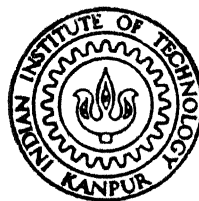


# **A STUDY OF THE PERFORMANCE OF THE EM — ALGORITHM IN A POSITRON EMISSION TOMOGRAPHY MODEL**

*by*

**RICHA RASTOGI**

NETP  
1988  
M  
RAS  
STU



**NUCLEAR ENGINEERING AND TECHNOLOGY PROGRAMME  
INDIAN INSTITUTE OF TECHNOLOGY, KANPUR**

**APRIL, 1988**

# **A STUDY OF THE PERFORMANCE OF THE EM — ALGORITHM IN A POSITRON EMISSION TOMOGRAPHY MODEL**

A Thesis Submitted  
In Partial Fulfilment of the Requirements  
for the Degree of  
MASTER OF TECHNOLOGY

*by*

**RICHA RASTOGI**

*to the*

**NUCLEAR ENGINEERING AND TECHNOLOGY PROGRAMME  
INDIAN INSTITUTE OF TECHNOLOGY, KANPUR**

**APRIL, 1988**

13 APR 1989  
CENTRAL LIBRARY  
I. I. T. KANPUR  
Acc. No. A104100

-T-21  
S39 7243  
R 18.6

NETP - 1980-M-RAS-STU

DEDICATED TO  
MY PARENTS



4/4/88 ii  
P2

Certificate

This is to certify that the work related to the project entitled "A STUDY OF THE PERFORMANCE OF THE EM-ALGORITHM IN A POSITRON EMISSION TOMOGRAPHY MODEL" has been carried out by Ms. RICHA RASTOGI under our supervision.

*mskalra*

Dr. M.S. KALRA  
DEPARTMENT OF NUCLEAR ENGINEERING  
INDIAN INSTITUTE OF TECHNOLOGY  
KANPUR

*R.K.S. Rathore*

Dr. R.K.S. RATHORE  
DEPARTMENT OF MATHEMATICS  
INDIAN INSTITUTE OF TECHNOLOGY  
KANPUR

*hatthal munshi*

Mr. P. MUNSHI  
DEPARTMENT OF NUCLEAR ENGINEERING  
INDIAN INSTITUTE OF TECHNOLOGY  
KANPUR.

Dated: April, 1988.

Acknowledgements

I wish to express my profound gratitude to my esteemed guides Dr. M.S. Kalra, Dr. R.K.S. Rathore and Mr. P.Munshi for their valuable guidance and unlimited co-operation during the course of this project. It was indeed a nice experience to work under them.

I am indebted to my parents for their constant encouragement and guidance.

I sincerely acknowledge the help rendered to me by the staff of the Nuclear Engineering Department.

My sincere thanks to my friends and colleagues for helpful discussions, inspiration and co-operation throughout my stay over here.

My thanks are also due to Shri G.L. Misra for his neat typing of the manuscript.

Dated: April, 1988.

Ms. RICHA RASTOGI

CONTENTS

	<u>Page</u>
LIST OF FIGURES	v
LIST OF TABLES	vi
NOMENCLATURE	vii
ABSTRACT	viii
CHAPTER 1 : A DISCUSSION OF POSITRON EMISSION TOMOGRAPHY	1
CHAPTER 2 : RECONSTRUCTION METHOD	6
(a) CONVOLUTION BACK PROJECTION METHOD	8
(b) EM ALGORITHM FOR PET	11
CHAPTER 3 : NUMERICAL SIMULATION AND CONCLUSION	21
REFERENCES	32
APPENDICES :	
A TIME COINCIDENCE TECHNIQUE	
B RECONSTRUCTED IMAGES	
C PROGRAM LISTING	

LIST OF FIGURES

<u>FIGURE</u>	<u>TITLE</u>	<u>PAGE NO.</u>
1	Positron detection Geometry	4
2	Parallel Beam Geometry	7
3	Variation of L-1 Error	28
4	Variation of L-2 Error	29
5	L-1 Error on Logarithmic Scale	30
6	L-2 Error on Logarithmic Scale	31

LIST OF TABLES

TABLE	TITLE	PAGE NO.
1	Principal Radioisotopes in diagnostic use	5
2	Comparison of Some Detector Materials	5
3	L-1 Error	26
4	L-2 Error	27

NOMENCLATURE

$B$	:	total no. of pixels
$c$	:	path of radiation
CAT	:	computer aided tomography
CBP	:	convolution back projection
$D$	:	total no. of detectors
$g_b$	:	<b>reconstructed pixel</b>
$f_b$	:	original pixel
$l(\lambda)$	:	$\log [L(\lambda)]$
$L(\lambda)$	:	likelihood function
$n(b,d)$	:	photons emitted in pixel $b$ and detected in tube $d$
NPIX	:	total number of considered pixels
$p(b,d)$	:	probability (emitted in $b$ detected in $d$ )
$p(t,\theta)$	:	projection data
PET	:	positron emission tomography
$t$	:	distance between $c$ and origin
$w(R)$	:	filter function
$\lambda$	:	<b>emission density</b>
$\mu$	:	attenuation co-efficient
$\Delta s$	:	distance between rays
$\Omega$	:	solid angle
$\tau$	:	resolving time
$\theta$	:	angle between $x$ -axis and the perpendicular on the path of radiation

ABSTRACT

The technique of positron emission tomography PET promises to open up new medical frontiers by enabling physicians to study the metabolic activity of the body in a pictorial manner. A suitable radio-active isotope [3], which emits positrons with a short half life time, is injected into the patients body. The radio-isotope flows with the blood stream and distributes itself in the various organs of the body. The positrons emitted by the radio-isotope interacts with the electrons in the nuclei of the surrounding material and get annihilated in the process. This annihilation produces a pair of photons which are subsequently detected in coincidence by an array of discrete detector elements surrounding the body. The short physical half-life of the majority of the positron emitting radio-nuclide lowers the radiation dose to the patient and permits repeat studies at short time interval [3]. Much as in X-Ray transmission tomography and other modes of computerized tomography the quality of the reconstructed image is very sensitive to the mathematical algorithm to be used for reconstruction. The objective of this study is to compare the performance of the EM algorithm [8] (specifically designed for PET) and an adaptation of the convolution back projection algorithm [7] widely used in transmission tomograph CAT scanner.

## Chapter 1

### A discussion of Positron emission tomography

Positron emission tomography (PET) is a medical diagnostic technique, which enables a physician to study blood flow and metabolic activity of an organ, in a visual way. For this, a biochemical metabolite labelled with a **positron** emitting radioactive material is introduced into the organ, under study. The radioactive emissions are then counted by using PET scanner- a machine consisting of detector elements mounted on one or more rings, positioned so that it surrounds the patient's body.

The choice of biochemical and the radioactive tracer depends on the organ to be studied and on the questions of interest. For example, labelled glucose is often used in PET studies of the brain while metabolism of the heart is measured with labelled deoxyglucose and labelled palmitic acid.

PET scans of brains of people suffering from schizophrenia and certain other diseases show distinctive metabolic patterns connected with these diseases. These metabolic portraits obtained from PET scans plays an important role in diagnosing such diseases and in assessing the effectiveness of various treatments.

An overview of the subject, including a discussion on clinical, biochemical, and other interesting aspects of PET



can be found in Brownell et al. (1932) and in Ter-Pogossian et al. (1980).

#### THE PHYSICS OF THE PET :

When a positron is emitted from a radioactive positron emitting material, it gets annihilated with a nearby electron. The annihilation creates two X-Ray photons that fly off the point of annihilation, at the speed of light, in (nearly) opposite directions, along a line with a completely random orientation. This pair of X-Ray photon is detected in coincidence by a pair of detector elements that define a cylindrical volume (to be referred to as a detector tube or, simply a tube).

The set of data collected in a PET scan is the tube counts  $n^*(1), n^*(2), \dots, n^*(D)$ , where  $n^*(d)$  is the total number of coincidences counted by the  $d^{\text{th}}$  detector tube and  $D$  is the total number of tubes.

Total tubes count is much smaller than the total number of emissions, because

- (1) Some of the photons do not get caught by detector ring.
- (2) Some of the photons are absorbed by the body's tissue.

These facts are schematically described in fig. (1.1). Table (1) shows the principal radioisotopes in diagnostic use.

### CHOICE OF DETECTOR MATERIALS :

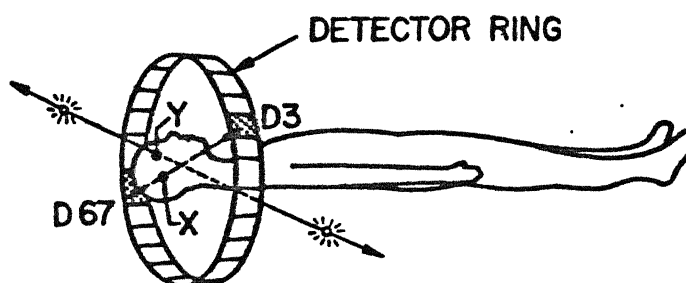
Three materials are under considerations for use in positron tomographs :

- (1) Sodium Iodide (NaI(Tl))
- (2) BISMUTH GERMANATE ( $\text{Bi}_4 \text{Ge}_3 \text{O}_{12}$ ); (BGO) (Cho and Farukhi 1977)
- (3) Caesium Fluoride (CsF)

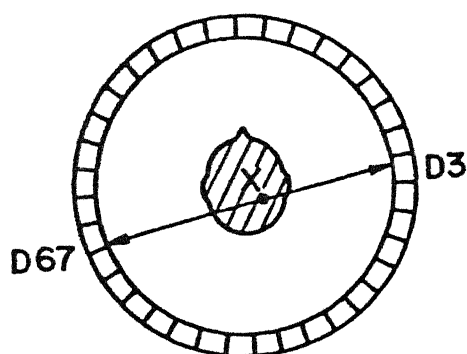
(Allemand et al. (1980)).

All these three have widely differing properties which are summarized in the table (2).

BGO is twice as dense as NaI(Tl) which results in a very high detection efficiency even for small crystals. CsF has excellent coincidence resolving time. Furthermore, BGO is not hygroscopic and therefore, does not need to be hermetically sealed as does NaI(Tl) and CsF. Most high resolution devices with detectors below 10 mm in size have BGO detectors (Derenzo et al. 1981 ; Erikson et al. 1980 ; Nohra et al. 1980 ; Brooks et al. 1980) because of the high detection efficiency and good packing fraction. CsF is preferred for lower resolution devices intended for fast dynamic studies (Yamamoto et al 1982).



a



b

Figure 1. (a) Two annihilations: one, at x, that is detected in tube (3, 67) and the other, at y, that passes undetected because the photon path does not intersect the detector ring. (b) Top view of the detector ring "plane" of a.

Ref. [9]

**Table 1.. Principal radioisotopes in diagnostic use (excepting C, N, O, F)**

Isotope	Radiopharmaceutical	Use	Reference
<sup>68</sup> Ga	Proteins	Regional blood-volume	Mazière, B. <i>et al.</i> (1982)
	Microspheres	Regional blood-flow	Yvert <i>et al.</i> (1979)
<sup>55</sup> Co	Bleomycin	Tumour tracer	Lagunas-Solar and Jungerman (1979)
<sup>82</sup> Rb	DTPA	CSF kinetics	Mazière, B. <i>et al.</i> (1981)
	—	Myocardial blood-flow	Lambrecht and Wolf (1979)
<sup>75,76</sup> Br	Bromocriptine	Dopamine receptors	Huang <i>et al.</i> (1981)
	Bromospiroperidol	Brain studies	Friedman <i>et al.</i> (1981)
<sup>73</sup> Se	Methionine	Protein metabolism	Guillaume <i>et al.</i> (1979)
<sup>51,52</sup> Mn	Chloride	Myocardial imaging	Ku <i>et al.</i> (1979)
	Chelate	Kidney function	Atcher <i>et al.</i> (1980)
<sup>122</sup> I	—	Cardiac angiography	Richards and Ku (1979)
<sup>19</sup> Ne	—	Local lung ventilation	Crouzel <i>et al.</i> (1980a,b)

Ref. [3, page 21 ]

**Table 2.. Comparison of some detector materials**

	NaI(Tl)	BGO	CsF
Density (g cm <sup>-3</sup> )	3.67	7.13	4.61
Atomic number	11, 53	82, 32, 8	55, 9
Relative light output	1.0	0.08	0.05
Scintillation peak wavelength (nm)	410	480	390
Index of refraction	1.78	2.15	1.48
Scintillation decay time (ns)	230	300	5
Time resolution* (2 $\tau$ , ns)	~12	~20	~6
Detection efficiency†			
Crystal width			
20 mm	61(41)%	90(88)%	68(49)%
8 mm	52(31)%	84(79)%	57(38)%
4 mm	46(25)%	78(71)%	50(29)%

\* Coincidence resolving time in positron system.

† For detector height = 3 cm, depth = 5 cm, packing fraction = 100 per cent, energy threshold = 100 keV for NaI(Tl) and CsF, 400 keV for BGO, number in parenthesis is photopeak efficiency.

Data from Derenzo (1981) and Ter-Pogossian *et al.* (1981).

Ref. [3, page 46 ]

## Chapter 2

### RECONSTRUCTION METHODS

In general terms the reconstruction problem is to determine the distribution of a function  $f(r, \varphi)$  from its projections  $p(t, \theta)$ . These two functions are related by,

$$p(t, \theta) = \int_{c(t, \theta)} f(r, \varphi) ds \quad (1.1)$$

where  $c(t, \theta)$  is a straight line that has a perpendicular distance,  $t$ , from the origin and the normal to which is at an angle,  $\theta$ , with respect to the  $x$ -axis, fig. (2). This problem has, of course, been solved and forms the basis of transmission computer tomography TCT.

In PET the unknown function is the activity distribution. Because of attenuation of the emitted gamma rays, the projections  $p(t, \theta)$  are not directly measured. Rather, the attenuated projection  $p_a(t, \theta)$  are measured. These are related to the unattenuated projection  $p(t, \theta)$  by

$$p_a(t, \theta) = p(t, \theta) p_\mu(t, \theta)$$

where  $p_\mu(t, \theta) = \exp \left[ - \int_{c(t, \theta)} \mu(r, \varphi) ds \right]$

$\mu(r, \varphi)$  = attenuation co-efficient and  $c(t, \theta)$  is the same as above.

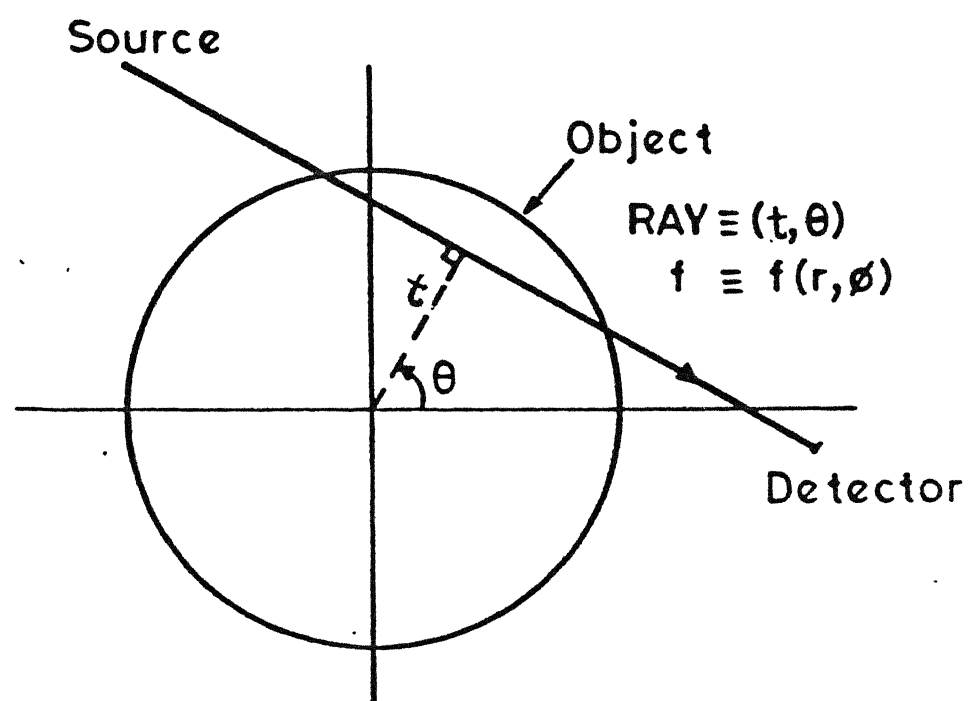


FIG. 2. PARALLEL-BEAM GEOMETRY.

Hence if  $p_{\mu}(t, \theta)$  is known, the  $p(t, \theta)$  can be calculated. The activity distribution  $f(r, \phi)$  can be computed using the same methods employed in TCT or by any method.

(1) Convolution Back Projection Method :

The data from the PET scanner is the attenuated projection  $p_a(t, \theta)$ . The projection data  $p(t, \theta)$  defined by

$$p(t, \theta) = \int_c \lambda(r, \phi) ds$$

is related to  $p_a(t, \theta)$  by

$$p(t, \theta) = p_a(t, \theta) / p_{\mu}(t, \theta)$$

where,

$$p_{\mu}(t, \theta) = \exp \left[ - \int_c \mu(r, \phi) ds \right]$$

$\mu$  = absorption co-efficient

$\lambda$  = emission density

$t$  = distance between origin and the path of radiation (RAY)

$\theta$  = angle between x-axis and the perpendicular on the path of radiation

$c$  = chord (path of radiation) with centre as the point  $(t \cos \theta, t \sin \theta)$

$\hat{p}(R, \theta)$  denotes the 1-D Fourier transform of projection with respect to  $s$ , at an angle  $\theta$ ,

$$\hat{p}(R, \theta) = \int_{-\infty}^{\infty} p(t, \theta) e^{i2\pi R t} dt \quad (2.3)$$

The projection theorem for Fourier transform or projection slice theorem [1], is

$$\hat{p}(R, \theta) = \hat{u}(R \cos \theta, R \sin \theta) \quad (2.4)$$

Taking the inverse Fourier transform of (2.4) we get,

$$u(x, y) = \int_0^{\pi} \int_{-\infty}^{\infty} \hat{p}(R, \theta) e^{i2\pi R(x \cos \theta + y \sin \theta)} |R| dR d\theta \quad (2.5)$$

For the computation of the integral involved in above equation, we need to make some approximation because limits  $-\infty$  to  $\infty$  on  $R$  introduces divergence. Therefore, a function  $w(R)$  is introduced in eqn. (2.5) called as window function or filter. Window function is chosen in such a way that

$$w(R) = \begin{cases} \text{some function of } R, & |R| \leq R_C \\ 0 & , |R| > R_C \end{cases}$$

where  $R_C = \frac{1}{2} \Delta s$ ,

$\Delta s$  = distance between rays.

After introducing the window function in equation (2.5) we get

$$u(x, y) = \int_0^{\pi} \int_{-R_C}^{R_C} \hat{p}(R, \theta) w(R) e^{i2\pi R(x \cos \theta + y \sin \theta)} |R| dR d\theta \quad (2.6)$$

Substituting for  $\hat{p}(R, \theta)$  from eqn. (2.3) and interchanging the order of integration over  $s$  and  $R$  we get



$$\mu(x,y) = \int_0^{\pi} \int_{-\infty}^{\infty} p(s,\theta) q(x \cos \theta + y \sin \theta - s) ds d\theta \quad (2.7)$$

If we assume object to be of unit radius then limits on  $s$  will be from  $-1$  to  $+1$ , so we get

$$\mu(x,y) = \int_0^{\pi} \int_{-1}^1 p(s,\theta) q(x \cos \theta + y \sin \theta - s) ds d\theta \quad (2.8)$$

where,  $1/2 \Delta s$

$$q(s) = \int_{-1/2 \Delta s}^{1/2 \Delta s} |R| w(R) e^{i2\pi R s} dR \quad (2.9)$$

$q(s)$  is called the convolving function.

The equation (2.8) and (2.9) form the basis of the method of convolution back projection [7]. If we break eqn. (2.8) into two equations :

$$\tilde{p}(s',\theta) = \int_{-1}^1 p(s,\theta) q(s'-s) ds \quad (2.10)$$

$$u(x,y) = \int_0^{\pi} \tilde{p}(x \cos \theta + y \sin \theta, \theta) d\theta \quad (2.11)$$

The operation represented by (2.10) is convolution and the operation represented by (2.11) is known as back projection. Thus the convolution back projection method applied to PET data consist of the following steps :

- (1) Estimation of  $p_{\mu}(t,\theta)$  by using transmission tomography
- (2) Obtaining  $p(t,\theta)$  by the relation

$$p(t,\theta) = p_a(t,\theta)/p_{\mu}(t,\theta)$$

- (3) Application of convolution back projection method to  $p(t, \theta)$ .

#### EM ALGORITHM FOR PET :

EM algorithm is derived [2] from the fact that each iteration of the method consists of an expectation step followed by a maximization step. The physical and statistical considerations that lead to a mathematical model of PET are discussed in detail in [4], [6] and [9].

The EM algorithm for PET has much in common with other iterative algorithms for image reconstruction from projections. It is an example of the finite series expansion reconstruction methods reviewed in [1] and discussion of its place, in the overall scheme, is given in [5]. We make the usual assumption that the image is subdivided into many small picture elements (pixels).

Let  $\lambda(b)$  be the (unknown) number of **positron** annihilation events that occurred in the  $b^{\text{th}}$  pixel ( $1 \leq b \leq B$ ), for which the corresponding pairs of photons were detected by the data acquisition system. The number of photon pairs detected in coincidence by the  $d^{\text{th}}$  pair of detector elements is denoted by  $n^*(d)$  ( $1 \leq d < D$ ). The probability that an event in the  $b^{\text{th}}$  pixel is detected by the  $d^{\text{th}}$  detector pair is denoted by  $p(b, d)$  while  $p(b)$  denotes the probability that an event in the  $b^{\text{th}}$  pixel is detected by the data acquisition system as a whole.

Therefore,

$$p(b) = \sum_{d=1}^D p(b,d) , \quad d = 1, \dots, D \quad (2.12)$$

Since the gamma rays are emitted at random angles in three dimensions, no practical detector system can intercept all of them. Hence the value of  $p(b)$  is less than one for all  $b$ .

Now consider further the time coincident gamma rays detected by the system as a whole for which the corresponding events occurred in the  $b^{\text{th}}$  pixel. Of these, let  $p(b,d)$  denote the fraction that is detected by the  $d^{\text{th}}$  pair of elements in the system.

By definition,

$$p'(b,d) = \frac{p(b,d)}{p(b)} \quad (2.13)$$

$$\text{and} \quad \sum_{d=1}^D p'(b,d) = 1 \quad (2.14)$$

Using the following notation for the inner product,

$$\langle p(d), \lambda \rangle = \sum_{b=1}^B p(b,d) \lambda(b) \quad (2.15)$$

the EM algorithm derived from the PET model [4], [6] and [9] may be written as

$$\lambda(b)^{k+1} = \lambda(b)^k \sum_{d=1}^D \left( \frac{n^*(d)}{\langle p(d), \lambda^k \rangle} \right) p'(b,d) \quad (2.16)$$

At each iteration (indexed by  $k$ ,  $k \geq 0$ ) the algorithm produces a new image vector  $\lambda^{(k+1)}$  from the old image vector  $\lambda^{(k)}$ . The initial image vector  $\lambda^{(0)}$  is chosen to satisfy,

$$\lambda^{(0)}(b) \geq 0, \quad b = 1, \dots, B.$$

Due to multiplicative nature of the iterative step any pixel of zero value will remain zero in subsequent iterations.

Two further properties of the iterative method are worth noting because they are particularly useful in PET :

- (1) Given a non-negative initial image  $\lambda^{(0)}$ , non-negative  $p(b,d)$  and  $n^*(d)$  (as is the case of PET), all images produced by the algorithm are non-negative.
- (2) For each image produced by the algorithm (i.e.  $\lambda^{(k)}$  for  $k > 1$ ), the sum of events in the image is equal to the sum of the counts in the data. In other words, the total number of  $\sum \lambda(b)$  of estimated counts is equal to the total number  $\sum n^*(d)$  of observed counts at each step  $\lambda^{(k)}$ ,  $k \geq 1$ .

The algorithm is therefore self-normalizing with each iteration producing a redistribution of the activity in the image, without any net increase or decrease in activity.

From the practical point of view, this property and the non-negativity of the image may be more important than the fact that the algorithm proceeds in the direction of maximizing the likelihood function.

The main disadvantage of this algorithm is the slow rate at which it iterates toward the acceptable image. But there are some modified version of EM algorithm which changes the image by a larger amount at each iterative step and also retains the non-negativity and self-normalization properties of the original algorithm.

CHOICE OF  $p(b,d)$  :

The EM iterative procedure (2.16) estimates  $\lambda^{\text{new}}$  from an old estimate  $\lambda^{\text{old}}$  by

$$\lambda^{\text{new}}(b) = \lambda^{\text{old}}(b) \frac{\sum_{d=1}^D \frac{n^*(d) p'(b,d)}{\sum_{b'=1}^B \lambda^{\text{old}}(b') p(b',d)}}{\sum_{b'=1}^B \lambda^{\text{old}}(b') p(b',d)}, \quad b = 1, \dots, B \quad (2.17)$$

Since we are interested only in those photons which have been detected in any of the detector tube, the conditional probability  $p'(b,d)$ , can be taken to be equal to  $p(b,d)$ .

According to Shepp and Vardi's assumption [8], a positron emitted in  $b^{\text{th}}$  pixel immediately runs to the centre of  $b$  and then travels a distance  $\rho$  with probability density

$$p(\rho) = \rho / (R \sqrt{R^2 - \rho^2}), \quad 0 < \rho < R, \quad (2.13)$$

in a random direction, to reach a point  $Q$  in the disk of radius  $R$ , about the centre of  $b$ . Upon reaching  $Q$  the positron annihilates and the photon pair chooses a line through  $Q$ , not at random, but uniformly over the  $n$  tube direction.

Based on the above assumption  $p(b,d)$  can be calculated as,  
 $p(b,d) = (2nR)^{-1} * (\text{width of the intersection of the circle}$   
 of radius  $R$  about the centre of  $b$  and the strip defined by the  
 tube  $d$ ),

where  $R$  = radius of the inscribed circle to  $b$

$n$  = no. of detector elements around the detector circle.

### Simulation :

For simulation Shepp and Vardi [9] use the phantom with density  $\lambda(x,y)$ .  $10^7$  points are then chosen independently from the density  $\lambda(x,y)/\iint \lambda$ . Each point is chosen by taking a uniform random point in the square  $|x|, |y| \leq 1$ . It is then accepted with probability  $\lambda$ . After choosing each point they choose a random line  $L$  through the point and increment the count for the detector unit corresponding to the two detector intervals that  $L$  passes through. This gives the numbers  $n^*(d)$ ,  $d = 1, \dots, D$ .

### MAXIMUM LIKELIHOOD FUNCTION OF $\lambda$ GIVEN $n^*$ :

The variable,  $n(b,d)$  the number of emissions in box  $b$  detected in tube  $d$ , are independent Poisson variables with mean

$$E n(b,d) = \lambda(b,d) = \lambda(b) p(b,d) \quad (2.19)$$

Therefore the likelihood function is given by,

$$L(\lambda) = p(n^* | \lambda) = \sum_A \prod_{\substack{b=1 \dots B \\ d=1 \dots D}} e^{-\lambda(b,d)} \frac{\lambda(b,d)^{n(b,d)}}{n(b,d)!} \quad (2.20)$$

where the sum is over all arrays  $A$  of  $n(b,d)$ 's with

$$n^*(d) = n(.,d) \stackrel{\text{def}}{=} \sum_{b=1}^B n(b,d), \quad d = 1, \dots, D \quad (2.21)$$

observed counts in the  $d^{\text{th}}$  detector tube. Also

$$n(b) = n(b,.) \stackrel{\text{def}}{=} \sum_{d=1}^D n(b,d) \quad (2.22)$$

is the (unobservable) number of emissions in the  $b^{\text{th}}$  box.

According to Shepp and Vardi [8] the concave nature of

$$l(\lambda) = \log [L(\lambda)] \quad (2.23)$$

can be proved as follows :

Differentiating (2.20) w.r.t. to  $\lambda(b_o, d)$  we get,

$$\begin{aligned} \frac{\partial L(\lambda)}{\partial \lambda(b_o, d)} &= \sum_A \left\{ \prod_{\substack{b=1 \dots B \\ d=1 \dots D}} e^{-\lambda(b,d)} \frac{\lambda(b,d)^{n(b,d)}}{n(b,d)!} \right\} \\ &\quad * \sum_{d=1}^D \left\{ -1 + \frac{n(b_o, d)}{\lambda(b_o, d)} \right\} \end{aligned} \quad (2.24)$$

Using (2.19),

$$\frac{\partial L(\lambda)}{\partial \lambda(b_o)} = \frac{\partial L(\lambda)}{\partial \lambda(b_o, d)} * p(b_o, d).$$

Therefore from (2.24) we get,

$$\begin{aligned} \frac{\partial L(\lambda)}{\partial \lambda(b_o)} &= \sum_A \left\{ \prod_{\substack{b=1, \dots, B \\ d=1, \dots, D}} e^{-\lambda(b,d)} \frac{\lambda(b,d)^{n(b,d)}}{n(b,d)!} \right\} \\ &\quad \cdot \sum_{d=1}^D \left\{ -p(b_o, d) + \frac{n(b_o, d)}{\lambda(b_o, d)} * p(b_o, d) \right\} \end{aligned} \quad (2.25)$$

On assuming that

$$\sum_{d=1}^D p(b_o, d) = 1$$

Eqn. (2.25) can be written as

$$\begin{aligned} \frac{\partial L(\lambda)}{\partial \lambda(b_o)} &= \sum_A \left\{ \prod_{\substack{b=1, \dots, B \\ d=1, \dots, D}} e^{-\lambda(b,d)} \frac{\lambda(b,d)^{n(b,d)}}{n(b,d)!} \right\} \\ &\quad \cdot \left[ -1 + \frac{1}{\lambda(b_o)} \sum_{d=1}^D n(b_o, d) \right] \end{aligned} \quad (2.26)$$

By definition of A on (2.20), the conditional expectation is given by

$$E [n(b_o) | n^*, \lambda] = \frac{1}{p(n^* | \lambda)} \sum_A \prod_{\substack{b=1, \dots, B \\ d=1, \dots, D}} e^{-\lambda(b,d)} \frac{\lambda(b,d)^{n(b,d)}}{n(b,d)!} n(b_o) \quad (2.27)$$

Comparing the second term in (2.26) with (2.27) and using (2.22) we get



$$\begin{aligned}
\frac{\partial l(\lambda)}{\partial \lambda(b_0)} &= \frac{1}{L(\lambda)} \frac{\partial L(\lambda)}{\partial \lambda(b_0)} = \frac{1}{p(n^*|\lambda)} \cdot \\
&\cdot \{-p(n^*|\lambda) + \frac{p(n^*|\lambda)}{\lambda(b_0)} E [n(b_0)|n^*, \lambda]\} \\
&= -1 + \frac{1}{\lambda(b_0)} \sum_{d=1}^D E [n(b_0, d)|n^*, \lambda] \quad (2.28)
\end{aligned}$$

Since  $n(b, d)$ 's are all mutually independent, the  $d^{\text{th}}$  term in the sum in (2.28) is given by

$$\begin{aligned}
E [n(b_0, d)|n^*, \lambda] &= E [n(b_0, d)|n^*(d), \lambda] \\
&= \frac{n^*(d) \lambda(b_0, d)}{\sum_{b'=1}^B \lambda(b', d)} \quad (2.29)
\end{aligned}$$

Putting the  $d^{\text{th}}$  term in (2.28) we get,

$$\begin{aligned}
\frac{\partial l(\lambda)}{\partial \lambda(b_0)} &= -1 + \frac{1}{\lambda(b_0)} \sum_{d=1}^D \frac{n^*(d) \lambda(b_0, d)}{\sum_{b'=1}^B \lambda(b', d)} \\
&= -1 + \frac{1}{\lambda(b_0)} \sum_{d=1}^D \frac{n^*(d) \lambda(b_0) p(b_0, d)}{\sum_{b'=1}^B \lambda(b') p(b', d)} \\
&= -1 + \sum_{d=1}^D \frac{n^*(d) p(b_0, d)}{\sum_{b'=1}^B \lambda(b') p(b', d)} \quad (2.30)
\end{aligned}$$

From (2.30) it follows that

$$\frac{\partial^2 l(\lambda)}{\partial \lambda(b_0) \partial \lambda(b_1)} = - \sum_{d=1}^D \frac{n^*(d) p(b_0, d) p(b_1, d)}{\left[ \sum_{b'=1}^B \lambda(b') p(b', d) \right]^2} \quad (2.31)$$

For any  $Z(1), \dots, Z(B)$ , (2.31) follows,

$$\begin{aligned} \sum_{b_0=1}^B \sum_{b_1=1}^B Z(b_0) Z(b_1) \frac{\partial^2 l(\lambda)}{\partial \lambda(b_0) \partial \lambda(b_1)} = \\ - \sum_{d=1}^D n^*(d) c^2(d) \end{aligned}$$

where  $c(d) = \frac{\sum_{b=1}^B Z(b) p(b, d)}{\sum_{b'=1}^B \lambda(b') p(b', d)}$  (2.32)

and since  $n^*(d) c^2(d) \geq 0$ , the quadratic form is negative semi-definite so that  $l(\lambda)$  is concave.

It has been proved in [2, Th. 1] that in each step the new estimate  $\lambda^{\text{new}}$  is an improvement over the old estimate  $\lambda^{\text{old}}$ :

$$L(\lambda^{\text{new}}) \geq L(\lambda^{\text{old}}) \quad (2.33)$$

with equality if and only if

$$L(\lambda^{\text{old}}) = \max_{\lambda} L(\lambda).$$

Therefore, it follows from the concavity of  $\log L(\lambda)$  that all maxima of  $L(\lambda)$  are global maxima and so the iteration scheme

gives a sequence  $\lambda^0, \lambda^1, \dots, \lambda^k \dots$  which converges to a global maximum likelihood estimator  $\lambda^\infty$ . If the maximum of  $L(\lambda)$  is not unique then by the concavity of  $\log L(\lambda)$  any convex combination of maxima is a maximum and  $\lambda^\infty$  depends on the initial choice  $\lambda^0$ .

### Chapter 3

#### Numerical Simulation and Conclusion

In our simulation we consider the case when there is no absorption of the photons. The measured data are  $n^*(1), \dots, n^*(D)$ , where  $n^*(d)$  is the total number of coincidences counted in the  $d^{\text{th}}$  detector tube. The simulation of  $n^*(d)$  is as follows :

At equidistant points in the detector tube  $d$  with uniform spacing 0.01, the positron activity proportional to the intensity of the picture, in the pixel, in which the point lies contributes to the tube  $d$ , data  $n^*(d)$ . This is done for  $128 \times 128$  tubes corresponding to 128 detectors mounted on the detector ring. 128 of these cases correspond to a null tube with zero data.

The iterative procedure for obtaining a new estimate  $\lambda^{\text{new}}$  from an old estimate  $\lambda^{\text{old}}$ ,

$$\lambda^{\text{new}}(b) = \lambda^{\text{old}}(b) \frac{\sum_{d=1}^D \frac{n^*(d) p(b,d)}{\sum_{b'=1}^B \lambda^{\text{old}}(b') p(b',d)}}{1}, \quad b = 1, \dots, B \quad (3.1)$$

is simulated as follows :

Let  $k(b,d)$  denotes the number of times pixel  $b$  has contributed to tube  $d$  and  $N(b)$  is the total contribution of pixel  $b$  to the detector ring, then  $p(b,d)$  is given by

$$p(b,d) = \frac{k(b,d)}{\sum_{d'} k(b,d')} = \frac{k(b,d)}{N(b)} \quad (3.2)$$

and we have

$$\sum_d p(b,d) = 1 \quad (3.3)$$

Now if  $PIC(b)$  is the value of pixel  $b$ , then

$$\lambda(b) \propto PIC(b) * N(b) \quad (3.4)$$

and

$$\begin{aligned} \sum_{b'} \lambda_o(b') p(b',d) &\propto \sum_{b'} PIC_o(b') N(b') * \frac{k(b',d)}{n(b')} \\ &= \sum_{b'} PIC_o(b') k(b',d) \\ &= n_o(d) \end{aligned} \quad (3.5)$$

Therefore (4.1) can be rewritten as

$$\begin{aligned} N(b) PIC_n(b) &= \frac{N(b) PIC_o(b)}{N(b)} \sum_d \frac{n^*(d) k(b,d)}{n_o(d)} \\ PIC_n(b) &= \frac{PIC_o(b)}{N(b)} \sum_d \frac{n^*(d) k(b,d)}{n_o(d)} \end{aligned} \quad (3.6)$$

Equation (3.6) has been implemented with various choice of initial approximation. L-1 and L-2 errors are then calculated as follows :

$$\begin{aligned} L-1 &= \frac{1}{NPIX} \sum_b (g_b - f_b) , \quad b = 1, \dots, B \\ L-2 &= \frac{1}{NPIX} \sqrt{\sum_b (g_b - f_b)^2} \end{aligned}$$

where,

$NPIX$  = Total no. of pixels considered

$g_b$  = Reconstructed pixel  $b$

$f_b$  = Original pixel  $b$ .

Four cases which we have considered are as follows :

- (1) Initial approximation is constant.
- (2) Initial approximation is from CBP having rebinning projection data from PET [PETCAT] .
- (3) Initial approximation is from CBP [CAT] .
- (4) Initial approximation is the last iterate of (1).

#### Observations :

- (1) Table [3] and Table [4] shows the corresponding  $L-1$  and  $L-2$  errors of each iteration for all the four cases respectively.
- (2) Figures of each iterations are in the appendix B.

#### CONCLUSION :

From the **figs.** [3-6] of error and iteration number ,  $n$ , we find that as  $n$  increases, the curve on the logarithmic scale approaches straight line with a negative gradient.

Hence for large  $n$ , the error values on the curve are of the form

$kq^n$  , where  $k$  is a constant and  $q$  is a positive number less than unity, implying that the convergence is of first order.

At the outset, from the reconstructions reported in Appendix B, it is clear that the CBP reconstruction in the parallel beam set up is generally the best and remains essentially unimproved by E-M iterates. The CBP algorithm applied on the rebinned PET data itself gives a reasonably good reconstruction which is only moderately improved by successive E-M iterates. Further starting with a constant initial approximation in the E-M algorithm seems to be quite time consuming.

The behaviour of errors in the three cases reveals the following information about EM-iterations :

- (i) If the initial approximation is crude the subsequent errors fall down rather quickly, till we get a good approximation of the cross-section.
- (ii) Starting with a good initial approximation the successive iterates improve the approximation till we get a close enough approximation of the cross-section. However, in this case the decrease in the error is rather slow.
- (iii) If the initial approximation is close enough the following iterates do not necessarily improve the approximation and the errors, infact, might even increase. However, this increase is rather marginal and the iterates continue to remain close enough to the desired cross-section. As the pattern of errors is more or less random apparently in this case the errors are solely due to round offs.

Combining (i), (ii) and (iii), it follows that one may start the procedure with an arbitrary initial approximation and continue the process till successive iterates keep on changing substantially. One then should stop the iterations when the changes are only marginal.

In conclusion, a practical strategy using EM algorithm would be :

- (a) Rebin the data
- (b) Apply CBP to get an initial approximation
- (c) Apply Em-algorithm with the initial approximation given by (b).

We may note at this point that rebining the PET data for adaptation to parallel beam geometry introduces interpolation errors to which it is well known that the CBP method is quite susceptible. On the other hand since the PET data is automatically a fan-beam geometry data, the corresponding fan-beam CBP may be used. The third alternative is to use iterative algebraic reconstruction technique ART, for the PET data. In view of the reported superior performance of iterative ART [4, 11.5], this possibly should be carefully examined since the time taken in EM iterations and ART iterations would be comparable, while the non-negativity and constant total activity by products of EM algorithm could be incorporated with equal ease in the ART case as well.



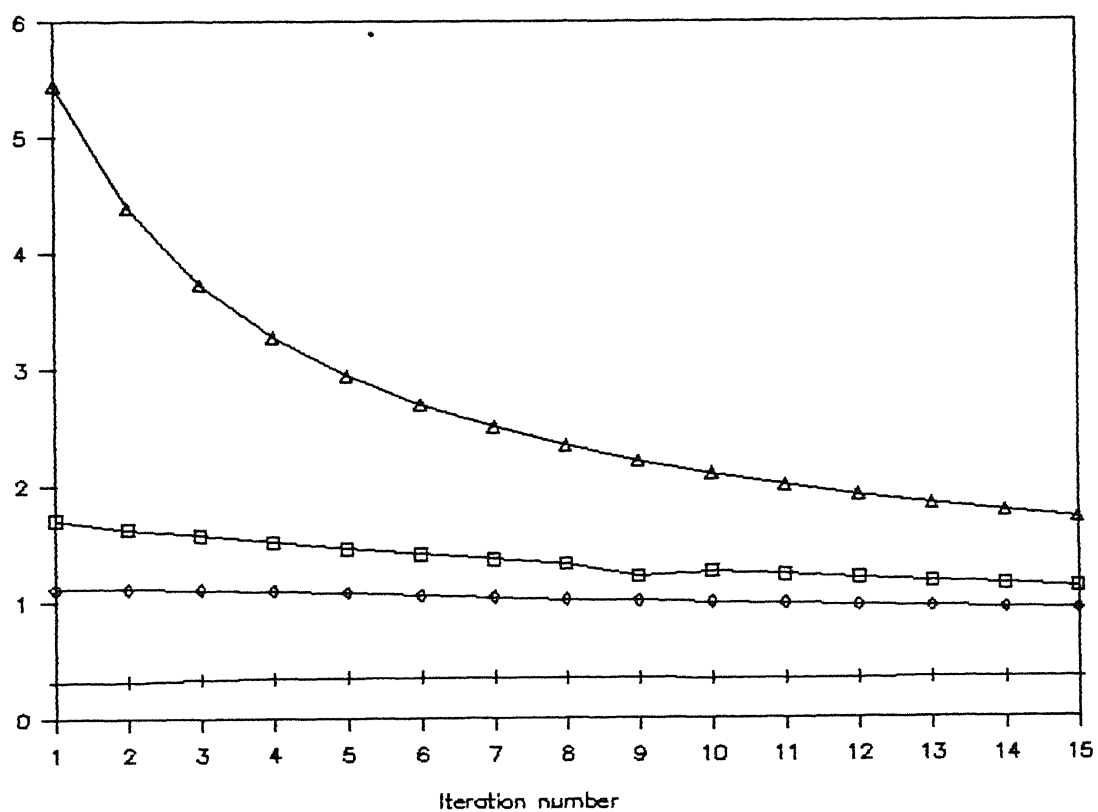
TABLE 3 : ERROR L-1

ITER. NO.	15 CONSTANT	CONSTANT	CAT	PETCAT
1	1.706590	5.446835	0.314174	1.115859
2	1.627746	4.390611	0.313572	1.111345
3	1.573578	3.723258	0.333133	1.107734
4	1.517605	3.274752	0.343665	1.098405
5	1.459325	2.943726	0.352091	1.081252
6	1.413181	2.692951	0.350587	1.058983
7	1.364129	2.502859	0.349082	1.037617
8	1.325308	2.343966	0.344568	1.019561
9	1.241002	2.210653	0.342462	1.009630
10	1.257899	2.096299	0.340355	0.992981
11	1.229010	1.999097	0.341860	0.980740
12	1.201023	1.915438	0.341860	0.969004
13	1.171833	1.836894	0.343966	0.956365
14	1.145652	1.772796	0.343966	0.943425
15	1.120975	1.714716	0.345170	0.932591

TABLE 4 : ERROR L-2

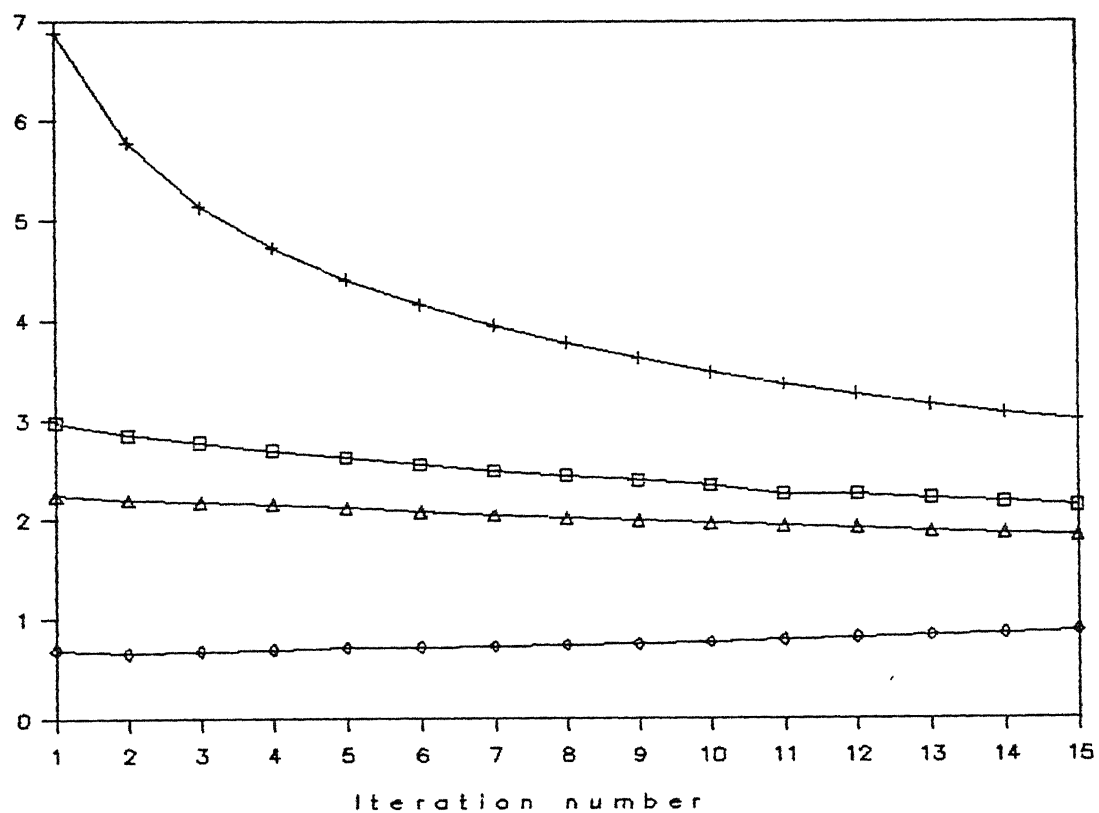
ITER. NO.	15 CONSTANT	CONSTANT	CAT	PETCAT
1	2.973299	5.878683	0.690418	2.239094
2	2.844712	5.777810	0.651357	2.188733
3	2.770215	5.141483	0.677438	2.172448
4	2.691199	4.748436	0.692160	2.153457
5	2.619115	4.409248	0.712723	2.119440
6	2.551191	4.159186	0.717143	2.081762
7	2.487102	3.953651	0.727351	2.042433
8	2.433466	3.775326	0.738234	2.009307
9	2.385380	3.622247	0.752966	1.983607
10	2.336820	3.475290	0.765845	1.957185
11	2.251358	3.359537	0.789641	1.932583
12	2.251358	3.254618	0.809959	1.910265
13	2.207148	3.153892	0.834120	1.876150
14	2.169815	3.067551	0.853909	1.854876
15	2.129921	2.988491	0.878574	1.836124

Fig.3. VARIATION OF L-1 ERROR



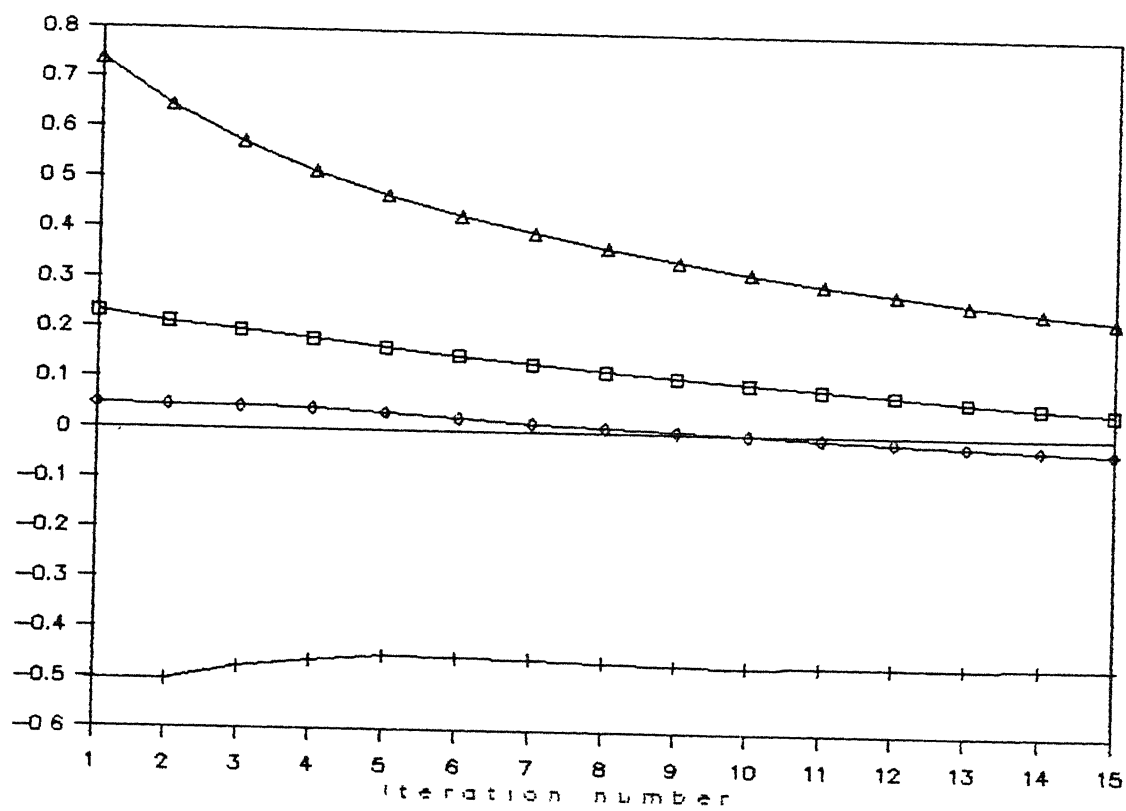
□ Petcat  
 Δ constant  
 ○ Petcat  
 + cat

Fig.4. VARIATION OF L-2 ERROR



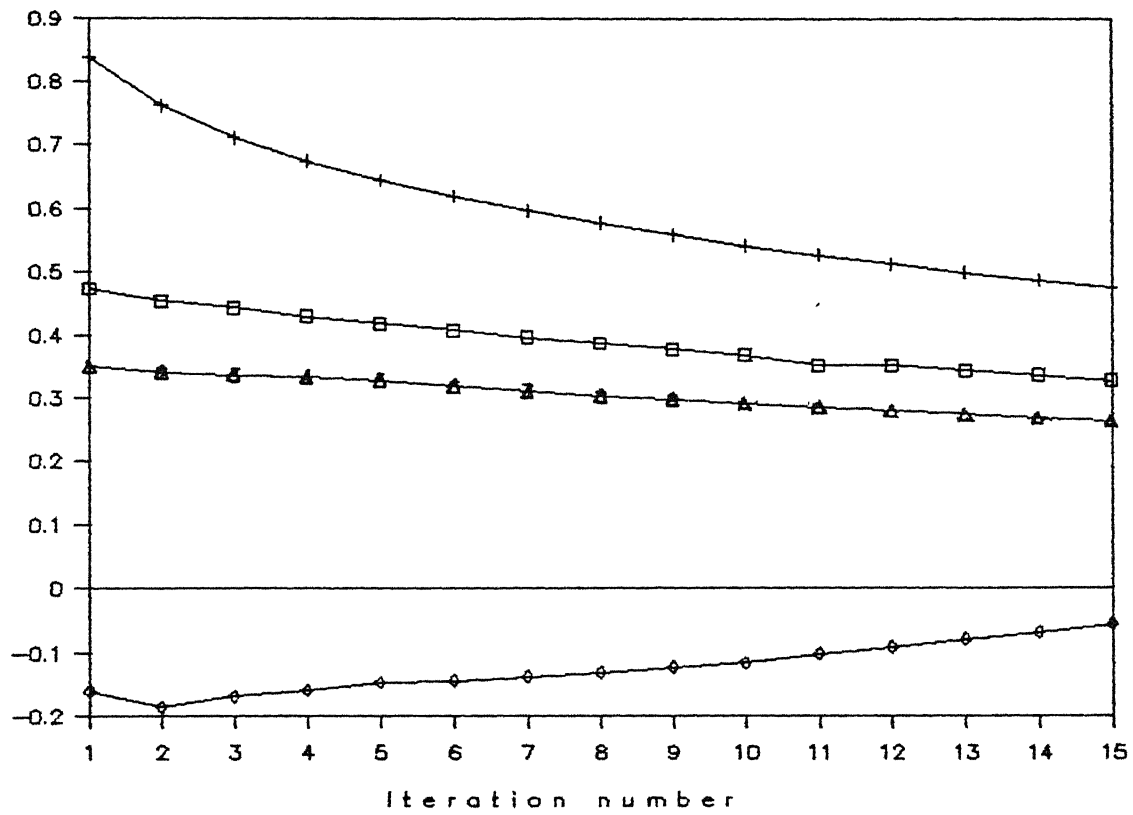
□ 15 constant  
 Δ Petcat  
 ○ cat  
 + constant

Fig.5. L-1 ERROR ON LOG SCALE



□ 15 constant  
 Δ constant  
 ○ Petcat  
 + cat

Fig.6. L-2 ERROR ON LOG SCALE



□ 15 constant  
△ Petcat  
◊ cat  
+ constant

### References

- 1     Y. Censor, "FINITE SERIES-EXPANSION RECONSTRUCTION METHODS," Proc. IEEE, Vol. 71, pp. 409-419, 1983.
- 2     A.P. Dempster, N.M. Laird, and D.B. Rubin, "MAXIMUM LIKELIHOOD FROM INCOMPLETE DATA VIA THE EM ALGORITHM," J. Royal Statist. Soc. (London) Series B, Vol. 39, pp. 1-38, 1977.
- 3     P.J. Ell and B.L. Holman, "COMPUTED EMISSION TOMOGRAPHY," Oxford Univ. Press, N.Y., 1982.
- 4     G.T. Herman, "IMAGE RECONSTRUCTION FROM PROJECTIONS : THE FUNDAMENTALS OF COMPUTERIZED TOMOGRAPHY," Academic Press, N.Y., 1980.
- 5     G.T. Herman, Y. Censor, D. Gordon, and R.M. Lewitt, "COMMENTS ON: A STATISTICAL MODEL FOR POSITRON EMISSION TOMOGRAPHY," J. American Statist. Assoc., Vol. 88, pp. 22-25, 1985.
- 6     K. Lange and R. Carson, "EM RECONSTRUCTION ALGORITHMS FOR EMISSION AND TRANSMISSION TOMOGRAPHY," J. Comput. Assist. Tomogr., Vol. 8, pp. 306-316, 1987.
- 7     R.M. Lewitt, "RECONSTRUCTION ALGORITHMS TRANSFORM METHOD," Proc. of IEEE, Vol. 71, pp. 390-409, 1983.
- 8     L.A. Shepp and Y. Vardi, "MAXIMUM LIKELIHOOD RECONSTRUCTION FOR EMISSION TOMOGRAPHY," IEEE Trans. Med. Imaging, Vol. MI-1, pp. 113-121, 1982.
- 9     Y. Vardi, L.A. Shepp and L. Kaufman, "A STATISTICAL MODEL FOR POSITRON EMISSION TOMOGRAPHY," J. Amer. Statist. Assoc., Vol. 80, pp. 8-37, 1985.

## Appendix A

### TIME COINCIDENCE TECHNIQUE

This technique identifies the time relationship between the radiations emitted by a radio-active source. In its simplest form, a double coincidence circuit, when fed with two input signals provides an output signal only if both of them arrive within a certain time  $\tau$  of each other. This time  $\tau$ , is known as the resolving time of the coincidence circuit.

In an overlap type coincidence circuit accepting two input signals each of width  $\tau$ , the resolving time is  $2\tau$  because coincidence output results only if one pulse lies within  $\pm \tau$  of other. Coincidence unit with a resolving time in nanosecond (nsec) range is termed as a fast coincidence unit. On the other hand, a coincidence unit with a resolving time in micro-second ( $\mu$  sec) range is called as a slow coincidence unit.

By using appropriate detector, coincidence measurements can be made between alpha- and gamma-rays, beta and gamma rays, gamma- and gamma rays, neutron and gamma-rays or between any such combination.

Normally the detectors are kept back to back. But by keeping one detector in a fixed position and moving the other in different angles, we can do angular (coincidence) correlation measurements. Such measurements are useful in determining the spins and parities of excited states of the nuclei.

---



The principal problem in the coincidence measurements are the accidental coincidences. To understand this, let us assume that angular distributions are isotropic, then, no. of coincidences detected per sec  $N_c$ , is given by

$$N_c = N_o \Omega_1 \Omega_2 \quad (A-1)$$

where

$N_o$  = No. of positron emissions occur/sec.

$\Omega_1$  = Solid angle subtended by detector 1

$\Omega_2$  = Solid angle subtended by detector 2.

If all detected photons are due to these  $N_o$  positron emissions, the total count rates in the two detectors  $N_1$  and  $N_2$  are,

$$N_1 = N_o \Omega_1 \text{ and } N_2 = N_o \Omega_2$$

If photons are detected in the two detectors within the resolving time of the coincidence analyzer  $\tau$ , they will be recorded as a coincidence. The chance that this will happen accidentally before or after each photon is received in the first detector is  $2\tau$  times the probability per second for a photon to reach the second detectors, or  $2\tau N_2$ . Since this situation occurs  $N_1$  times per second, the total number of accidental coincidences per second,  $N_a$ , is

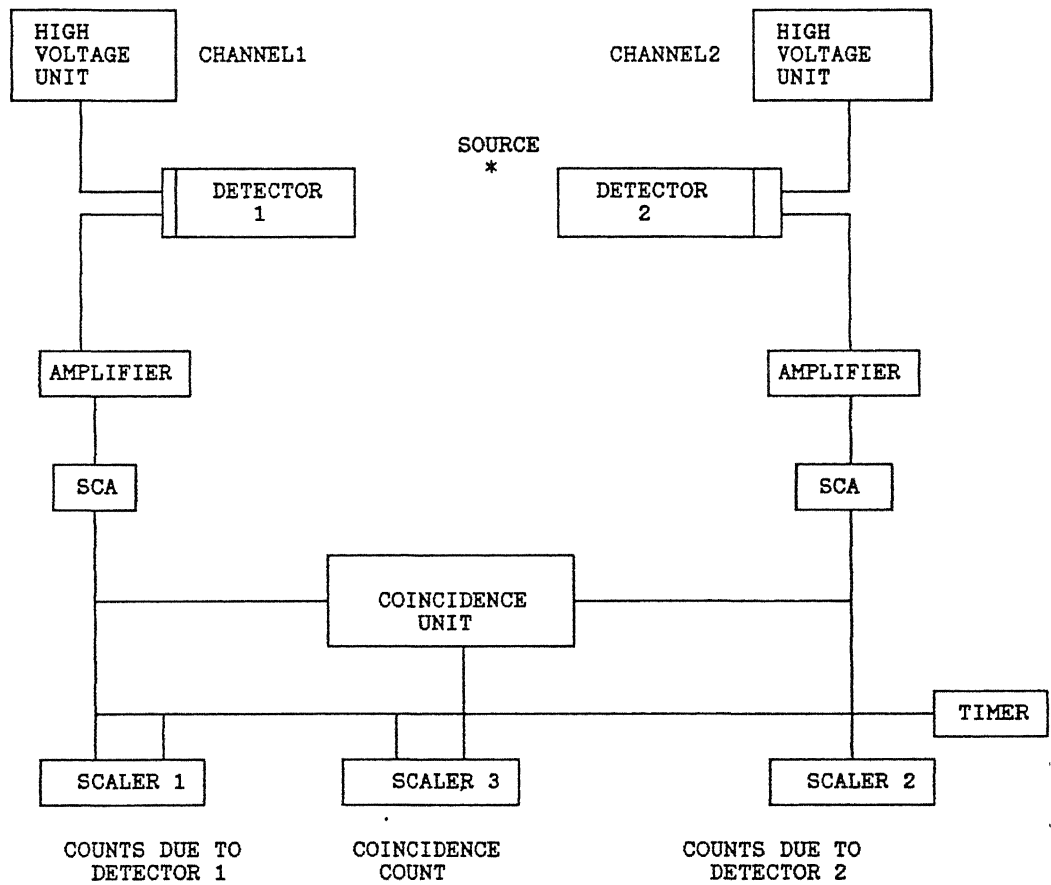
$$N_a = 2\tau * N_1 N_2$$

Therefore, the ratio of true to accidental coincidences is,

$$\frac{N_c}{N_a} = \frac{N_o \Omega_1 \Omega_2}{2N_o^2 \Omega_1 \Omega_2 \tau} = \frac{1}{2N_o \tau} .$$

For good coincidence measurement, this ratio should be sufficiently large. The ratio can be increased by reducing  $N_o$  or  $\tau$ . Since reducing  $N_o$  means reducing  $N_c$  i.e. rate of data accumulation it is advisable to keep  $\tau$  as small as possible.

SET-UP FOR COINCIDENCE MEASUREMENT



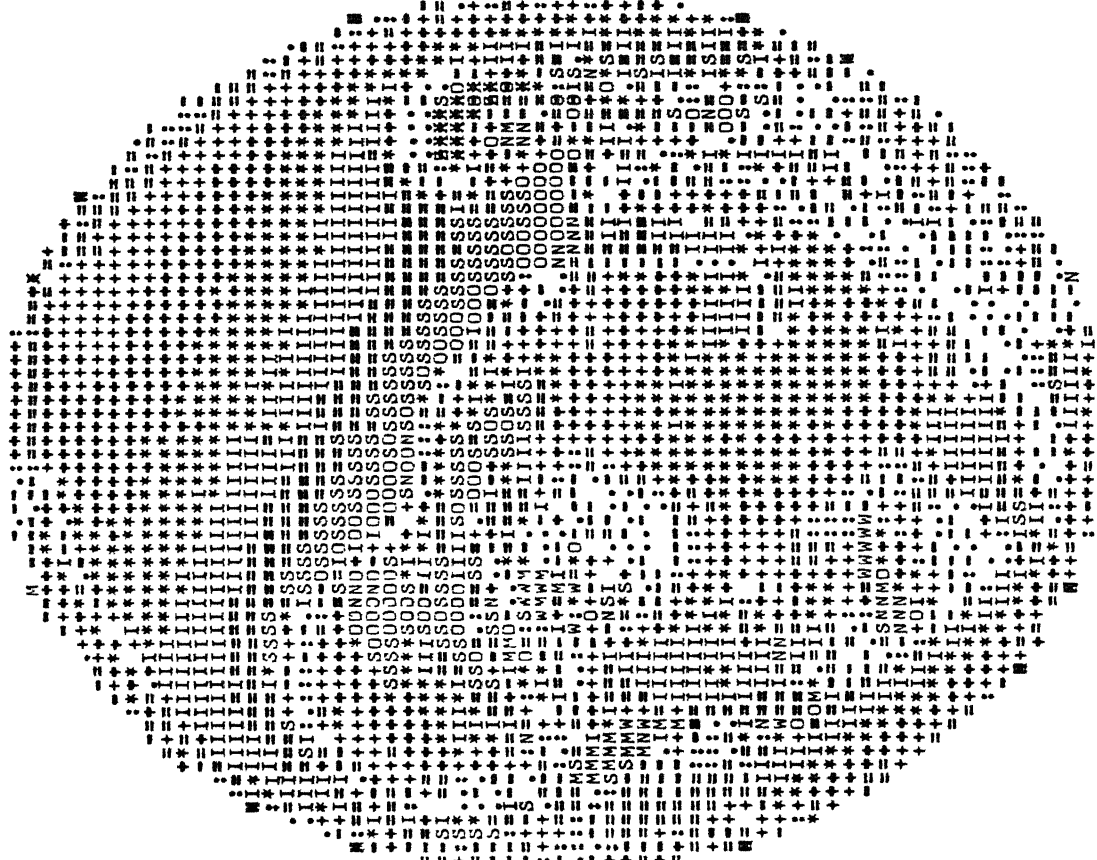
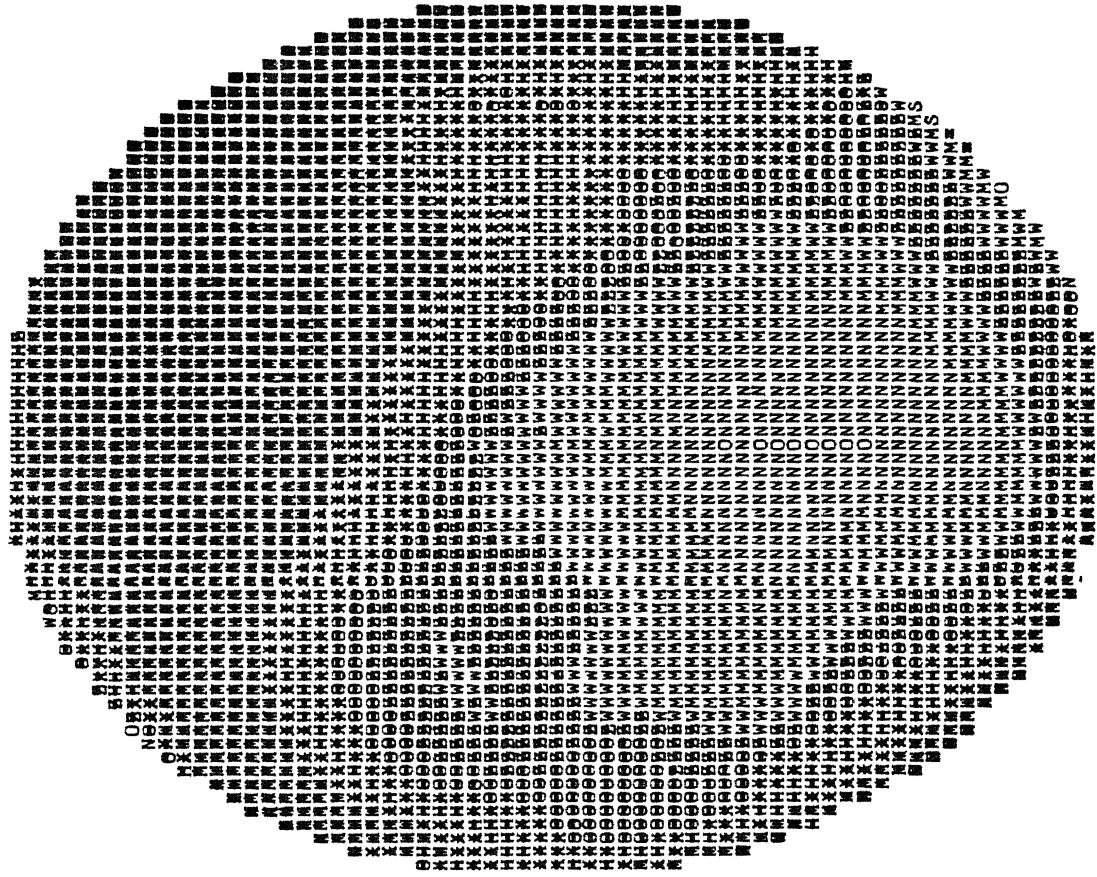
**APPENDIX B**  
**RECONSTRUCTED IMAGES**

[illegible]

# INITIAL APPROXIMATION TO CAT

# INITIAL APPROXIMATION TO PETCAT

RKSFIL INITIAL=CONSTANT DATA=FACE OF A GIRL ITERATION NUMBER= 1 NO. OF DETECTORS = 128 NRAY = 128



RKSPIL

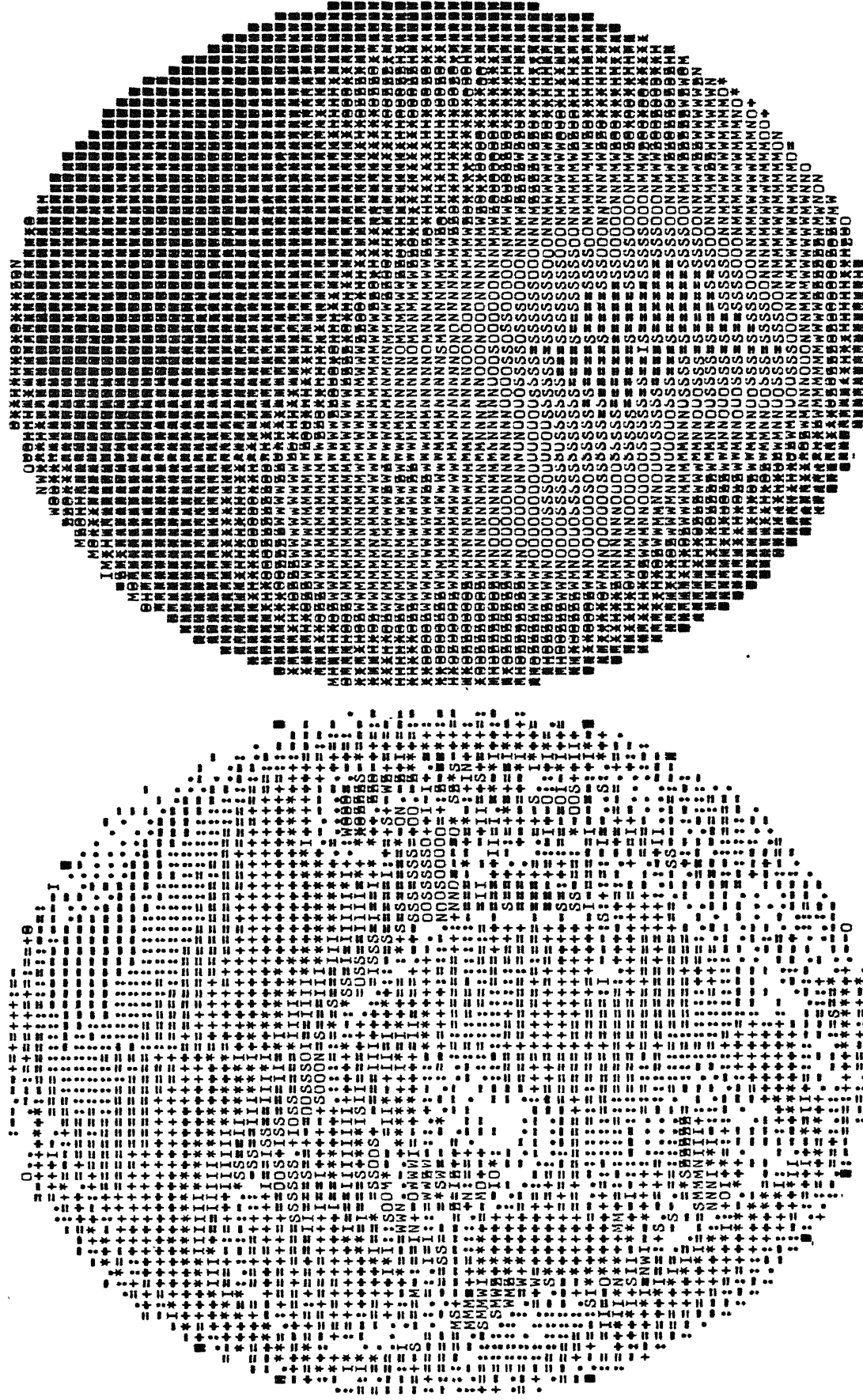
INITIAL=CONSTANT

DATA=FACE OF A GIRL

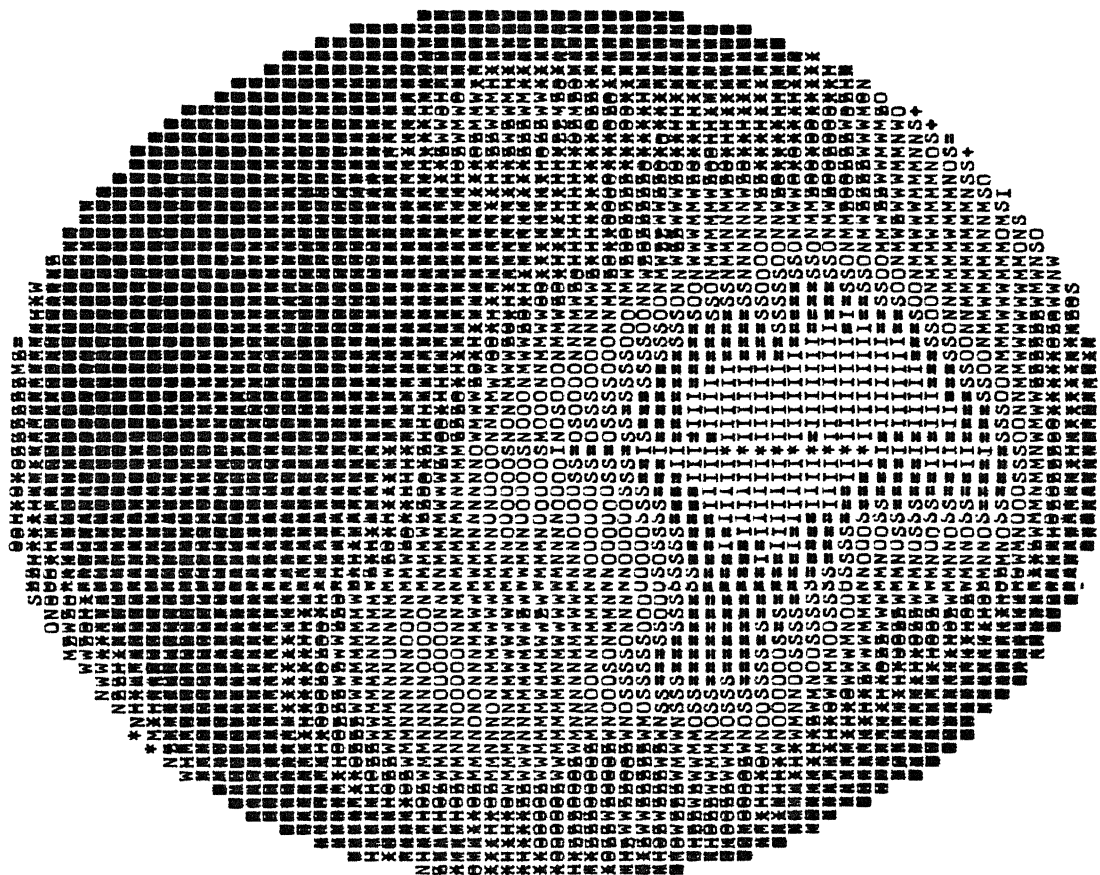
ITERATION NUMBER= 2

NO. OF DETECTORS = 128

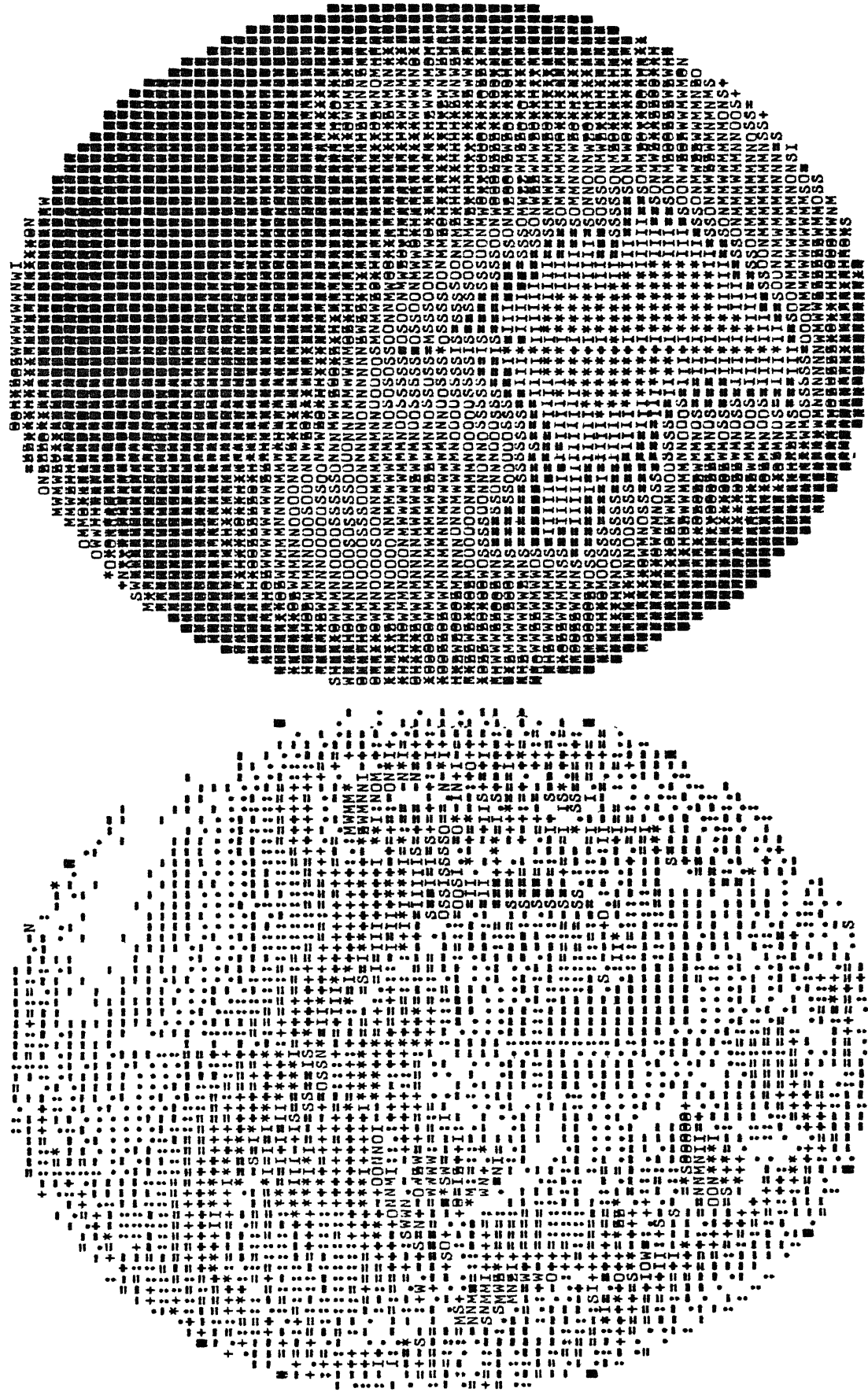
NRAY = 128

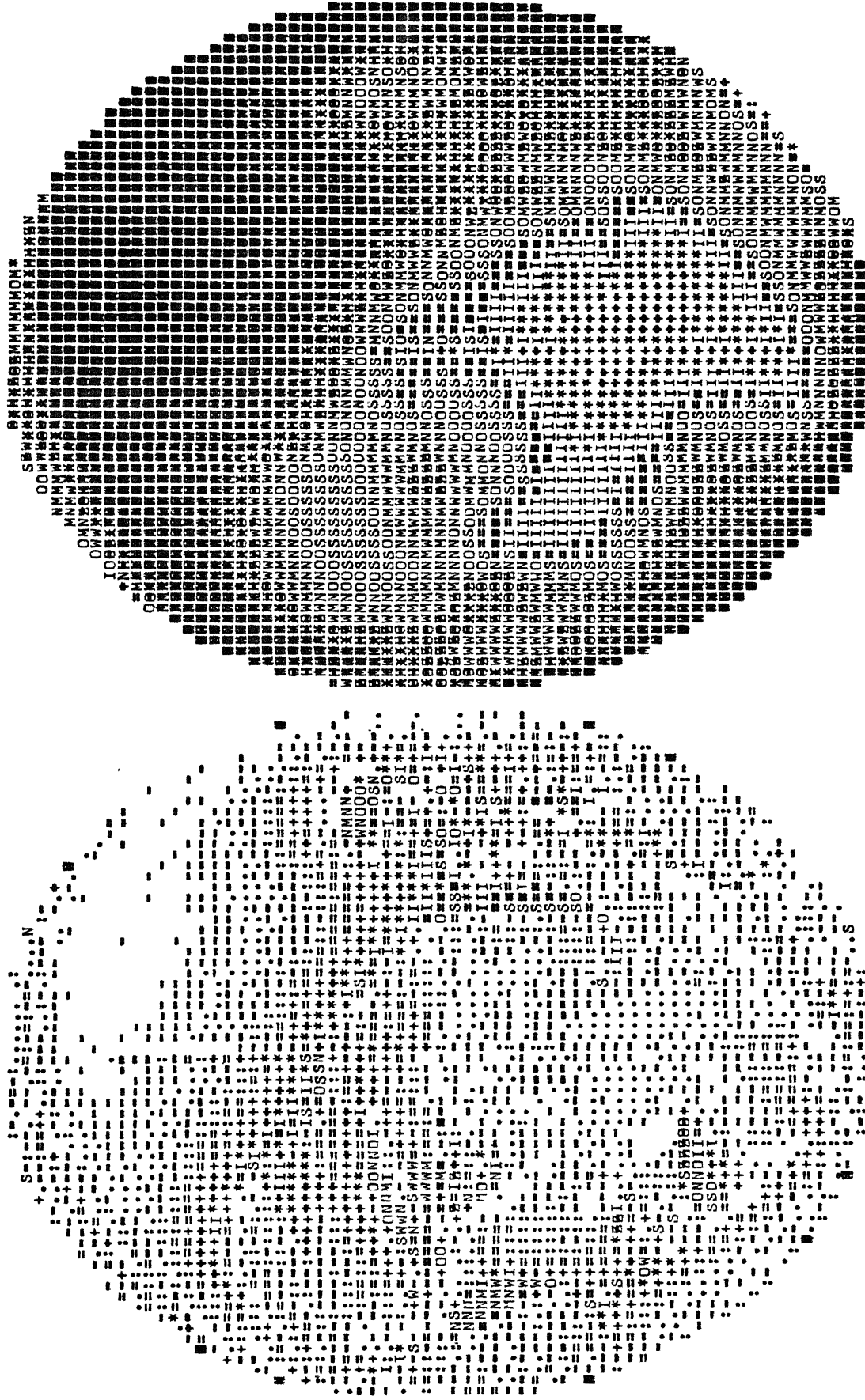


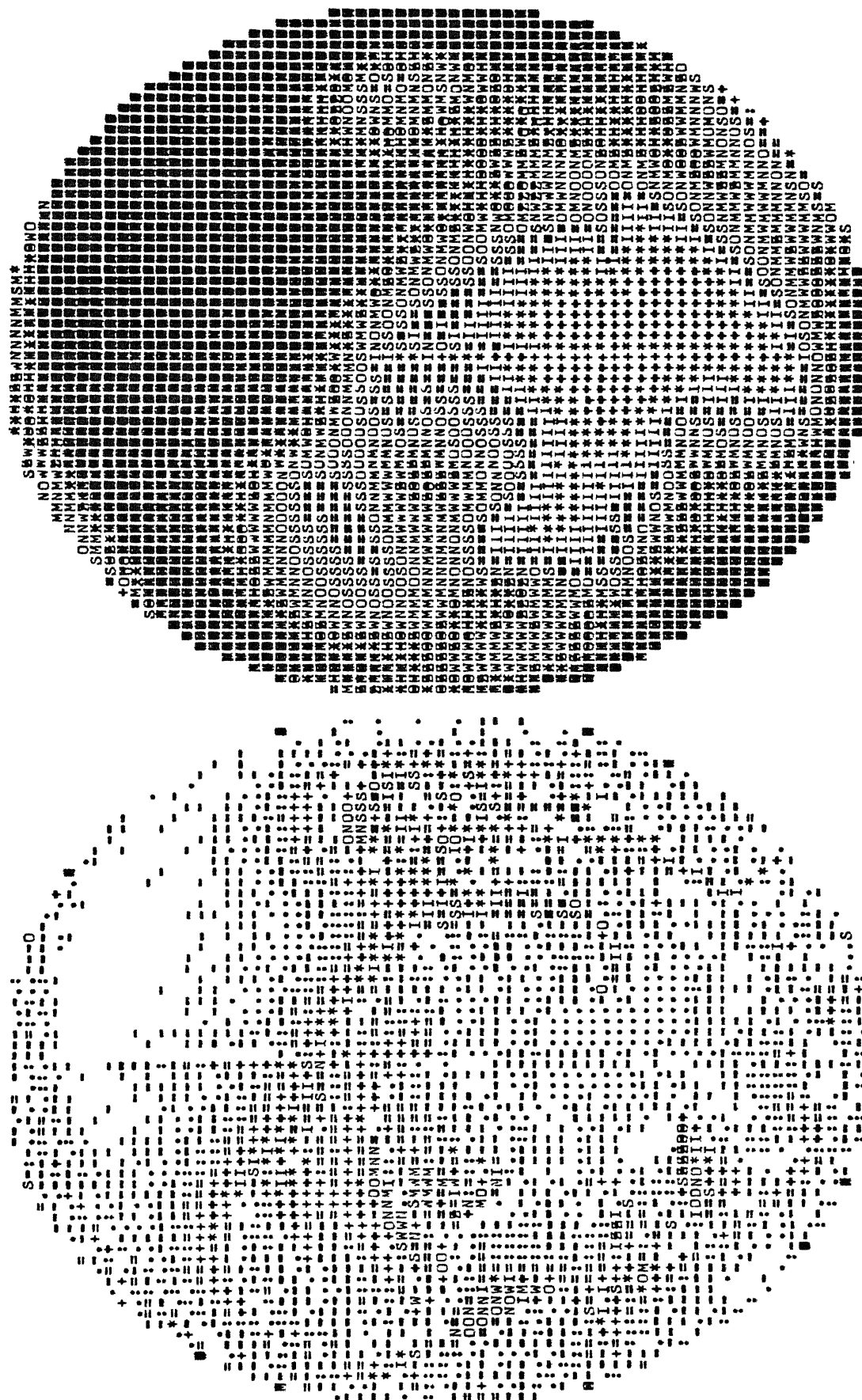




RKSFIL INITIAL=CONSTANT DATA=FACE OF A GIRL ITERATION NUMBER= 4 NO. OF DETECTORS = 128 NRAY = 128







RKSPIL

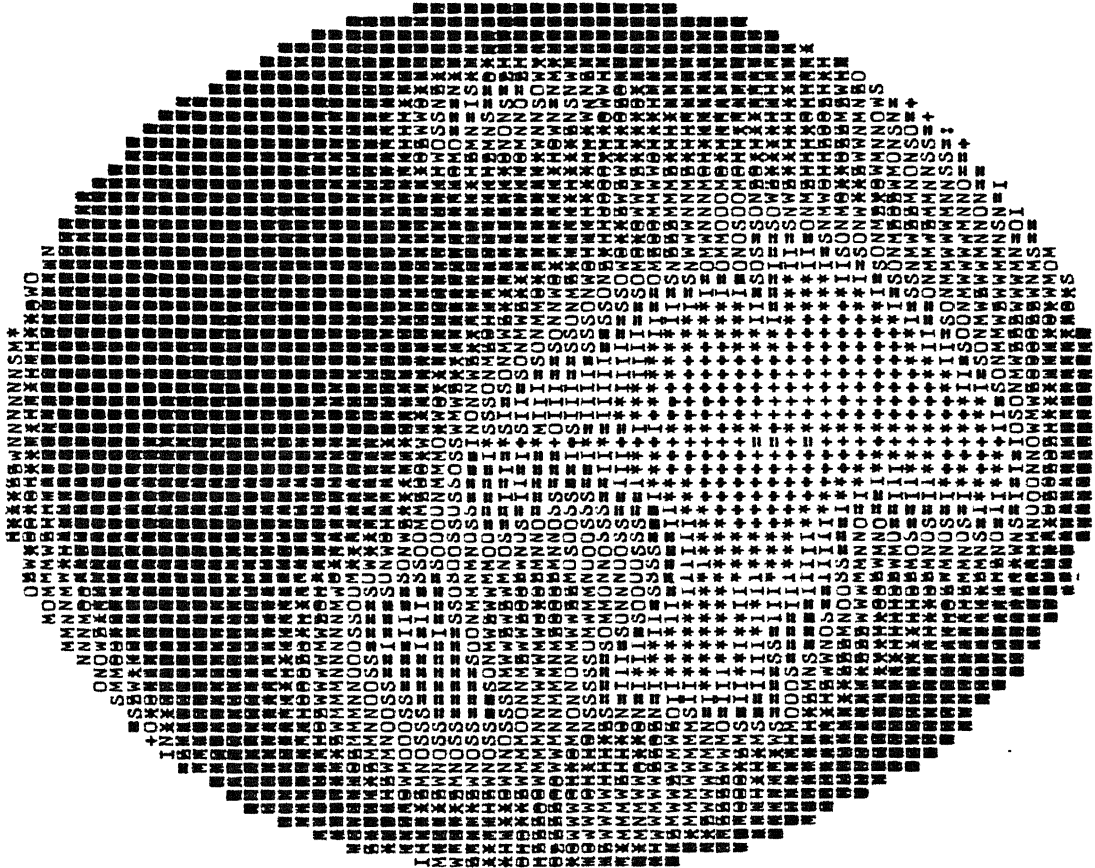
INITIAL=CONSTANT

DATA=FACE OF A GIRL

ITERATION NUMBER= 7

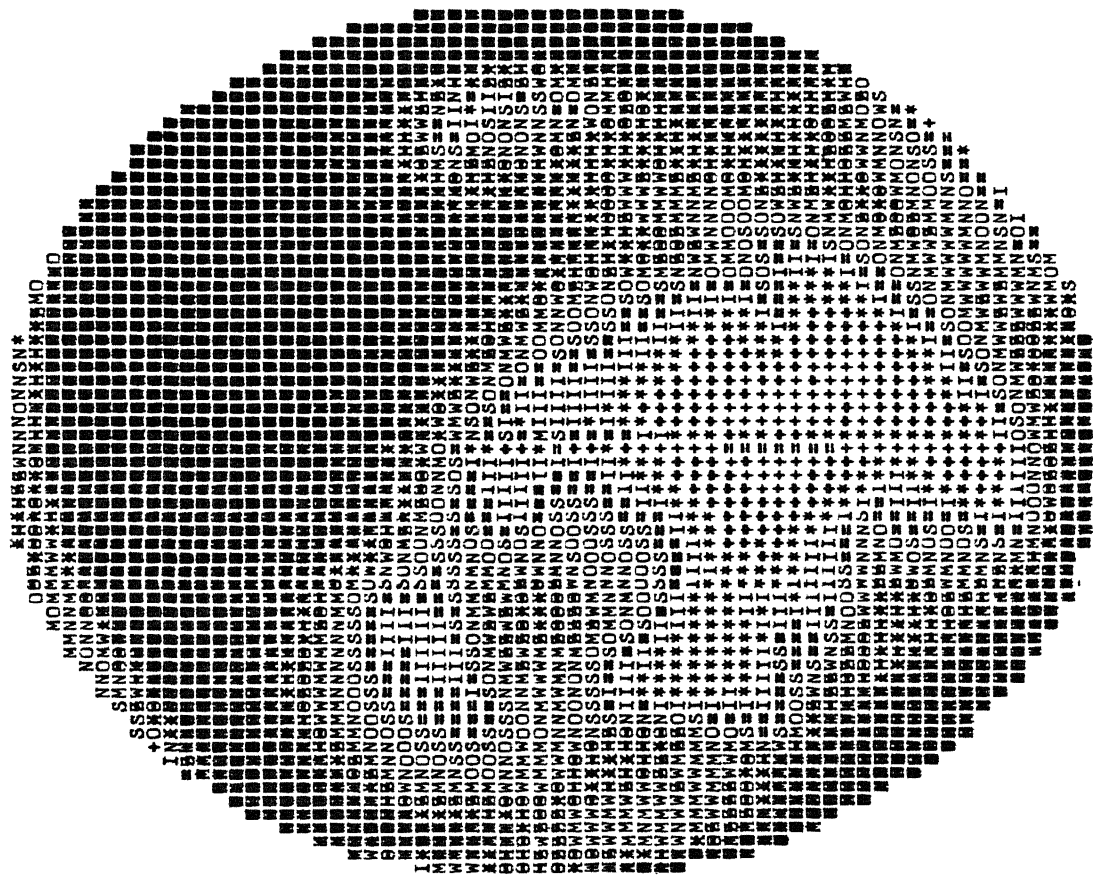
NO. OF DETECTORS = 128

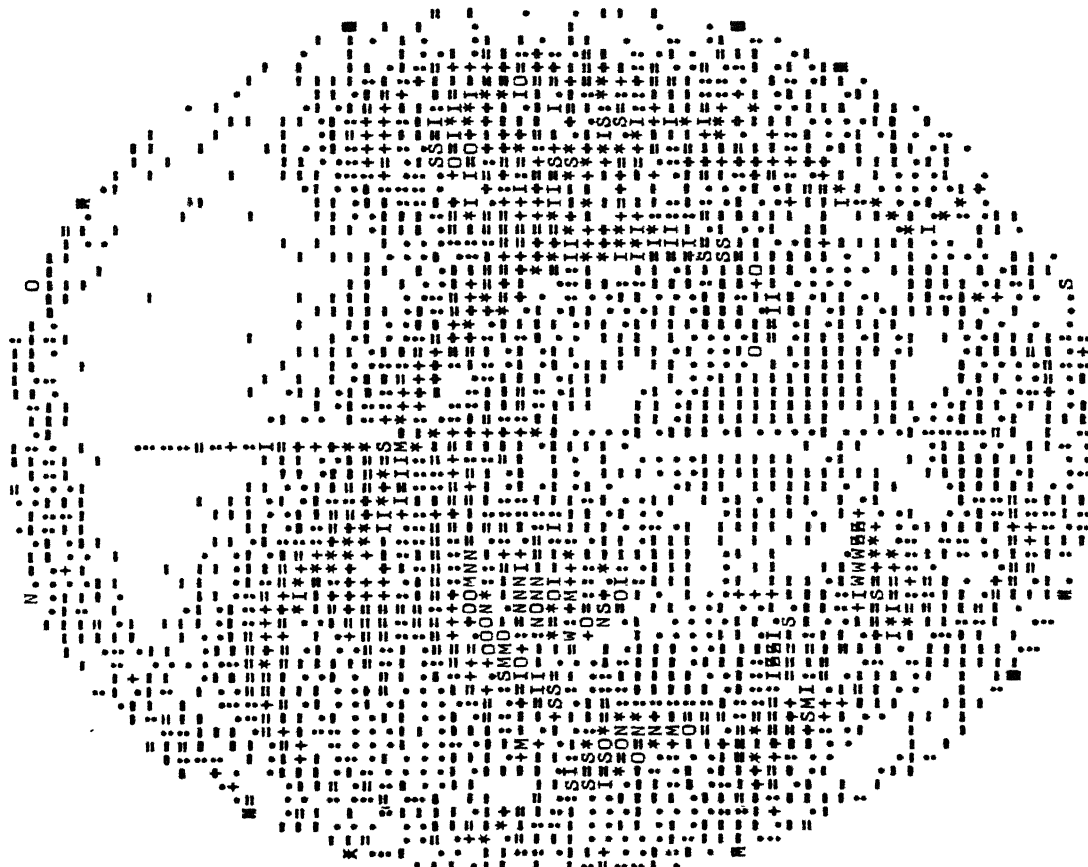
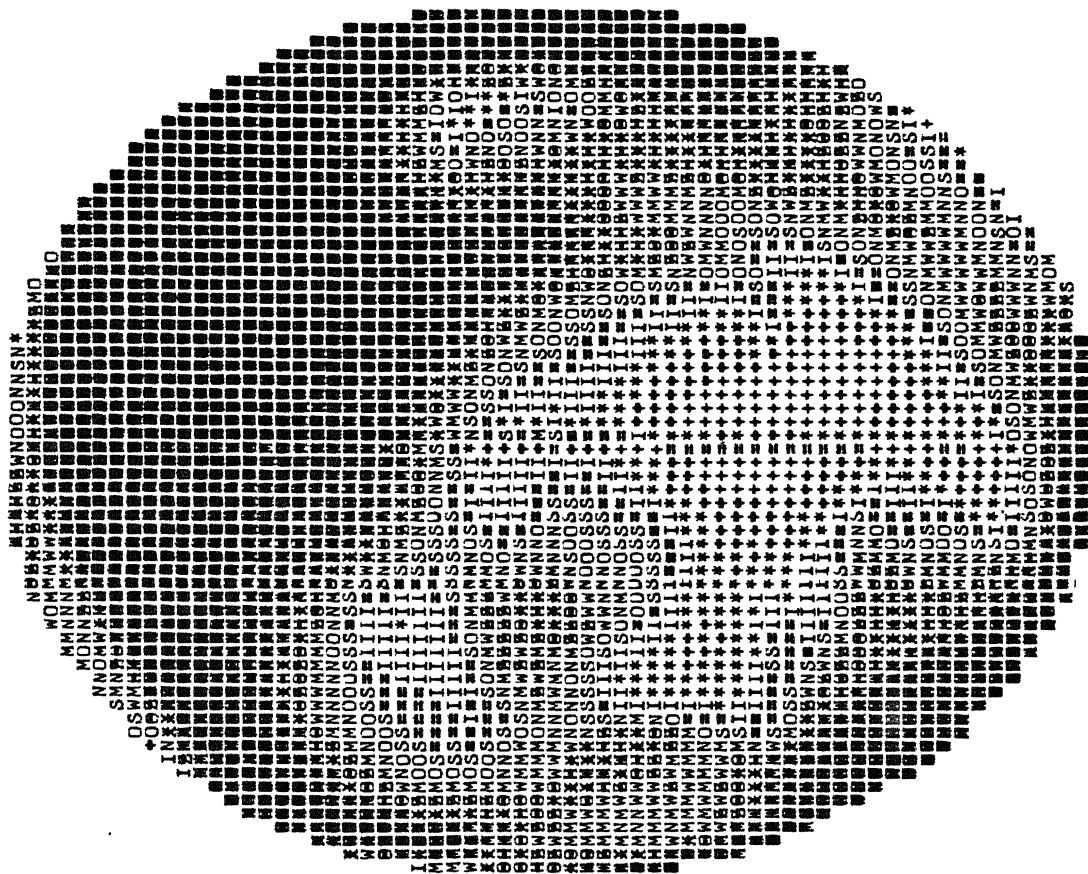
NRAY = 128





ITERATION NUMBER= 8 NO. OF DETECTORS = 128 NRAY = 128

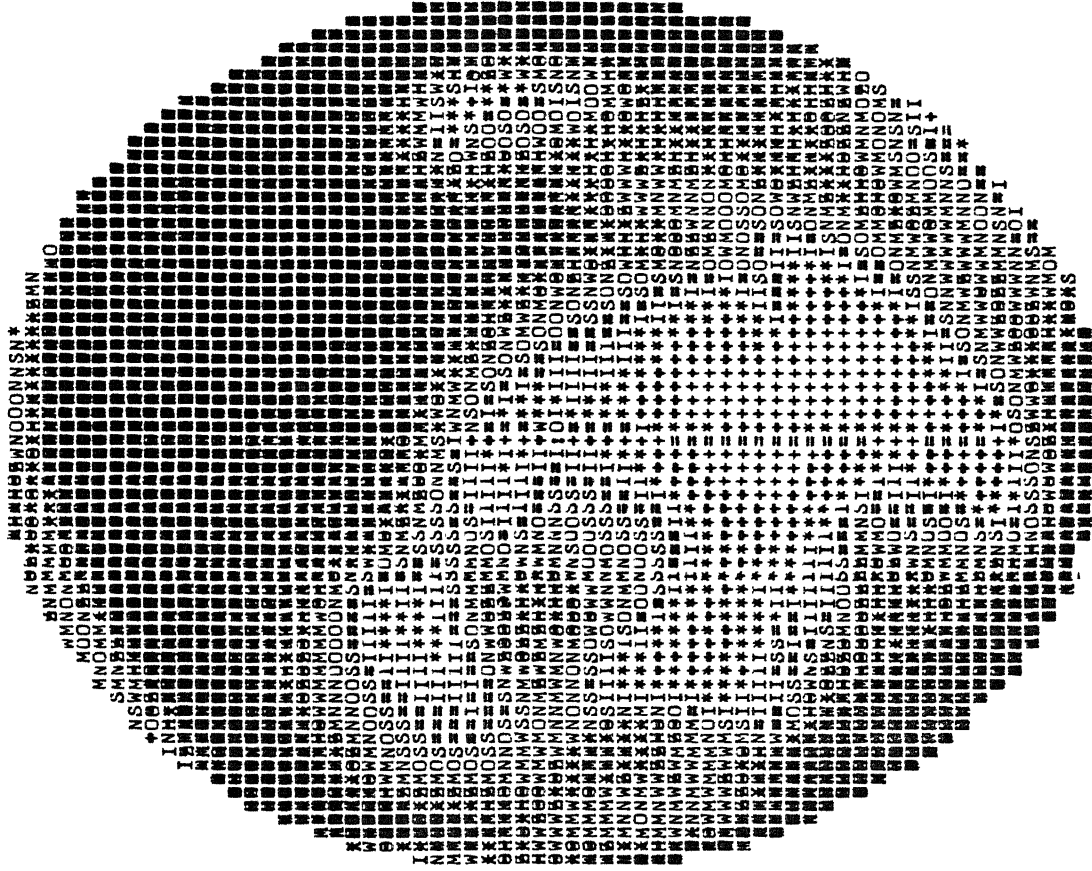




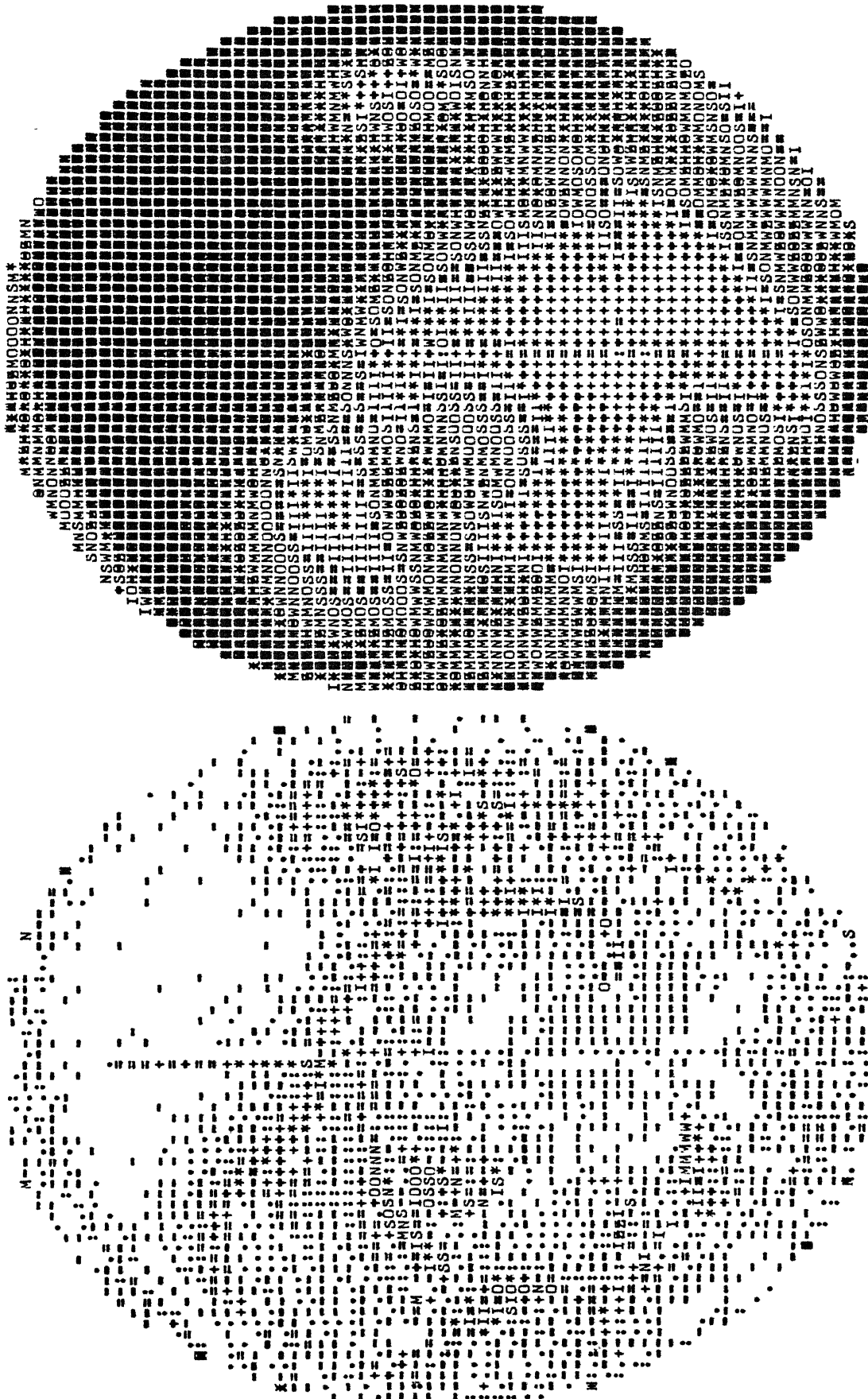
```

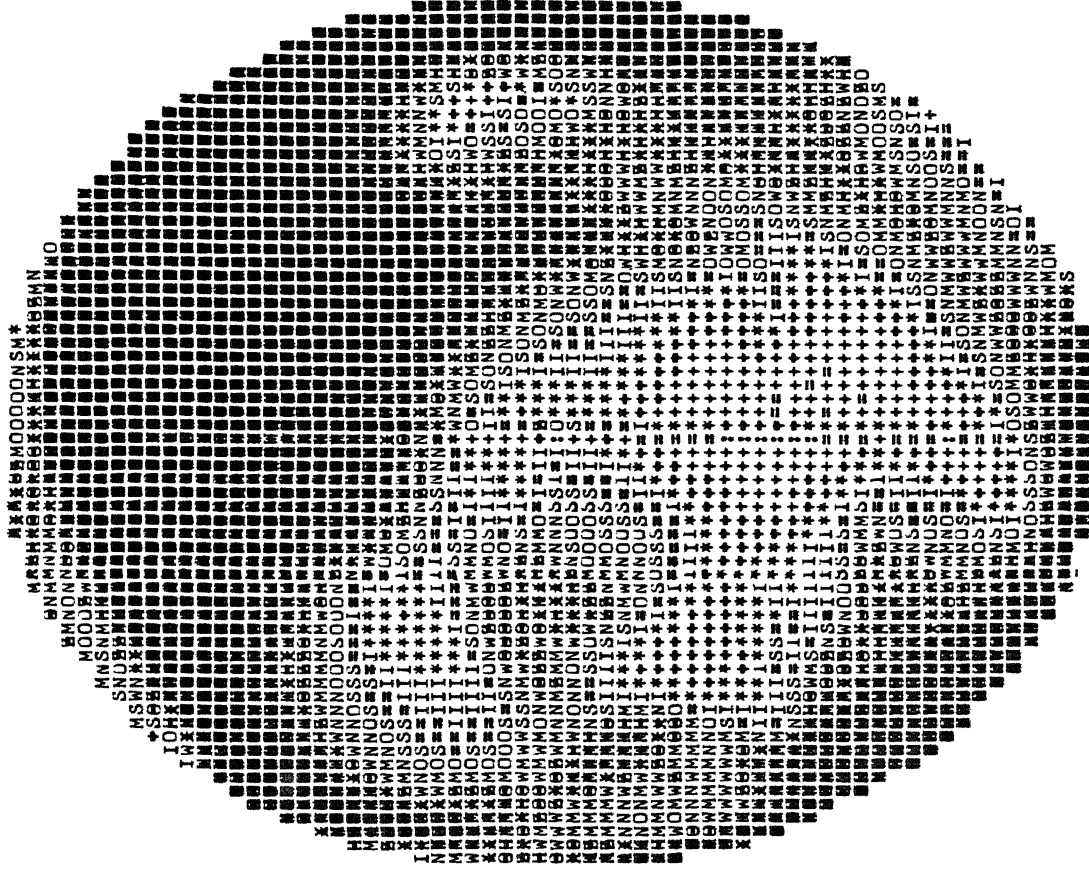
RKSFIL      INITIAL=CONSTANT      DATA=FACE OF A GIRL      ITERATION NUMBER= 10  NU. OF DETECTORS = 128  NRAY = 128

```

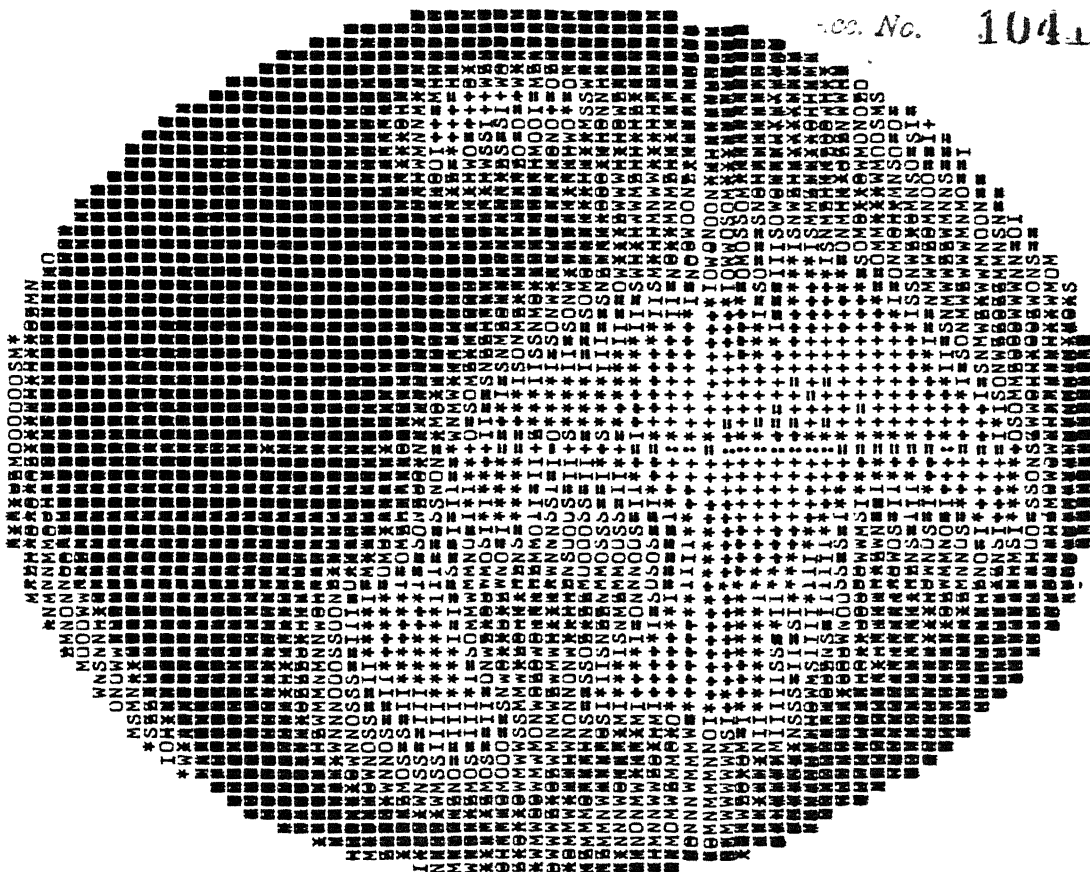




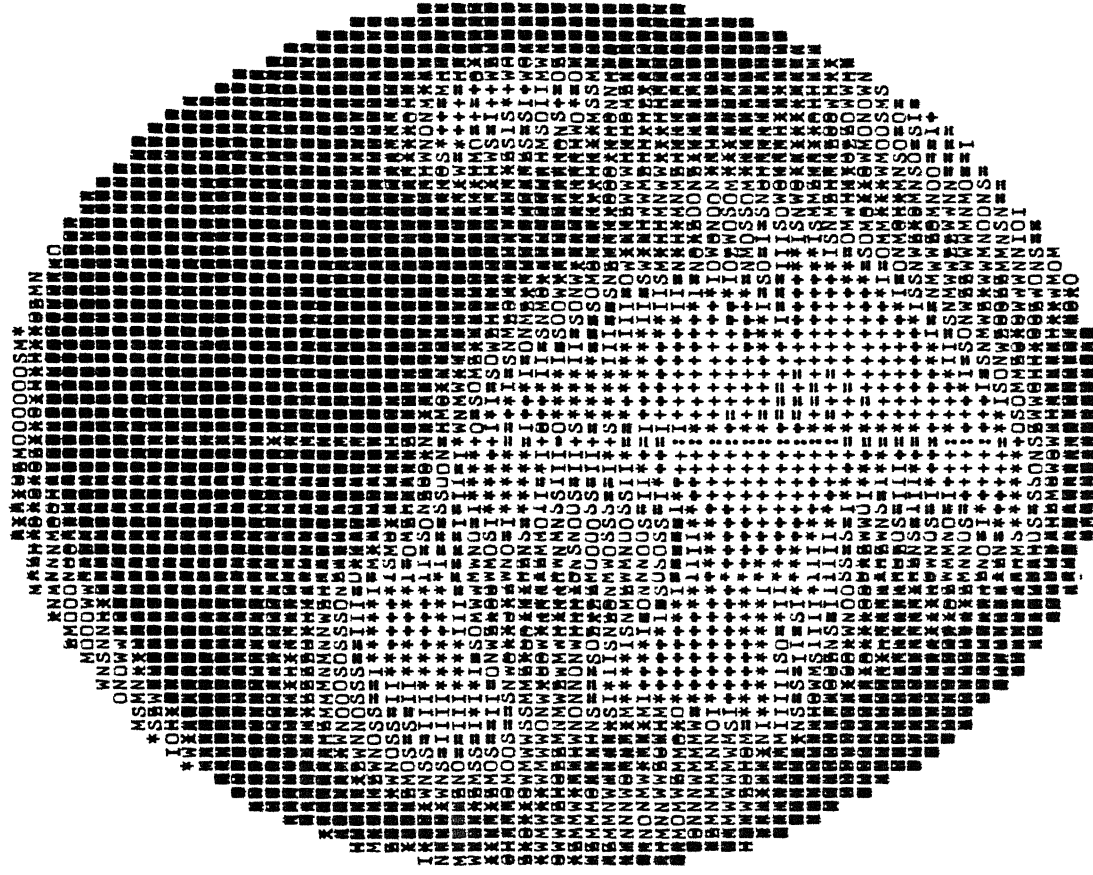




RKSFIL INITIAL=CONSTANT DATA=FACE OF A GIRL ITERATION NUMBER= 13 NO. OF DETECTORS = 128 NRAY = 128



Doc. No. 104460.



PKSFIL

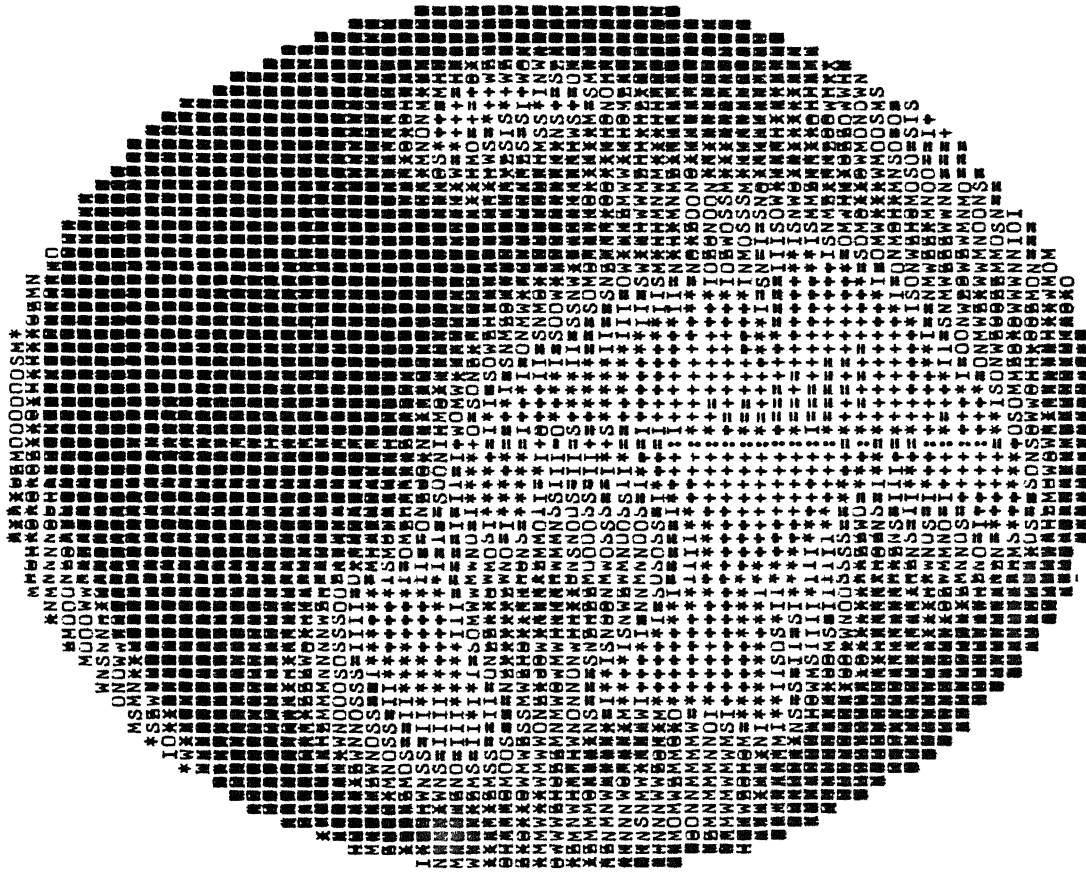
INITIAL=CONSTANT

DATA=FACE OF A GIRL

ITERATION NUMBER= 15

NU. OF DETECTORS = 128

NRAY = 128



RFSPID INITIAL=15-CONSTANT DATA=FACE OF A GIRL

ITERATION NUMBER= 1 NO. OF DETECTORS = 128 NRAY = 128



PIXEL CONSIDERED = 4096 ERMIN = -16 ERMAX = 11 ERSUM = 5671 ERSQSUM = 29377 ERL1 = 1-706590 ERL2 = 2.973299



123456/890123456/890123456/890123456.

RYFSFIL INITIAL=15CO,STANT DATA=FACE OF A GIRL

PJYCL CONSIDERED = 4096 ERMIN = -16 ERMAX =









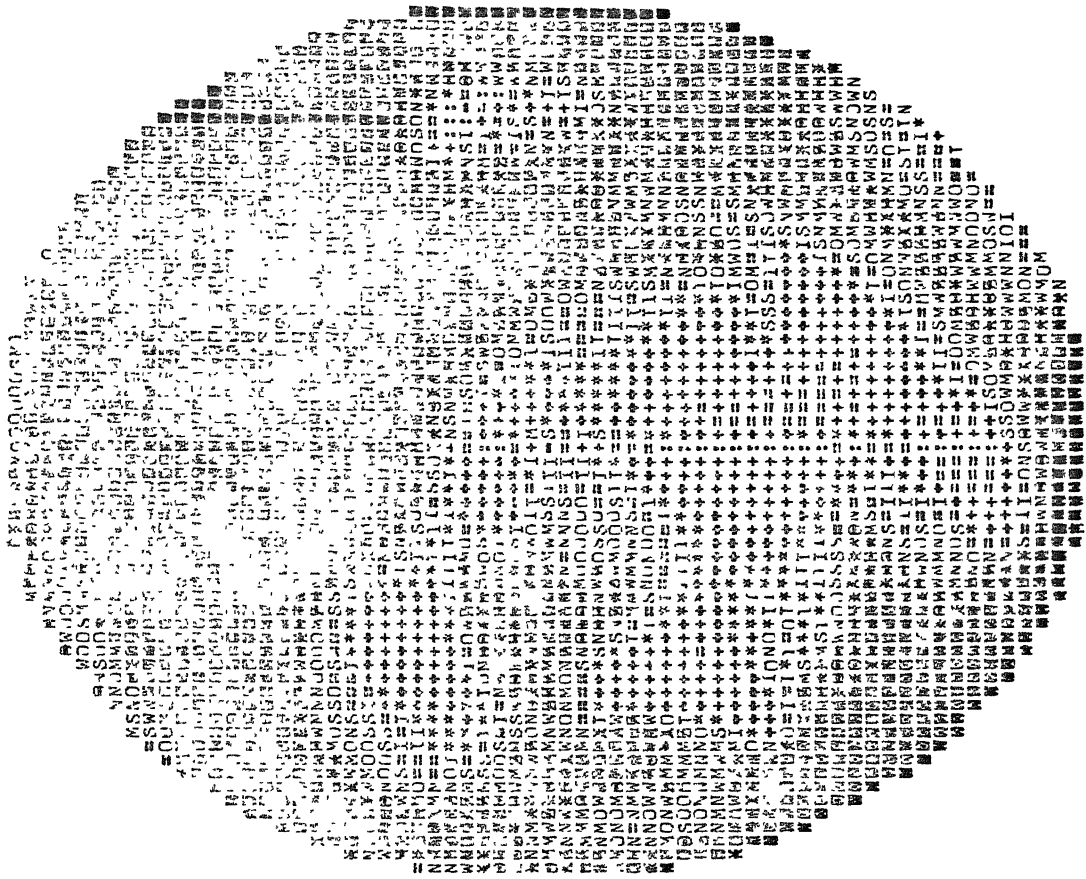
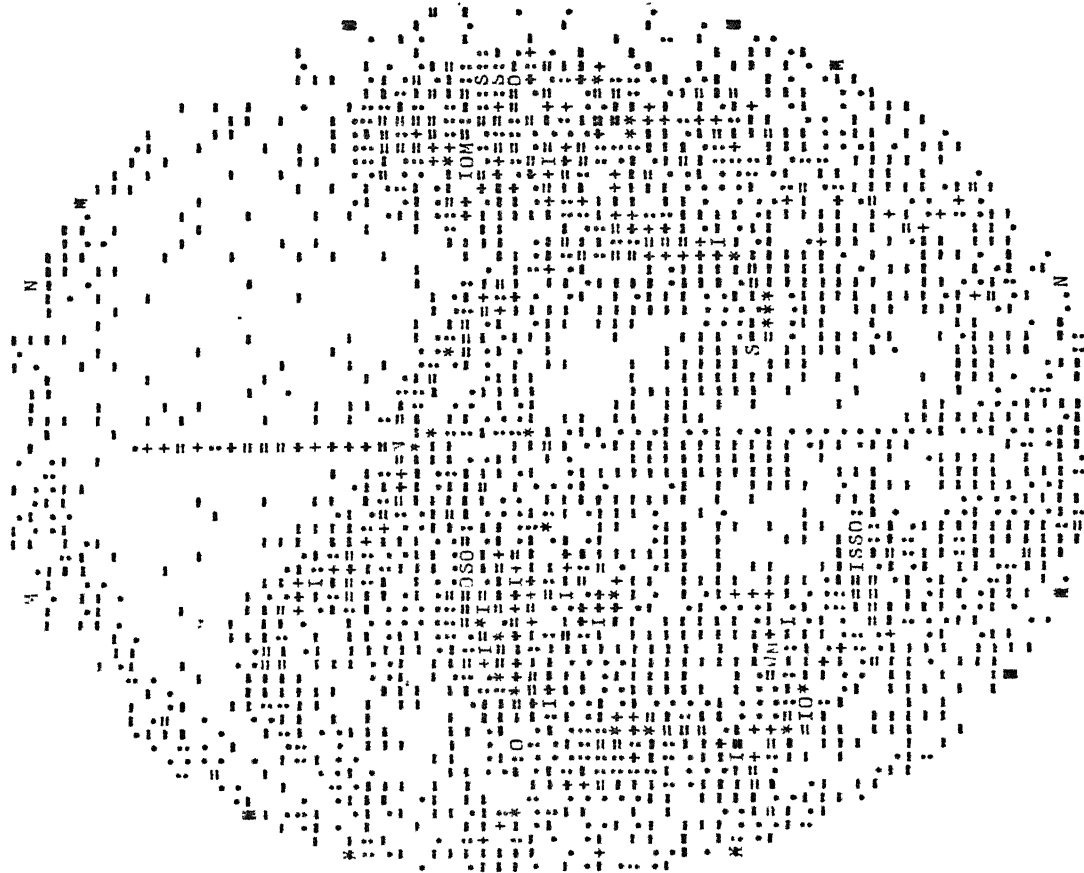
ITERATION NUMBER= 6 NU. OF DETECTORS = 128 NRAY = 128

[illegible]

PIXEL CONSIDERED = 4096 ERMIN = -15 ERHAX = 9 ERSUM = 4696 ERSQSUM = 21628 ERL1 = 1-413181 ERL2 = 2.551191

P&S FIL INITIAL=15 CONSTANT DATA=FACE OF A GIRL

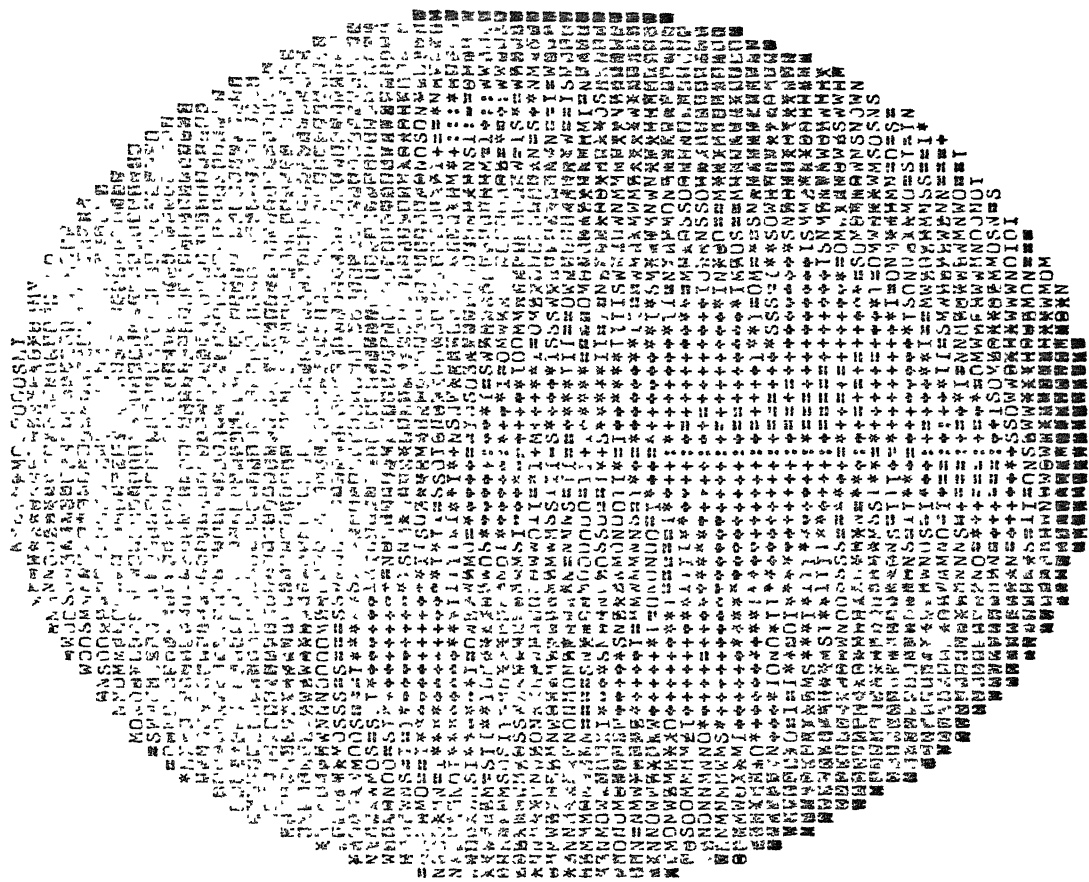
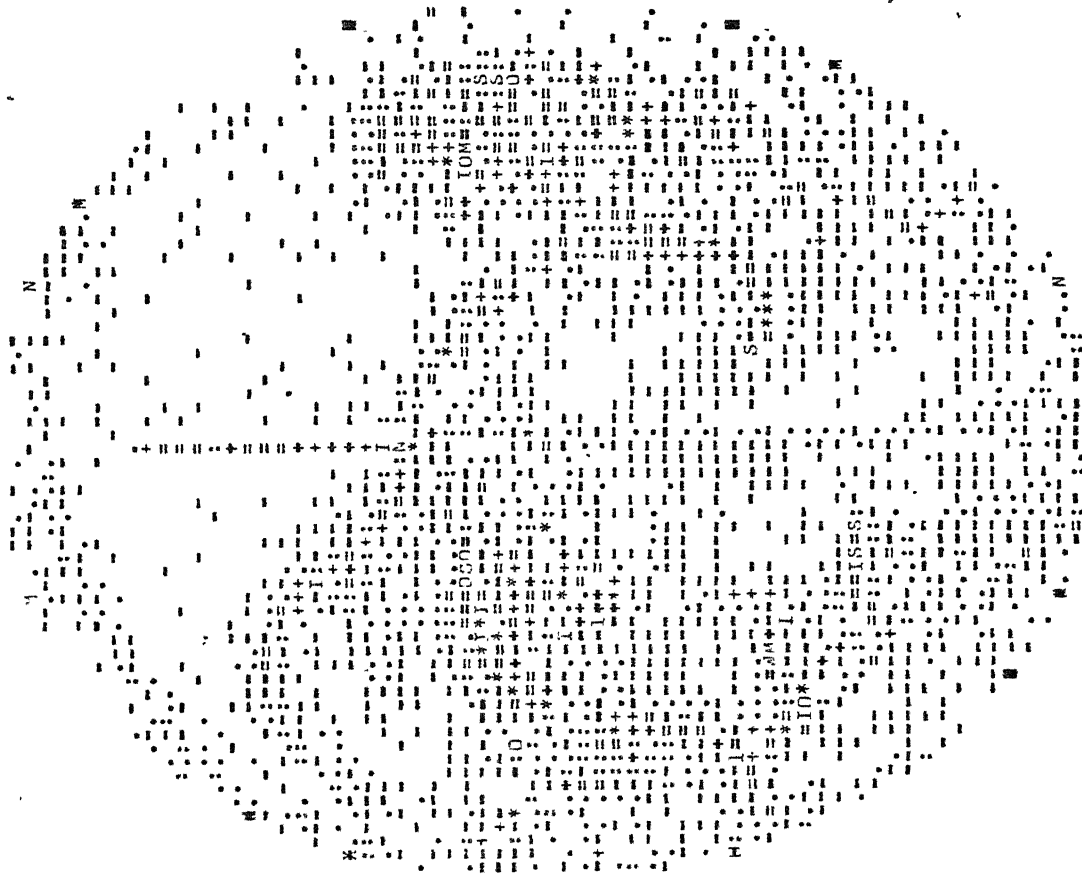
ITERATION NUMBER= 7 NO. OF DETECTORS = 128 NRAY = 128



PIXEL CONSIDERED = 4096 ERMIN = -15 ERMAX = 8 ERSUM = 4533 ERSQSUM = 20555 FRL1 = 1.364129 ERL2 = 2.487102

PFSFIL INITIAL=15CONSTANT DATA=FACE OF A GIRL

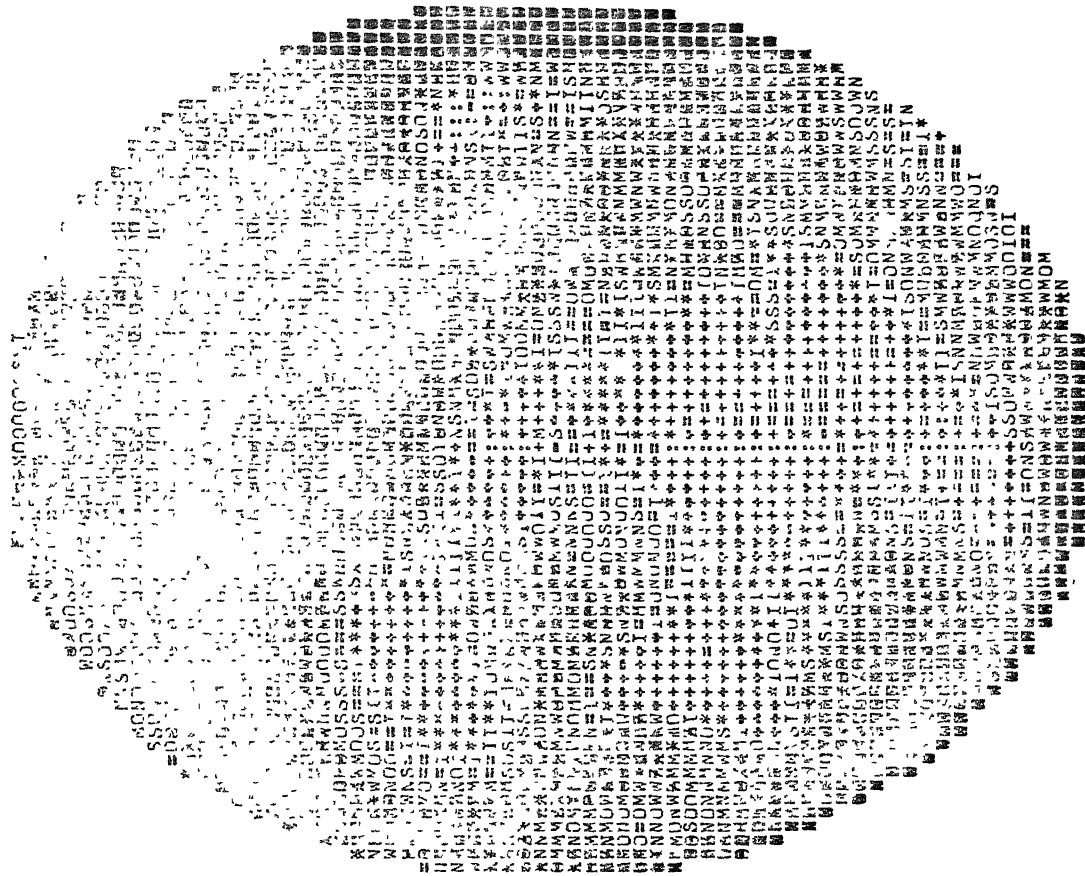
ITERATION NUMBER= 8 NO. OF DETECTORS = 128 NRAY = 128



PIXEL CONSIDERED = 4096 ERMIN = -15 EPVAX = 8 ERSUM = 4404 ERSOSUM = 19678 ERL1 = 1.325308 ERL2 = 2.433466

RKSFIL INITIALC=150CONSTANT DATA=FACE OF A GIRL

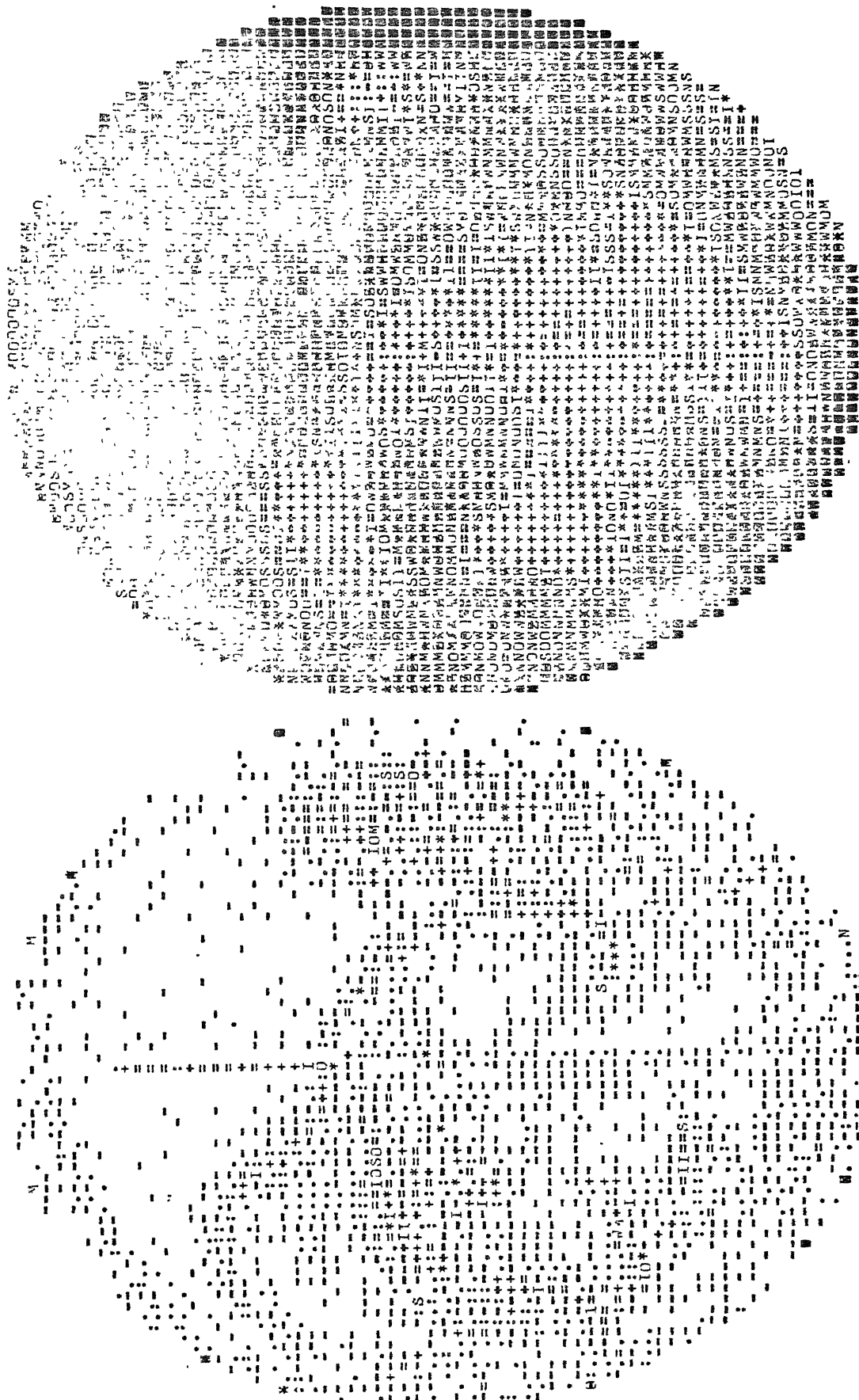
ITERATION NUMBER= 9 NO. OF DETECTORS = 128 NRAY = 128



PIXEL CONSIDERED = 4096 ERMIN = -15 ERMAX = 8 ERSUM = 4290 ERSQSUM = 18908 ERL1 = 1.291002 ERL2 = 2.365380

ITERATION NUMBER= 10 NO. OF DETECTORS = 128 NRAY = 128

RKSFIL INITIAL=15CONSTANT DATA=FACE OF A GIRL

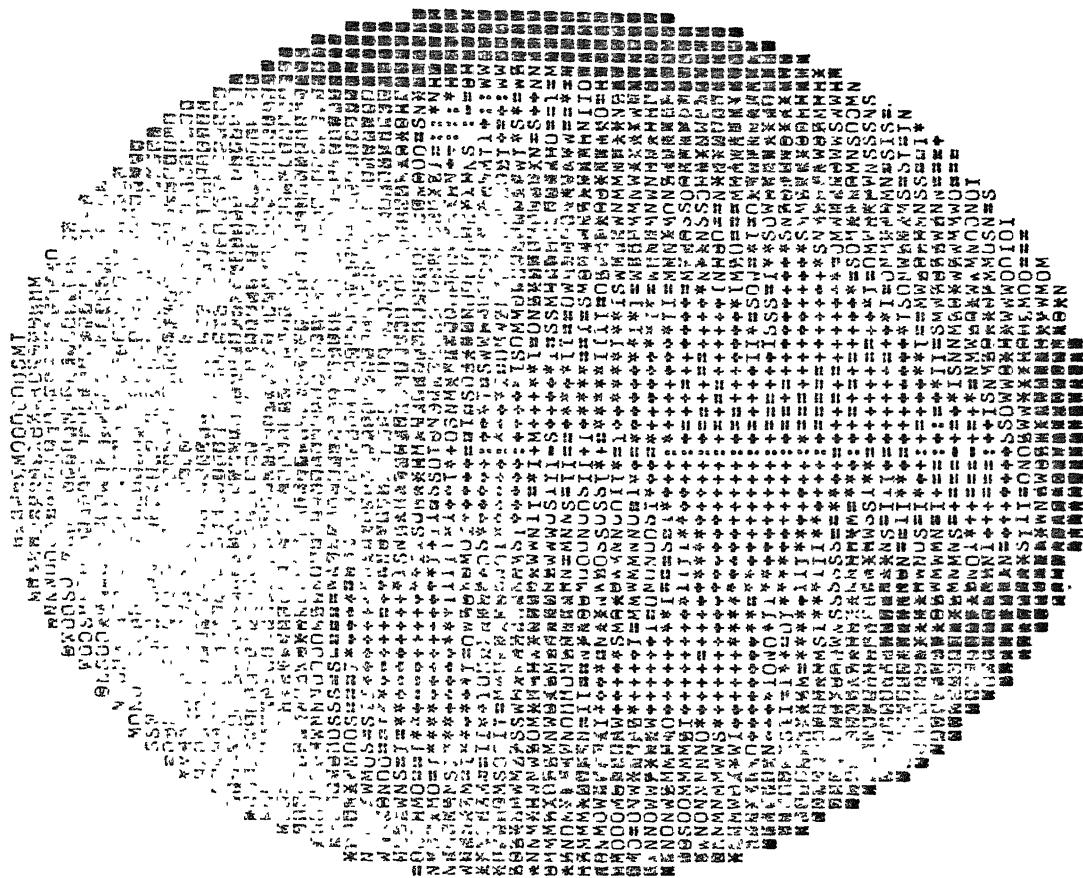


PIXEL CONSIDERED = 4096 ERMIN = -15 ERMAX = 8 ERSUM = 4180 ERSOSUM = 18146 ERL1 = 1.257899 ERL2 = 2.336820



RKSFIL INITIAU=15CONSTANT DATA=FACE OF A GIRL

ITERATION NUMBER= 11 NO. OF DETECTORS = 128 NRAY = 128

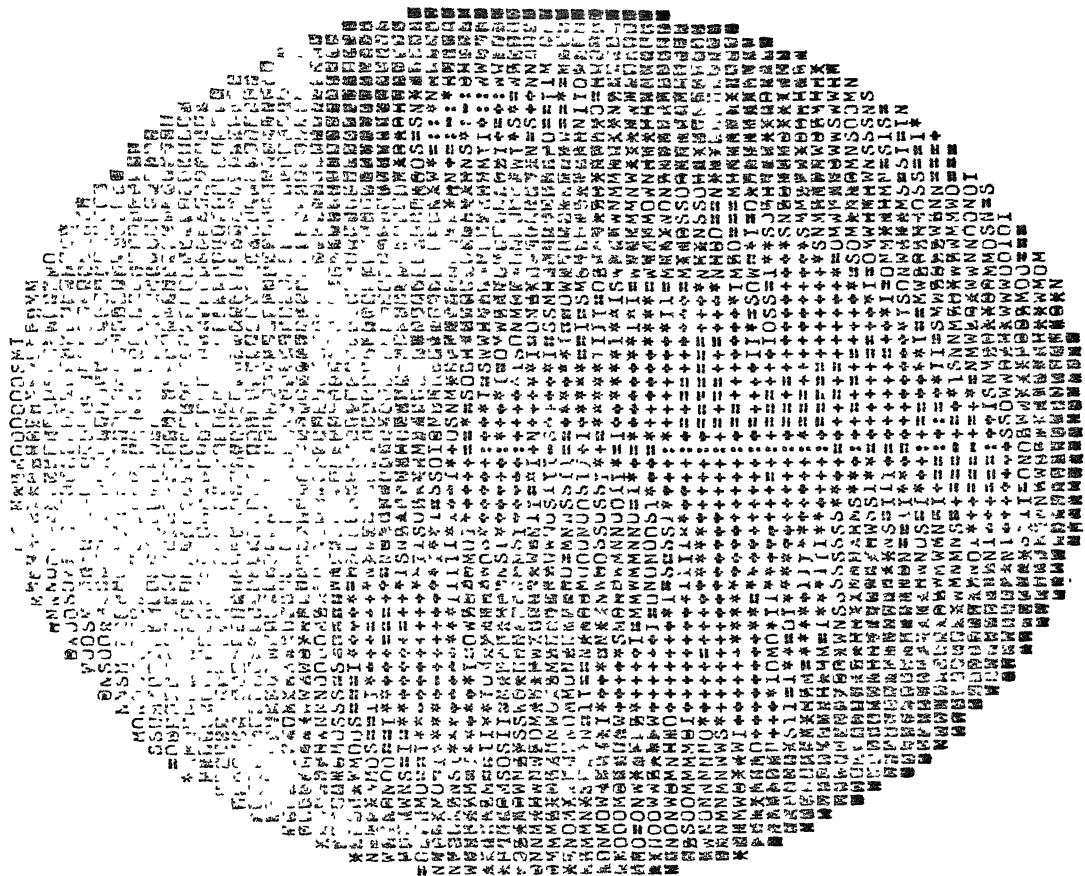
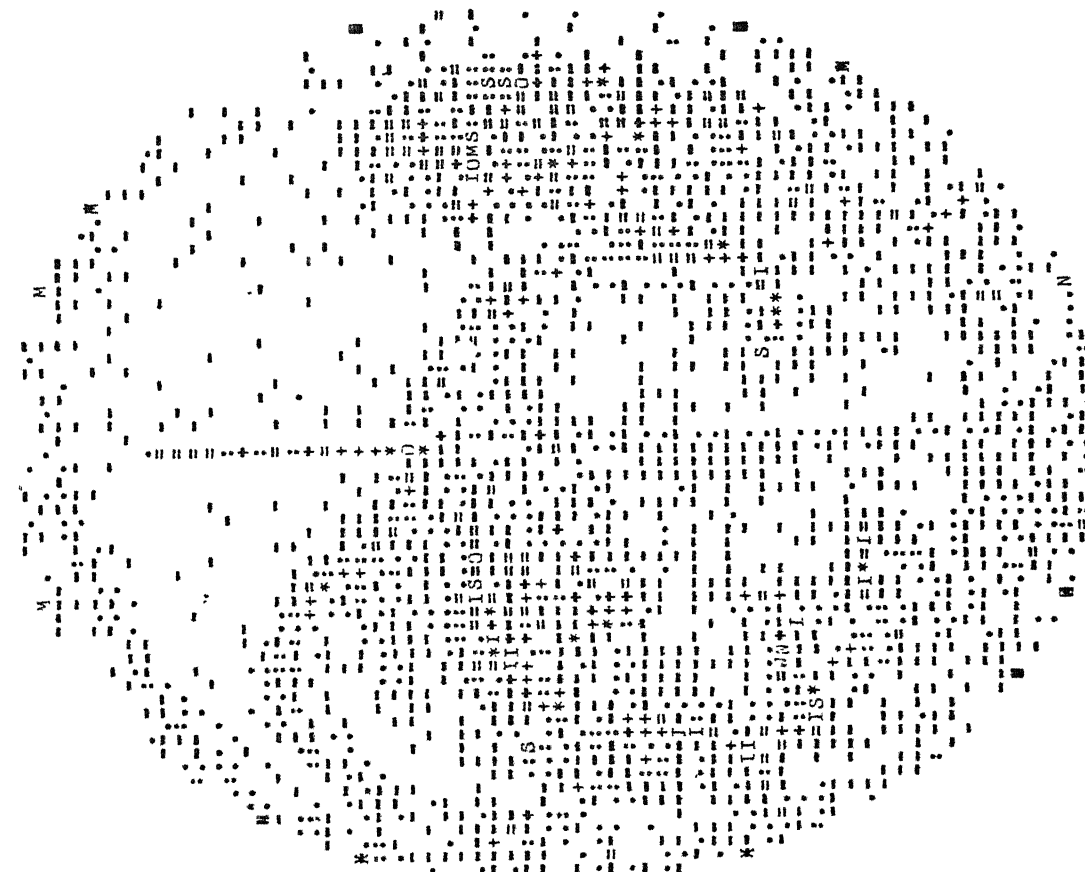


PIXEL CONSIDERED = 4096 ERMIN = -15 ERMAX = 8 ERSUM = 4084 ERSOSUM = 17526 ERL1 = 1.239010 ERL2 = 2.296552



RKSFIL INITIAL=15CONSTANT DATA=FACE OF A GIRL

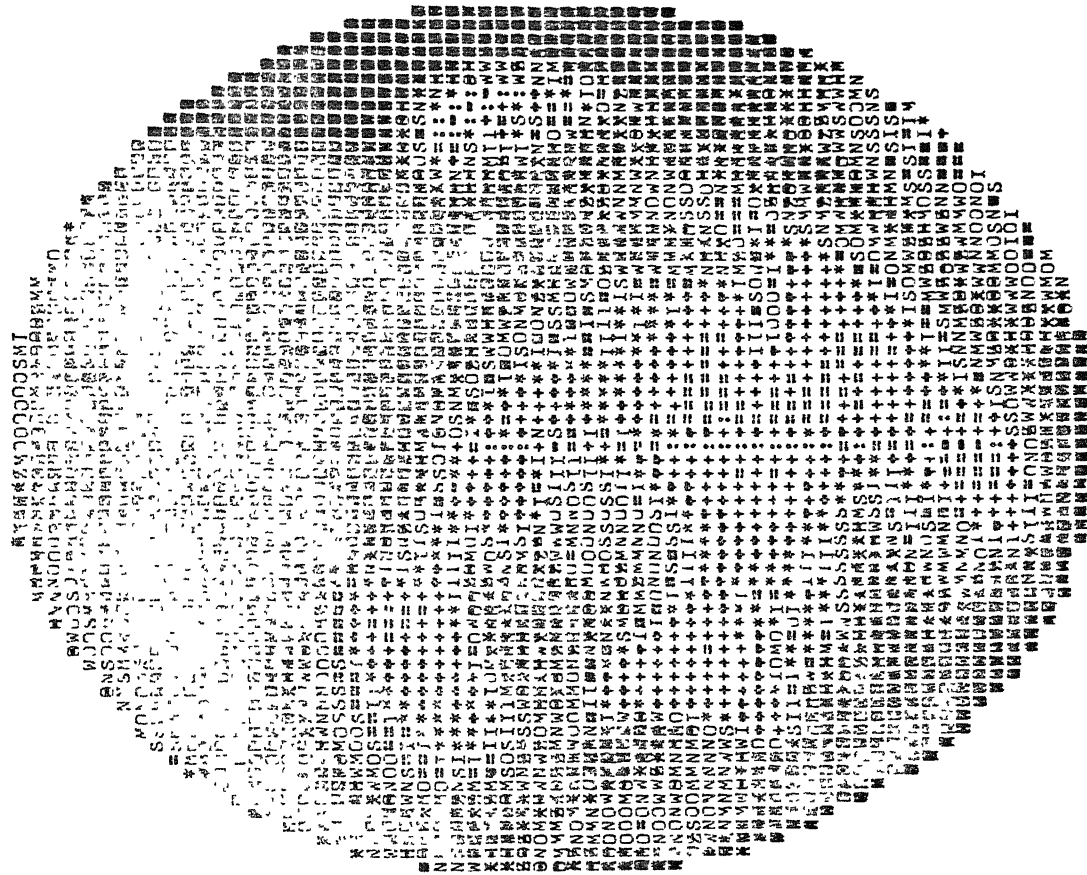
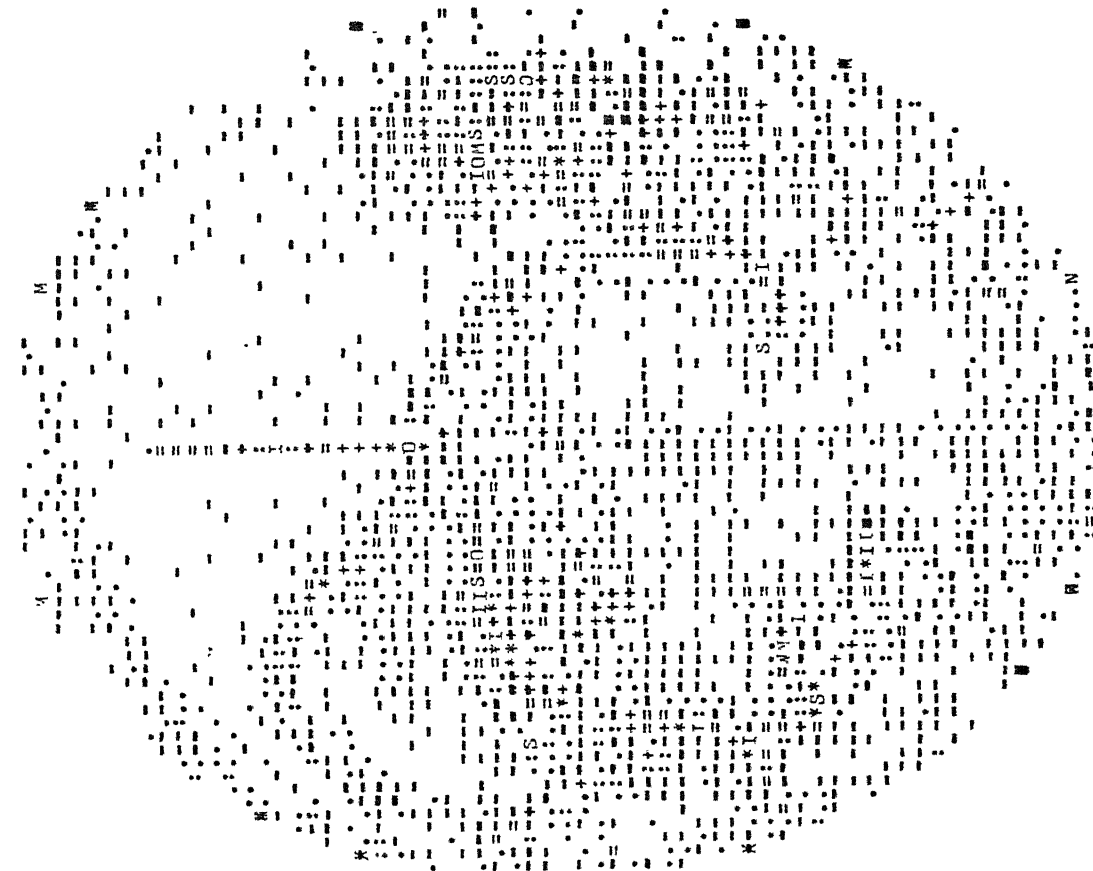
ITERATION NUMBER= 12 NO. OF DETECTORS = 128 NRAY = 128



PIXEL CONSIDERED = 4096 ERMIN = -15 ERMAX = 8 ERSUM = 3991 ERSQSUM = 16843 EXL1 = 1.201023 EXL2 = 2.251358

RKSFIL INITIAL=1500 INSTANT DATA=PAGE OF A GIRL

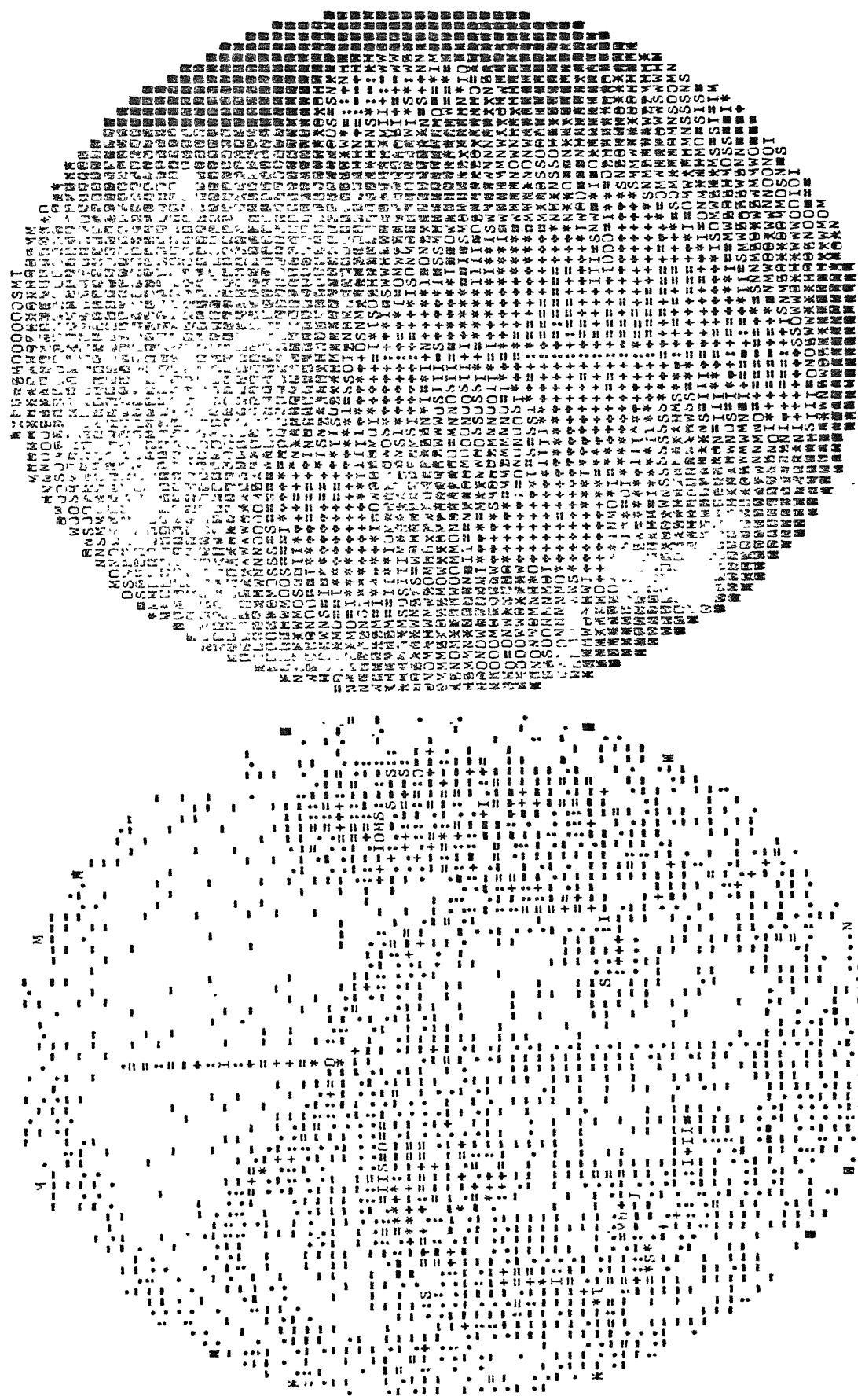
ITERATION NUMBER= 13 NO. OF DETECTORS = 128 NRAY = 128



PLACL CONSIDERED = 4096 ERMIN = -15 ERMAX = 7 ERSUM = 3894 ERSOSUM = 16188 ERL1 = 1.171833 ERL2 = 2.207148

RKSFIL INITIAL=15CONSTANT DATA=FACE OF A GIRL

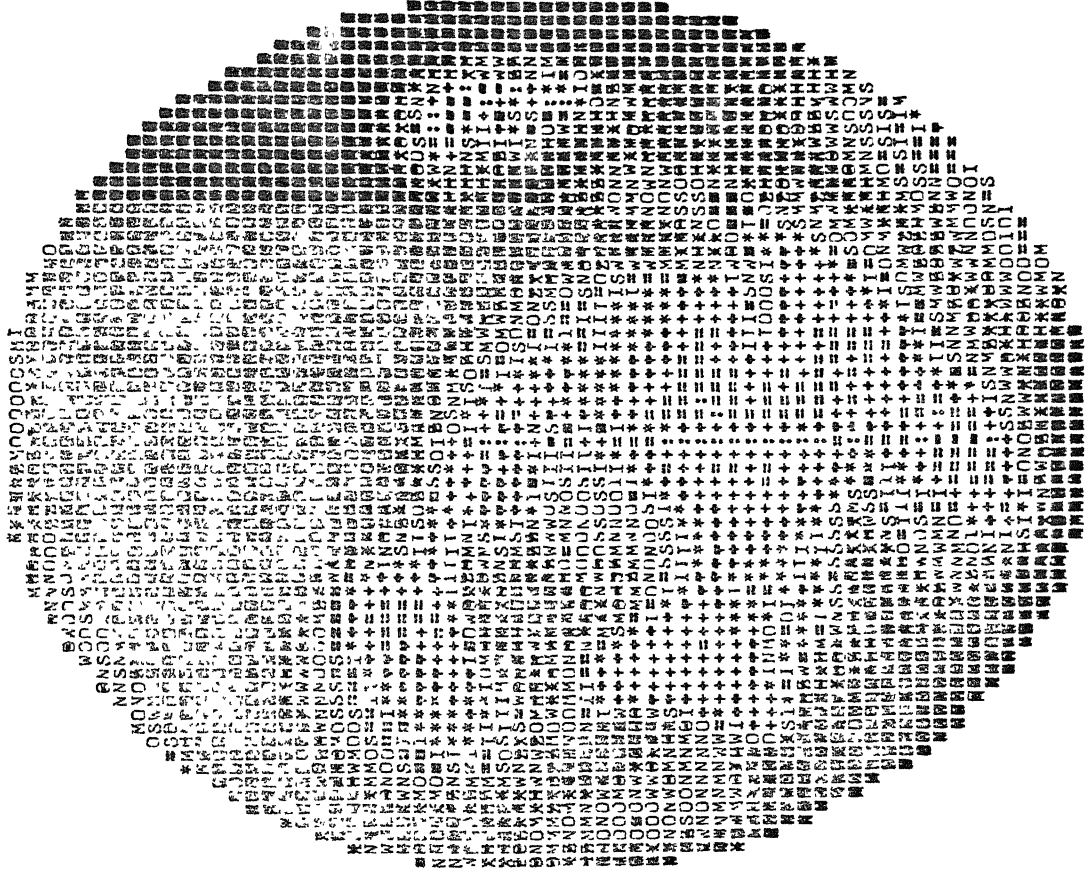
ITERATION NUMBER= 14 NO. OF DETECTORS = 128 NRAY = 128



PIXEL CONSIDERED = 4096 ERMIN = -14 ERMAX = 7 ERSUM = 3807 ERSQSUM = 15645 ERL1 = 1.145652 ERL2 = 2.169815

RKSFIL INITIAL=15CONSTANT DATA=FACE OF A GIRL

ITERATION NUMBER= 15 NO. OF DETECTORS = 128 NRAY = 128



PIXEL CONSIDERED = 4096 ERMIN = -14 ERMAX = 7 EPSUM = 3725 ERSQSUM = 15075 ERL1 = 1-120975 ERL2 = 2.129921

RKSFTL

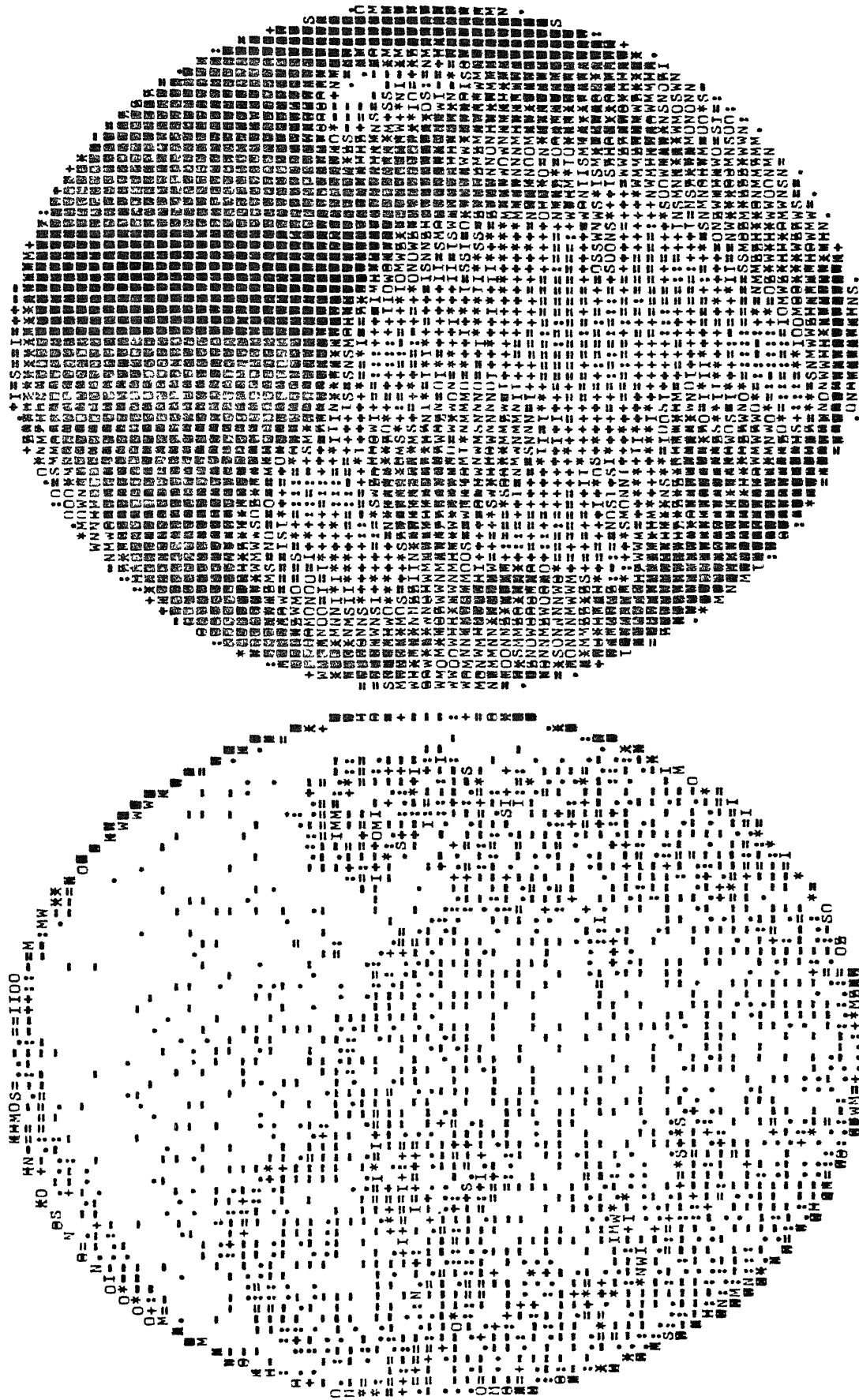
INITIAL=PETCAT

DATA=FACE OF A GIRL

ITERATION NUMBER= 1

NO. OF DETECTORS = 128

NRAY = 128



RKSFIL

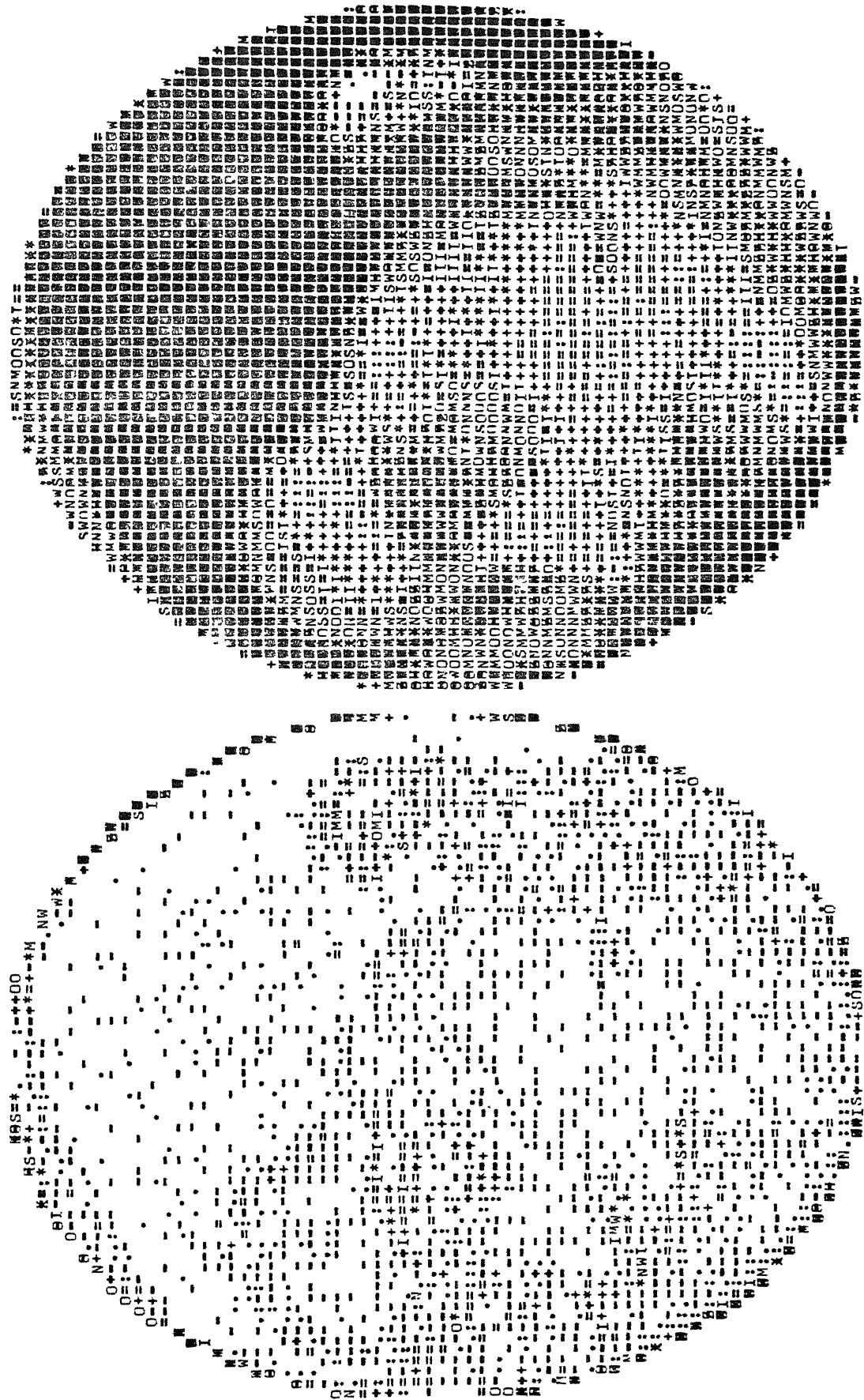
INITIAL=PETCAT

DATA=FACE OF A GIRL

ITERATION NUMBR= 2

NO. OF DETECTORS = 128

NRAY = 128





PKSFIL

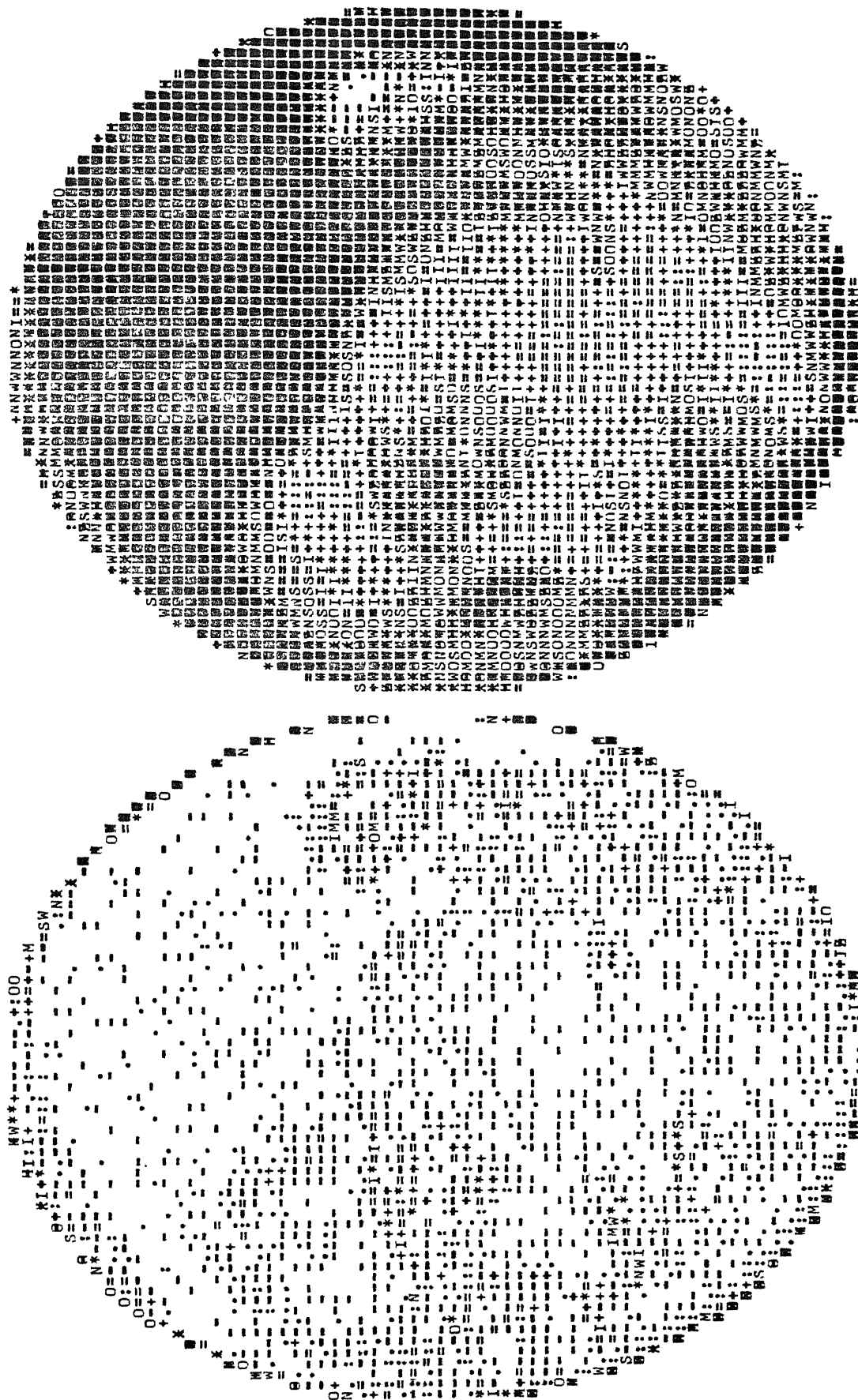
INITIAL=PEICAT

DATA=FACE OF A GIRL

ITERATION NUMBER= 3

NO. OF DETECTORS = 128

NRAY = 128



PKSFIL

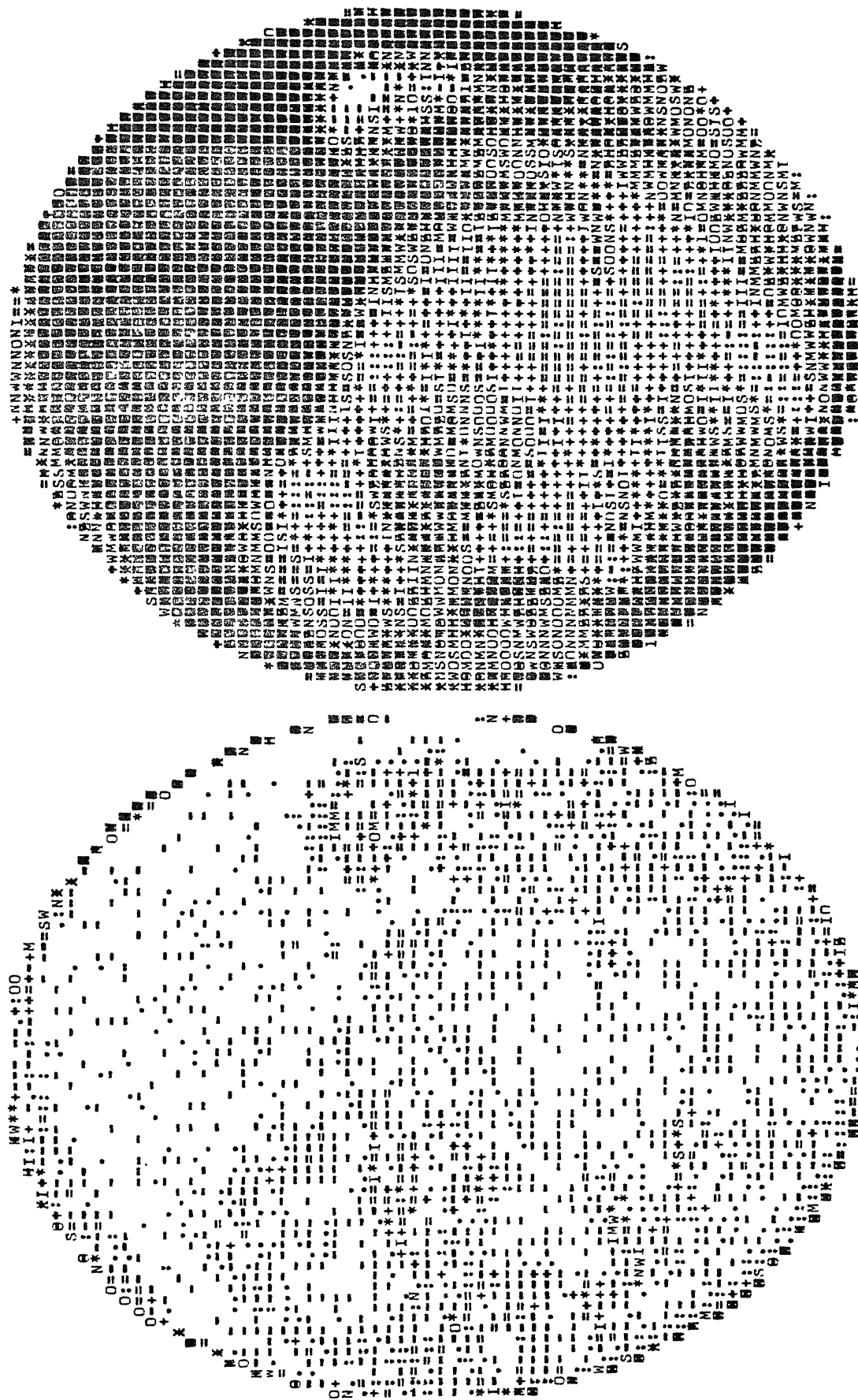
INITIALC=PEICAT

DATA=FACE OF A GIRL

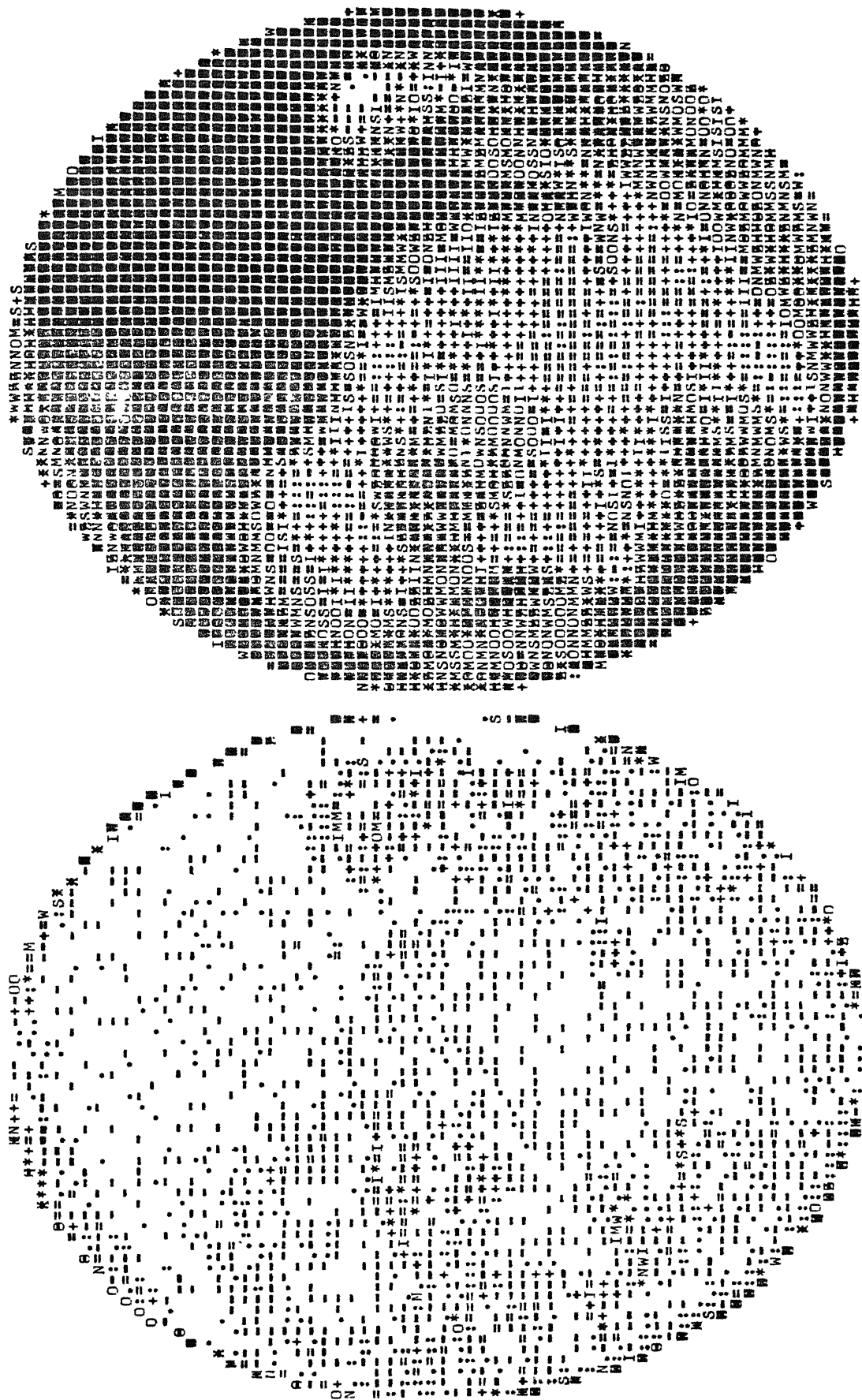
ITERATION NUMBER= 3

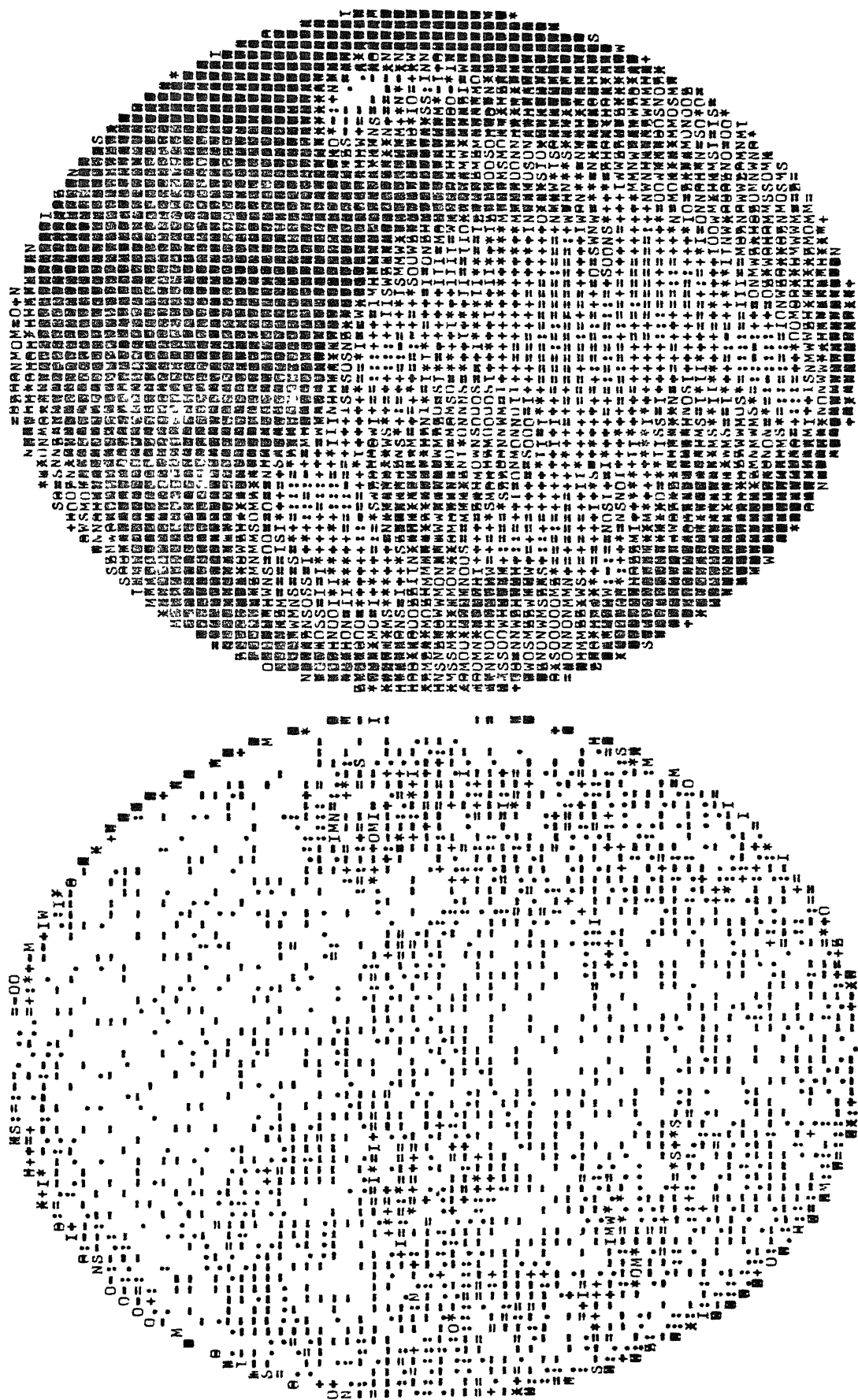
NO. OF DETECTORS = 128

NRAY = 128









RKSFIL

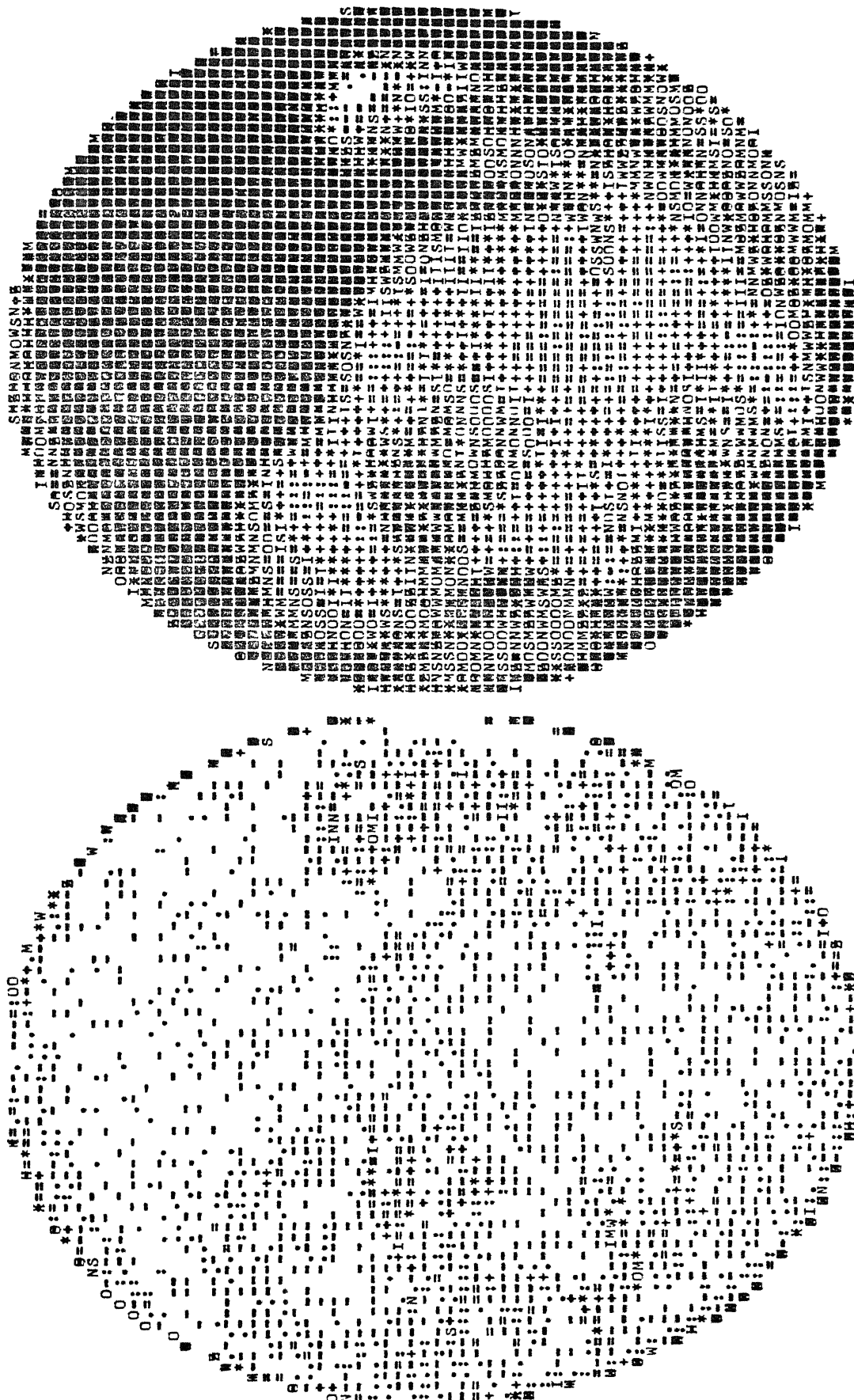
INITIAL=PETCAT

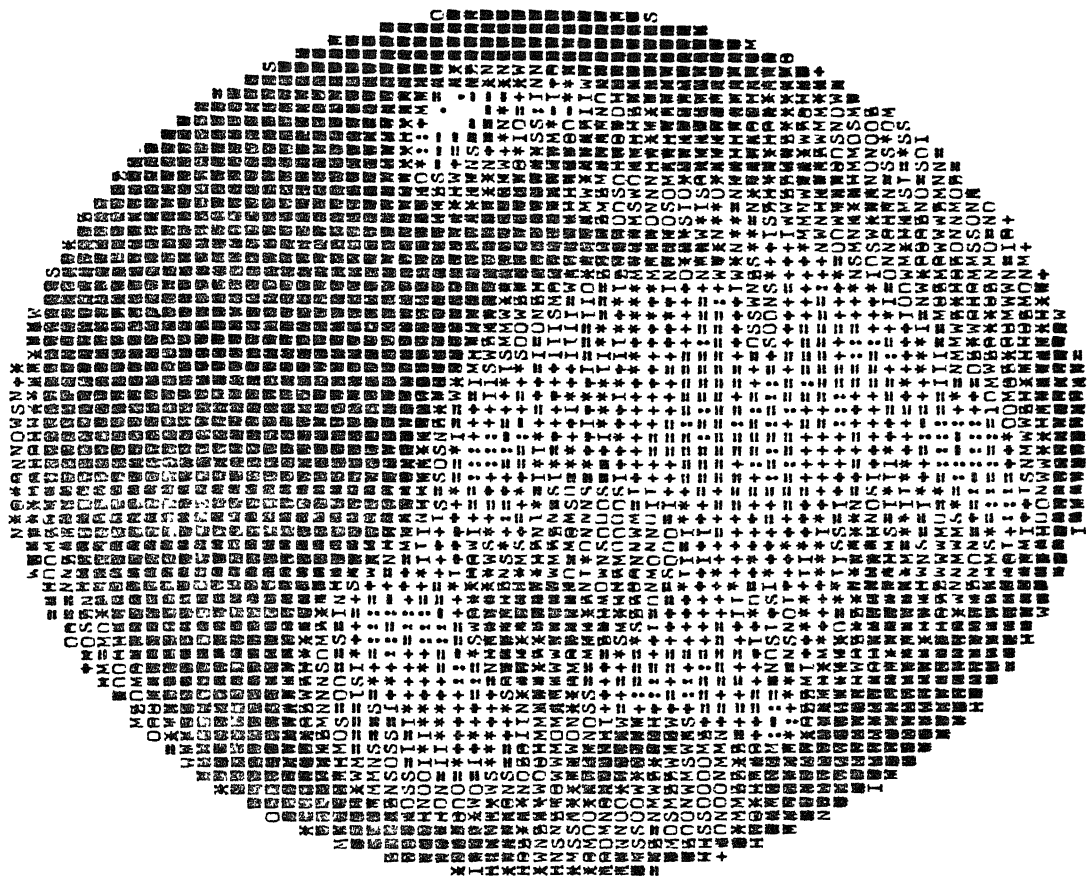
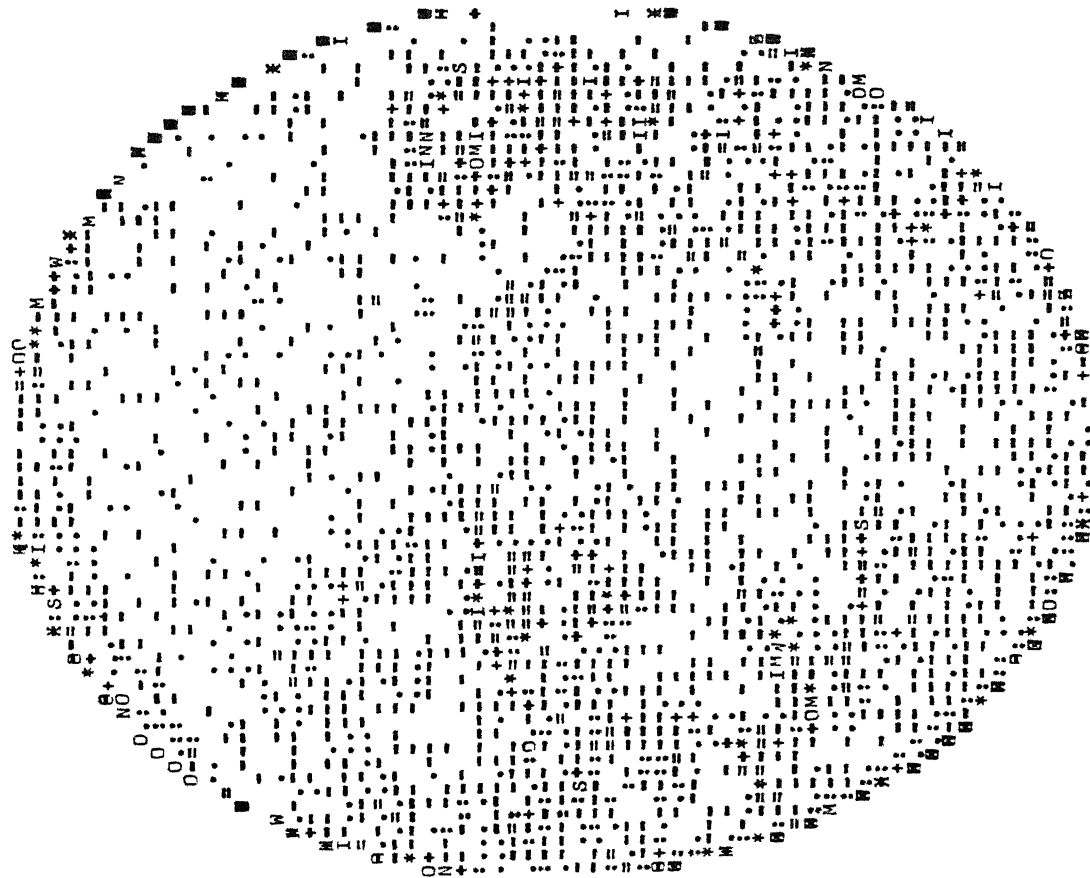
DATA=FACE OF A GIRL

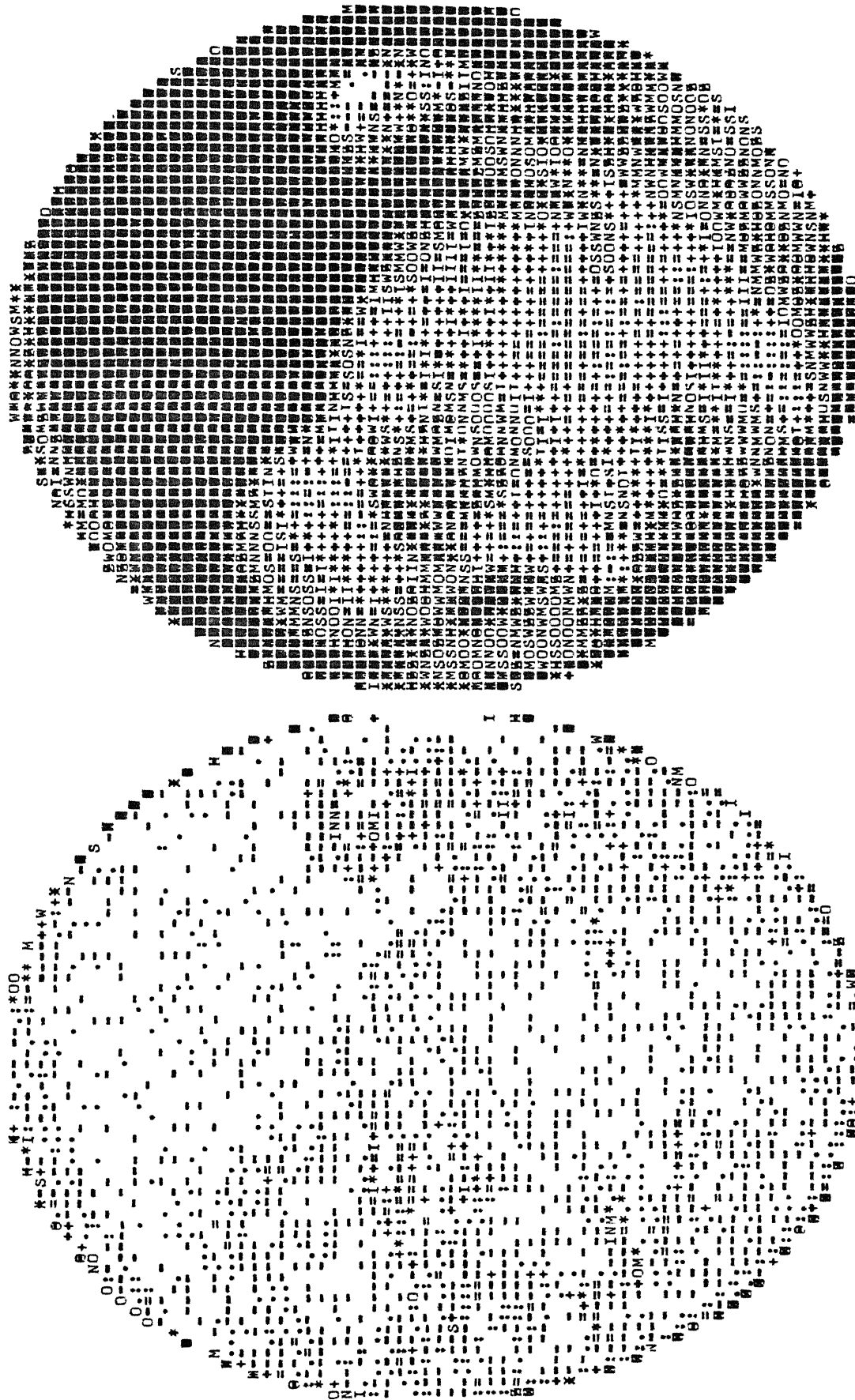
ITERATION NUMBER= 6

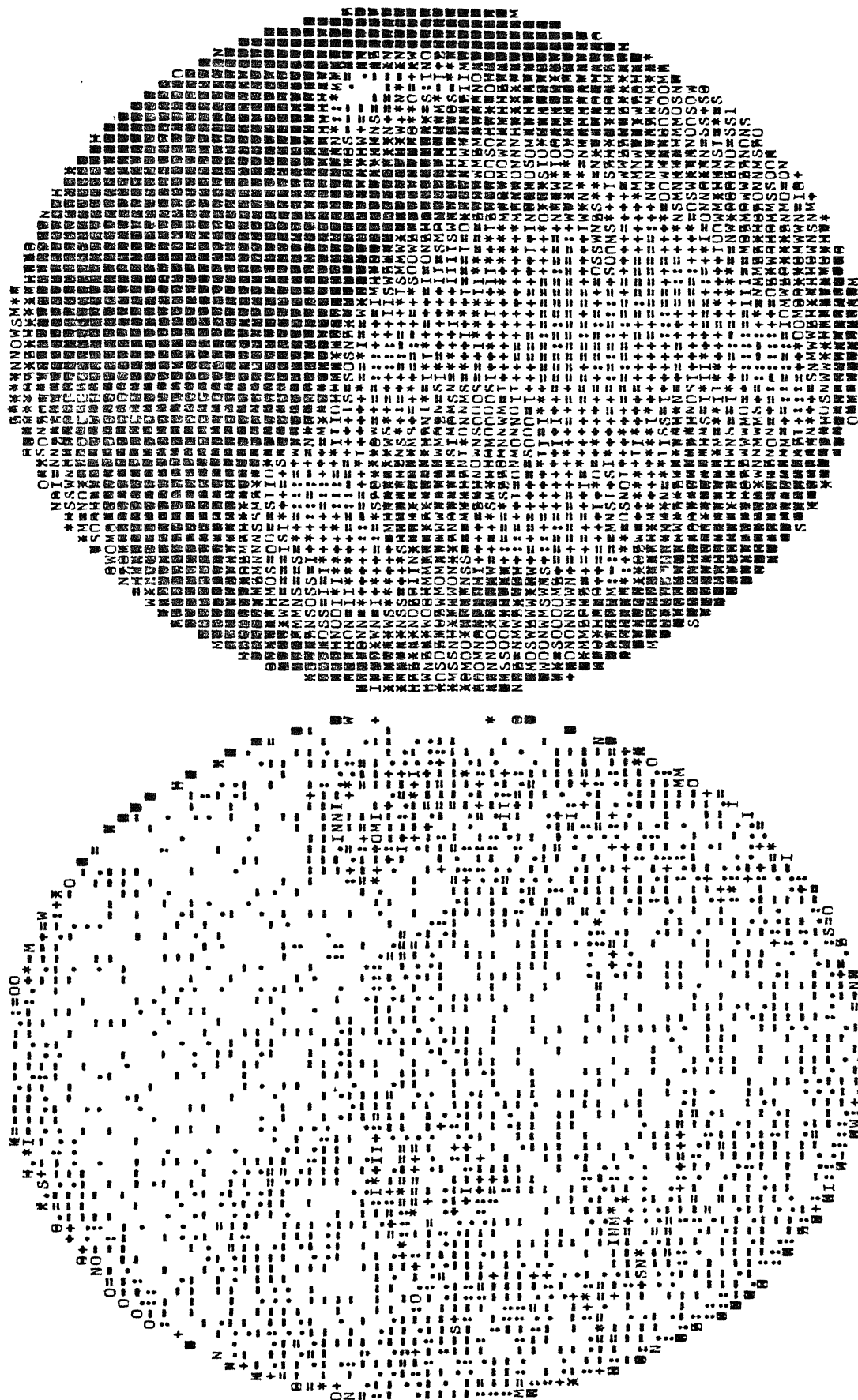
NO. OF DETECTORS = 128

NRAY = 128





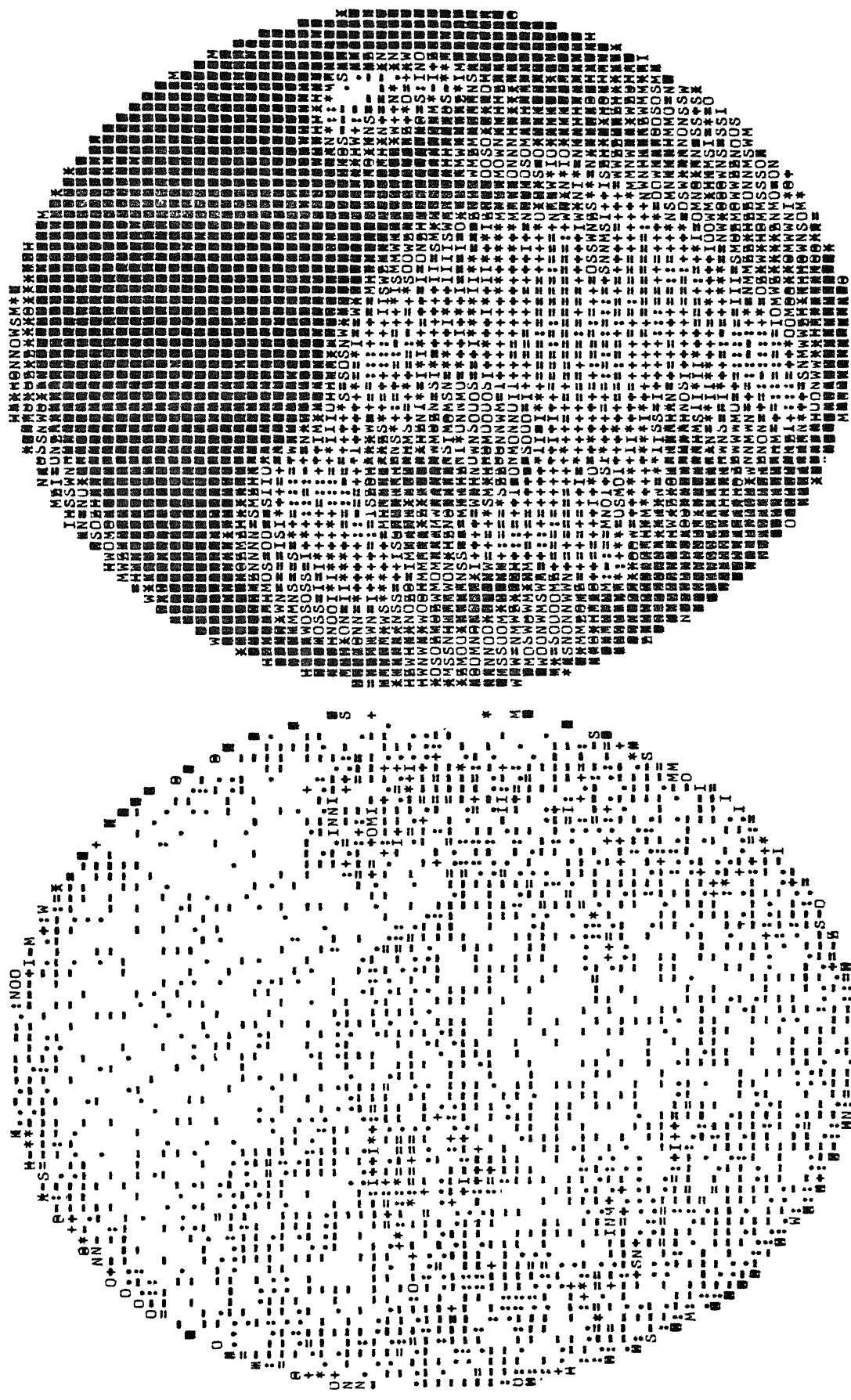






```
ITERATION NUMBER= 10 NO. OF DETECTORS = 128 NRAY = 128
```

```
PIXEL CONSIDERED = 4096 ERMIN = -14 ERMAX = 9 ERSUM = 3303 ERSQSUM = 12729 FRL1 = 0.993981 ERL2 = 1.957185
```



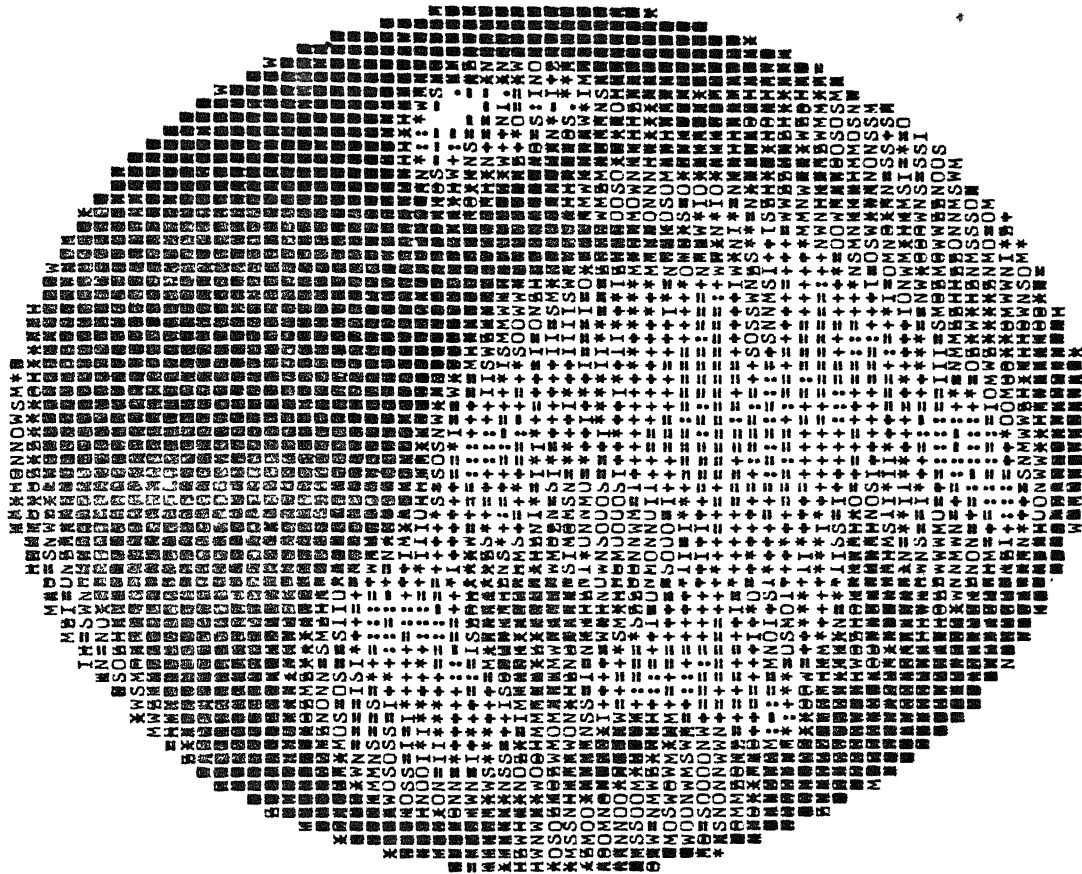
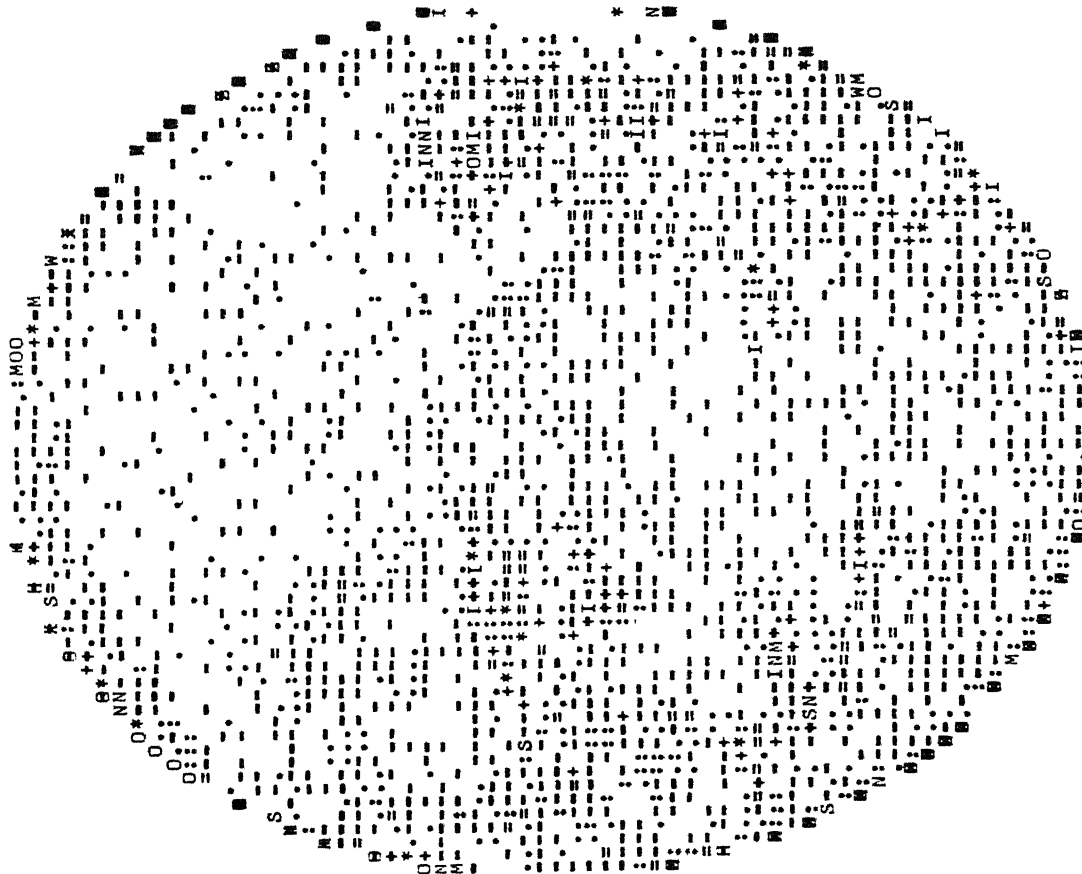


RKSFIL

INITIAL=PETCAT

DATA=FACE OF A GIRL

ITERATION NUMBER= 12 NO. OF DETECTORS = 128 NRAY = 128

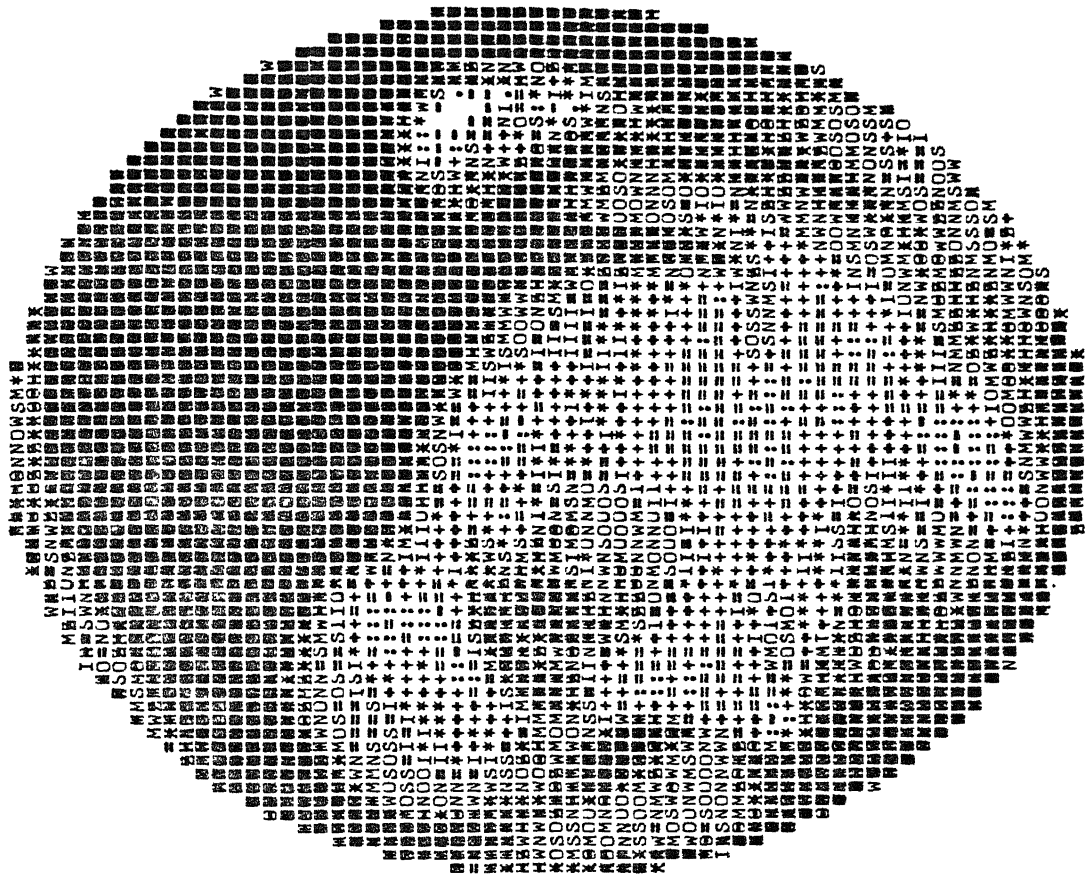
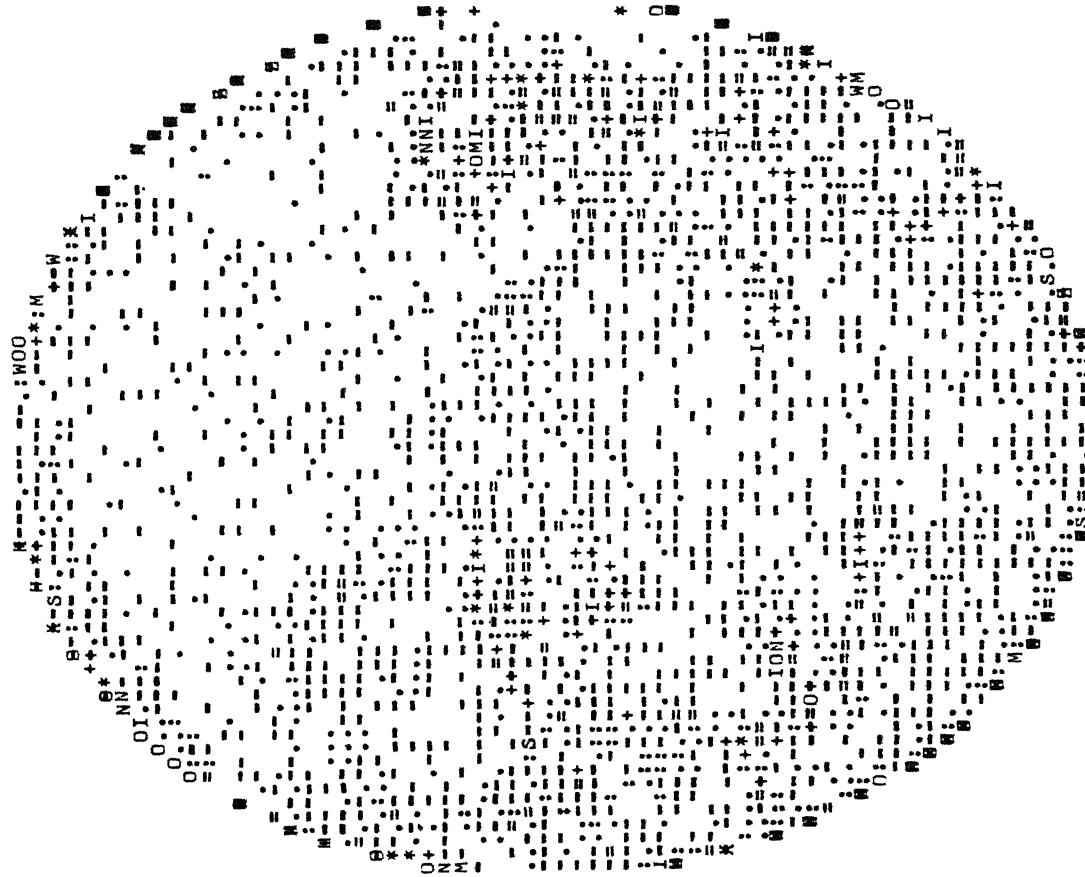


PIXEL CONSIDERED = 4096 ERMIN = -14 ERMAX = 9 ERSUM = 3220 ERSQSUM = 12126 ERL1 = 0.969004 ERL2 = 1.910265

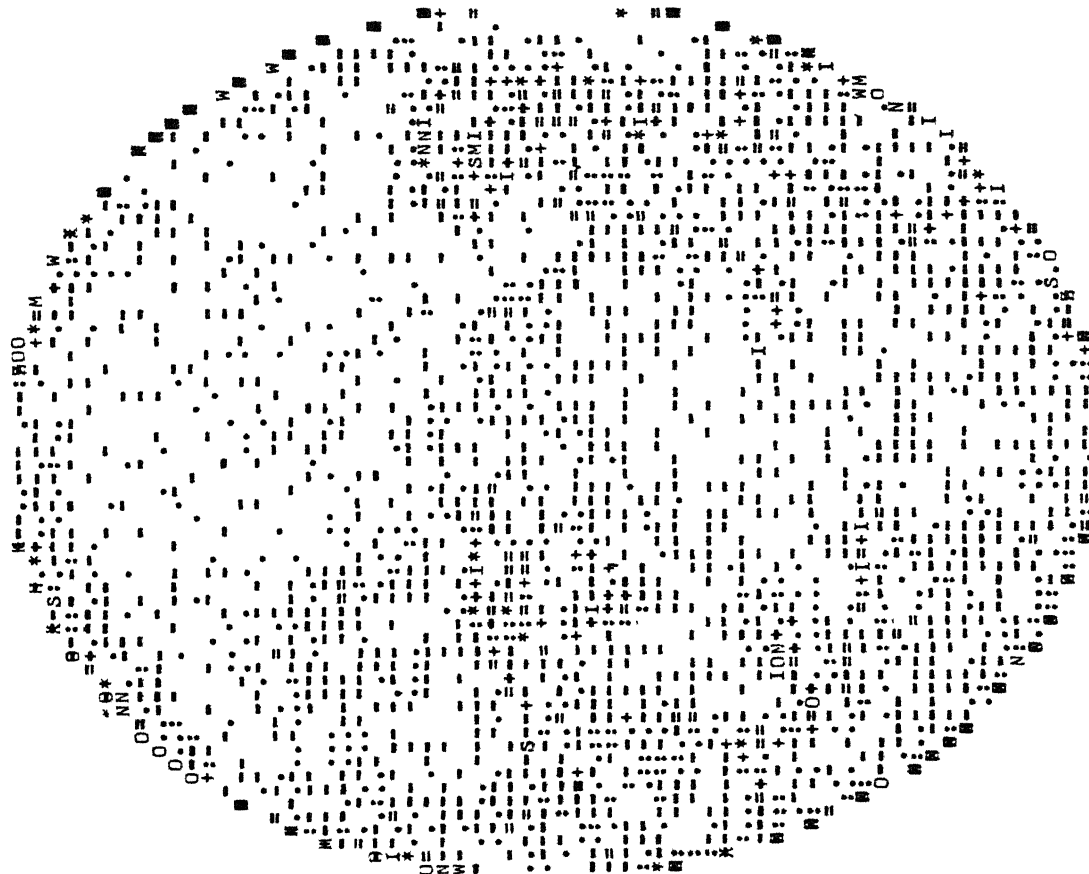
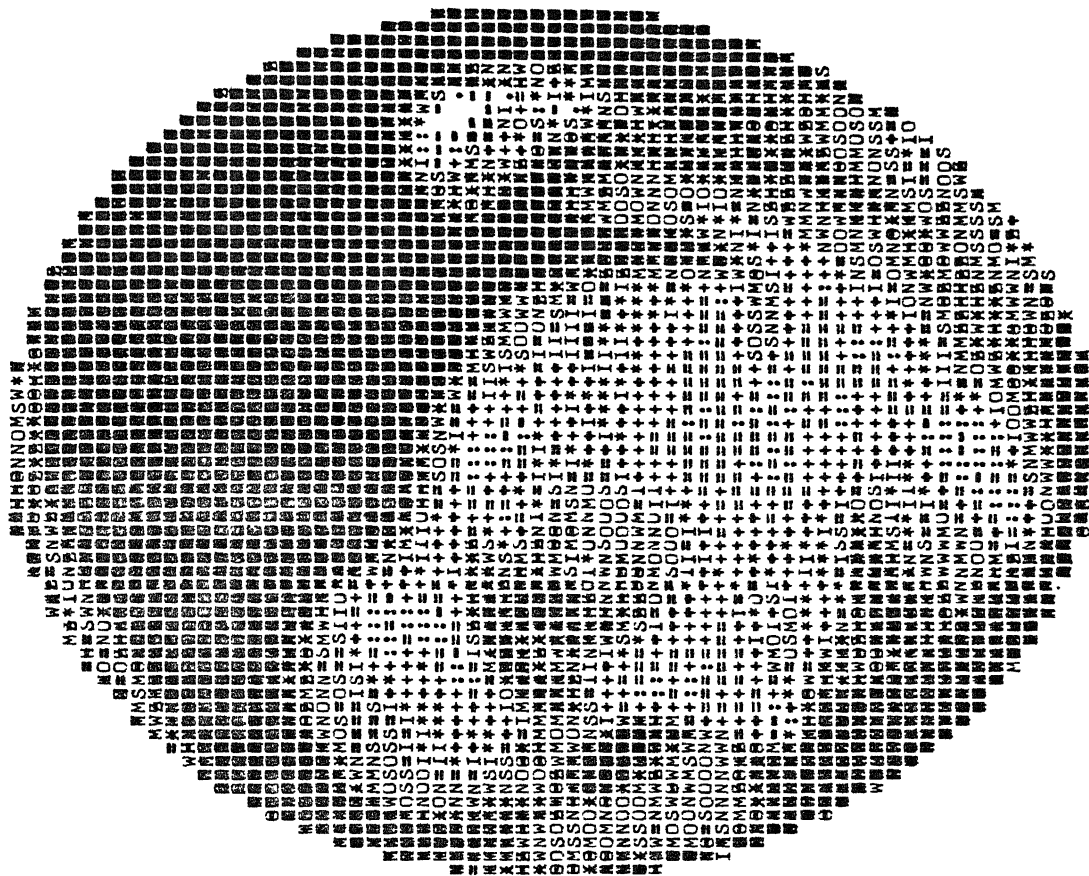
```

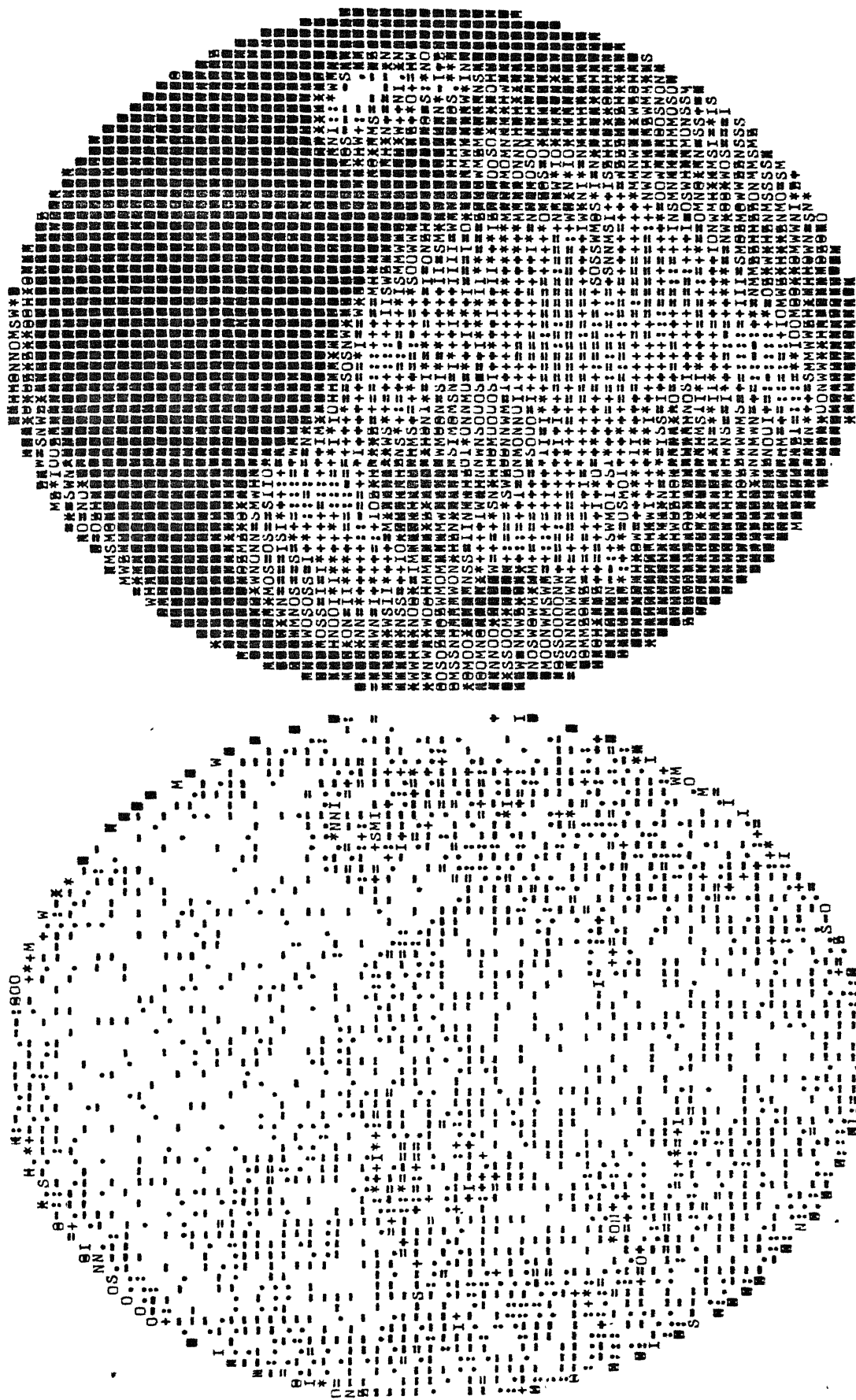
ITERATION NUMBER= 13  NO. OF DETECTORS = 128  NRAY = 128

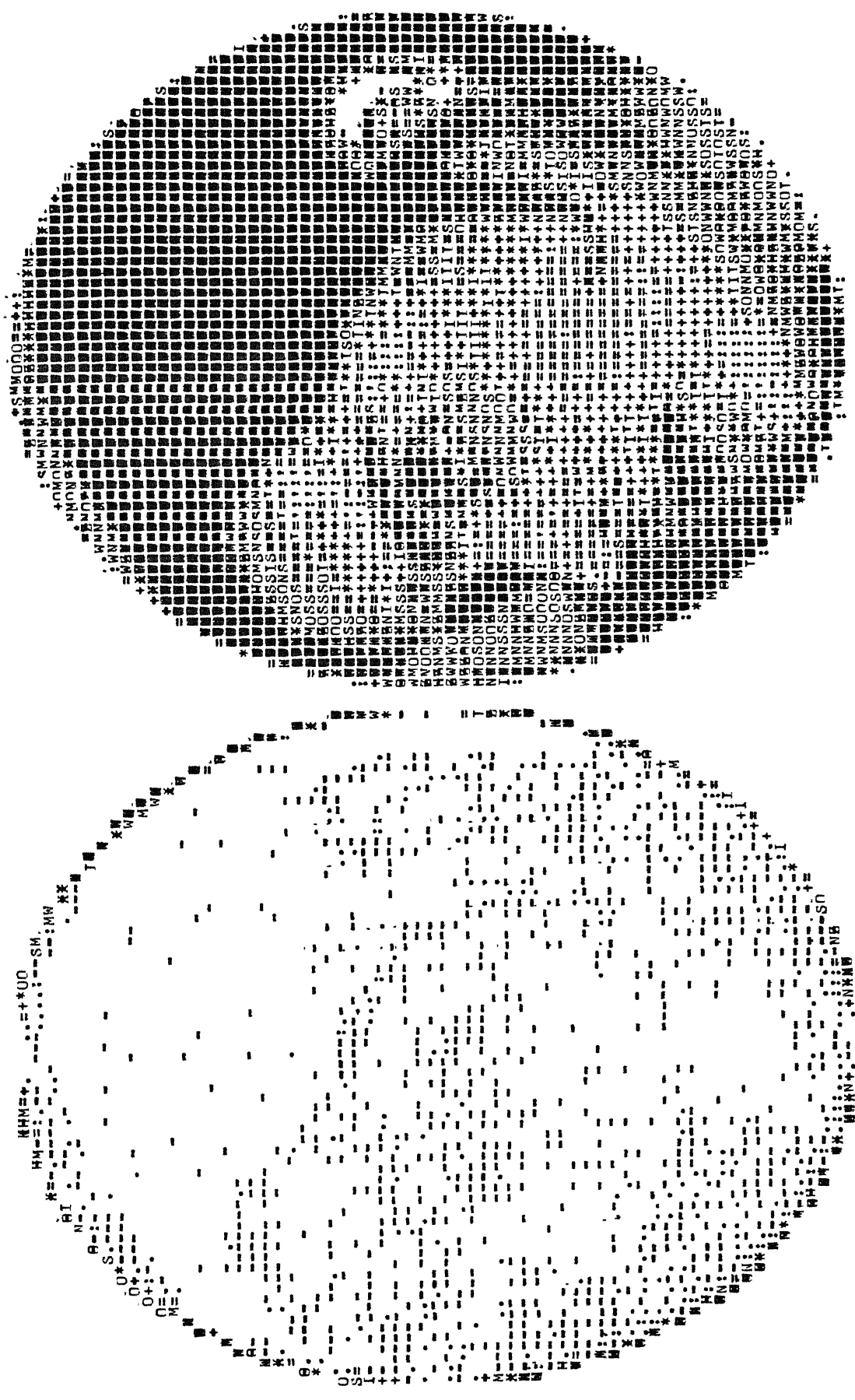
```



```
PIXEL CONSIDERED = 4096 ERMIN = -14 ERMAX = 9 ERSUM = 3178 ERSQSUM = 11740 ERL1 = 0.956365 ERL2 = 1.879615
```







RKSFIL

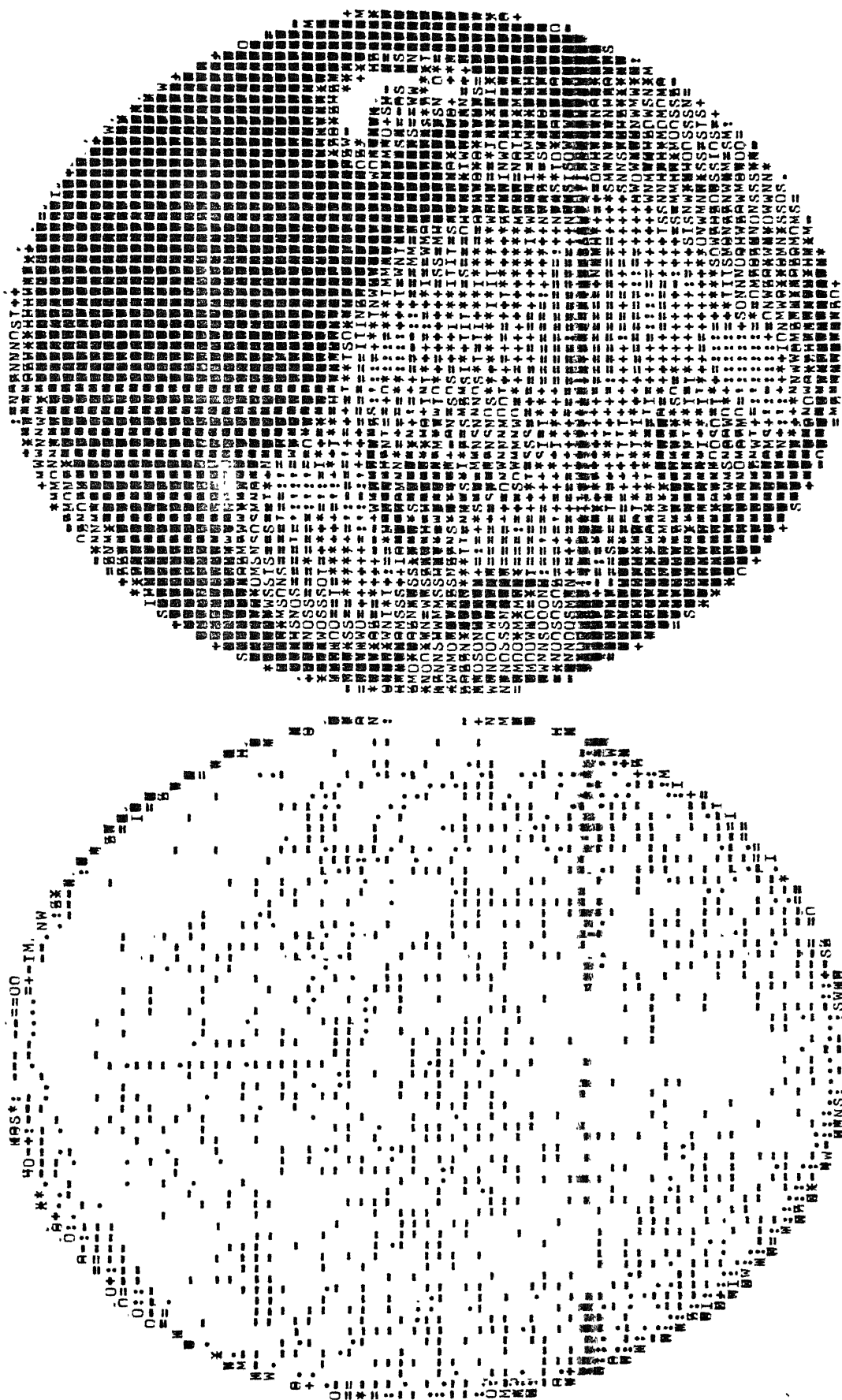
INITIAL=CAT

DATA=FACE OF A GIRL

ITERATION NUMBPR= 2

NO. OF DETECTORS = 128

NRAY = 128



PIXEL CONSIDERED = 4096 ERMIN = -4 EPMAX = 3 ERSUM = 1042 ERSOUM = 1412 ERL1 = 0.313572 ERL2 = 0.651857



RKSFIL

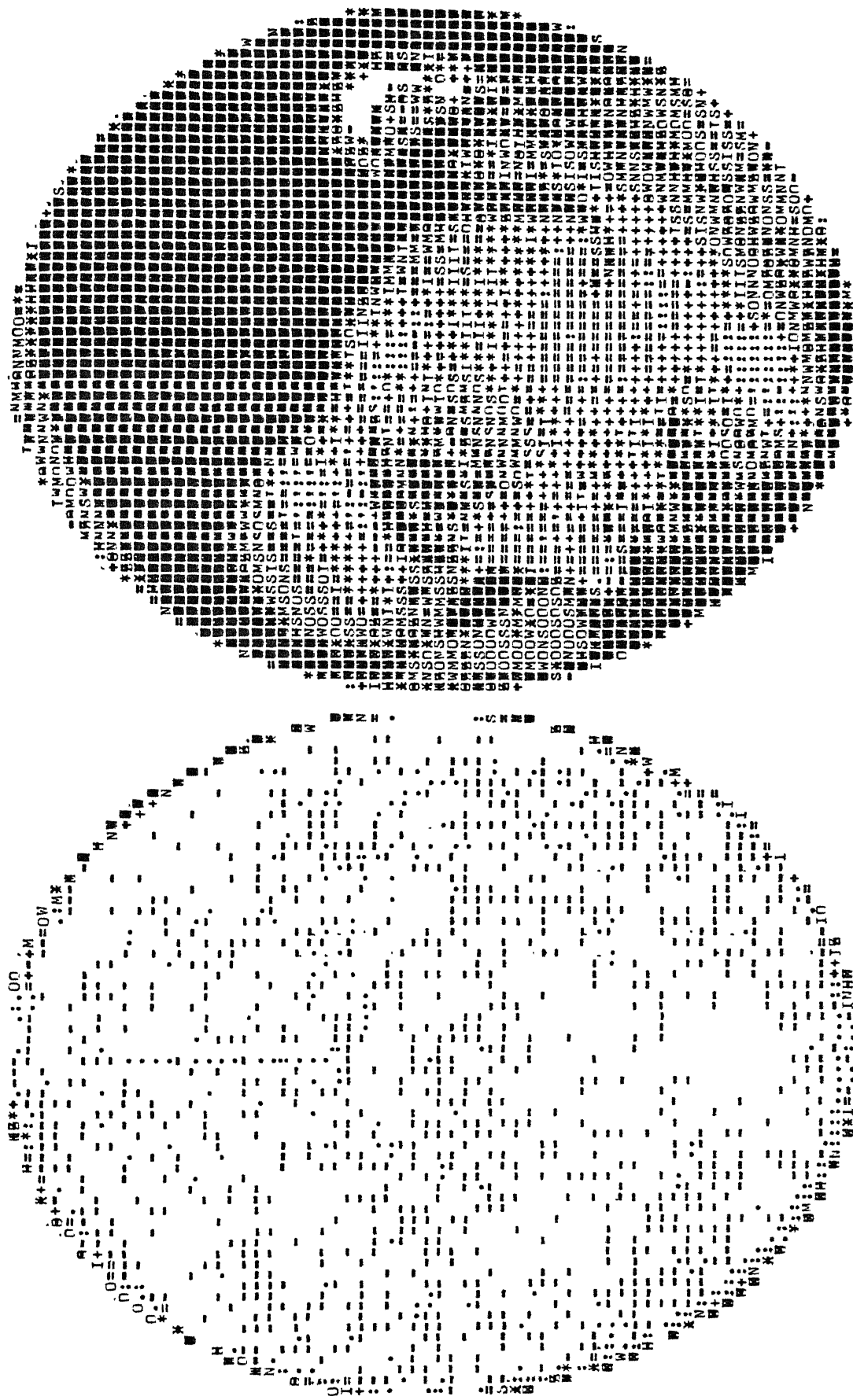
INITIAL=CAT

DATA=FACE OF A GIRL

ITERATION NUMBPR= 3

NO. OF DETECTORS = 128

NRAY = 128



FILE CONSIDERFD = 4096 FRMIN = -4 ERMAX = 4 ERSUM = 1107 ERSOSUM = 1525 FRI1 = 0.633333 ERI2 = 0.67743R

RKSPIL

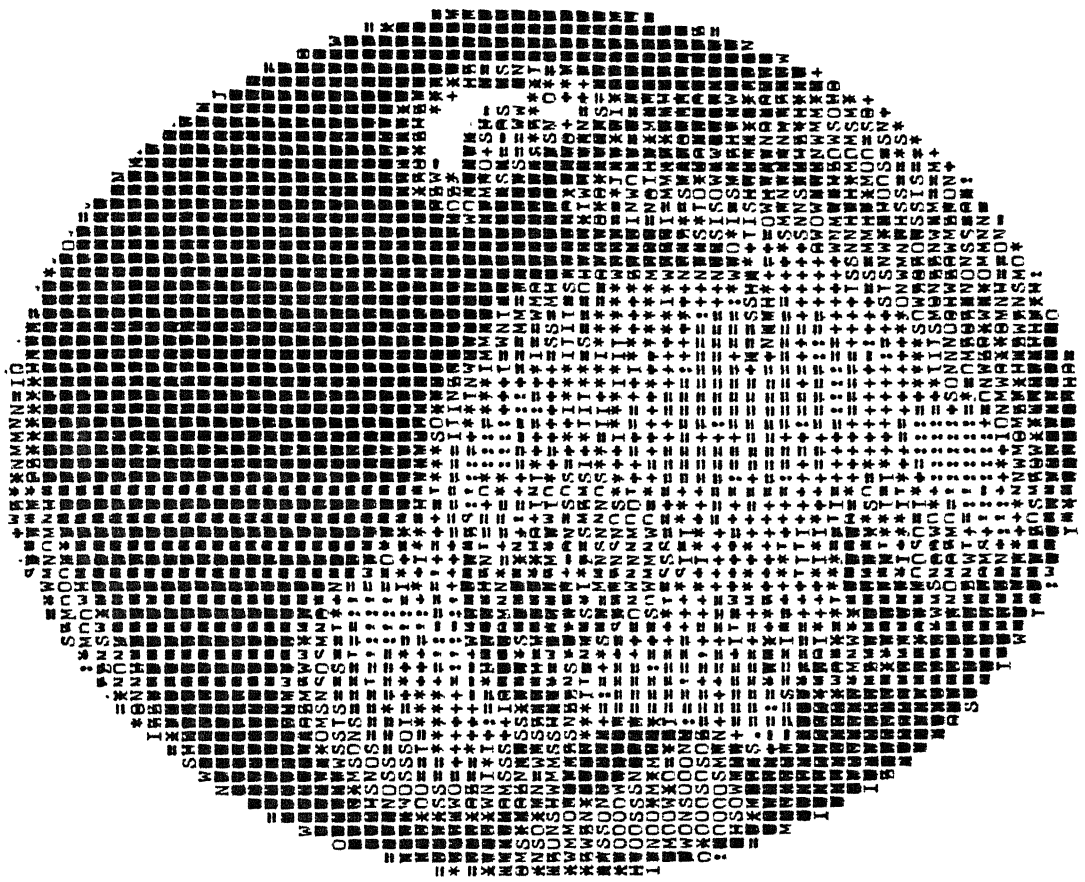
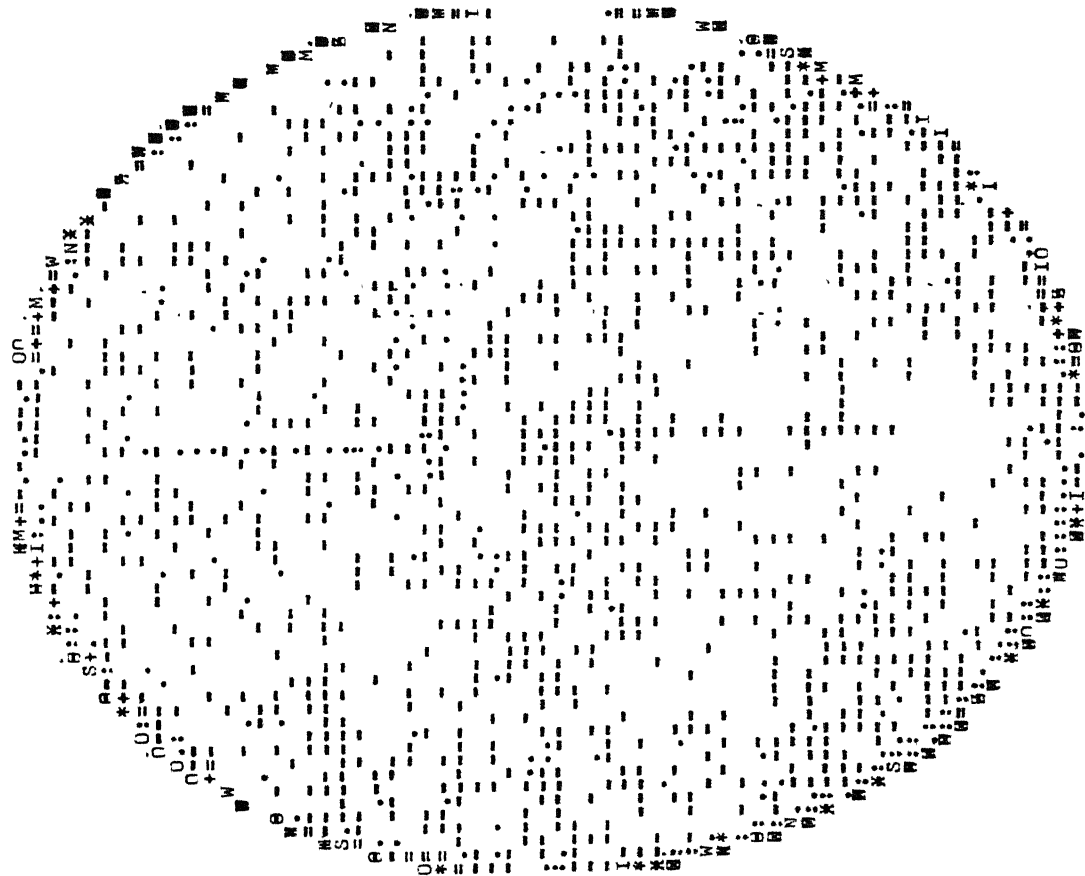
INITIAL=CAT

DATA=FACE OF A GIRL

ITERATION NUMBER= 4

NO. OF DEFECTORS = 128

NRAY = 128





RKSFIL

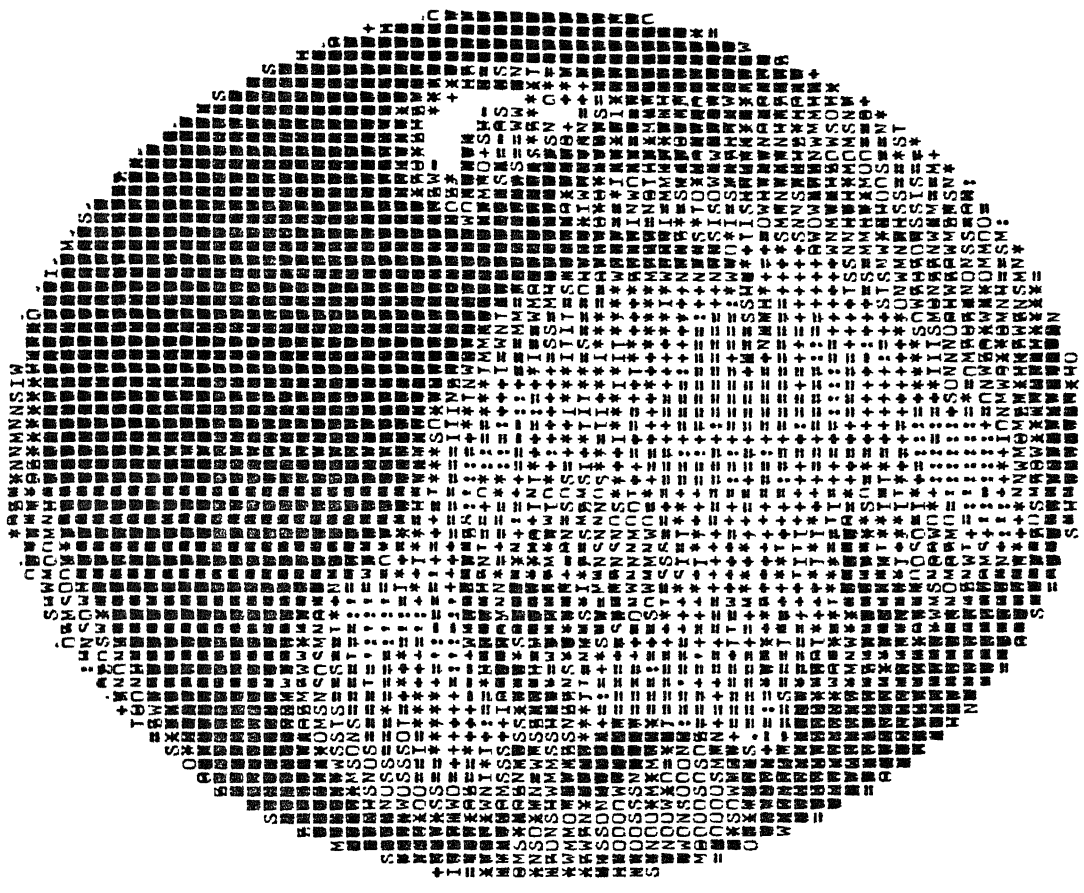
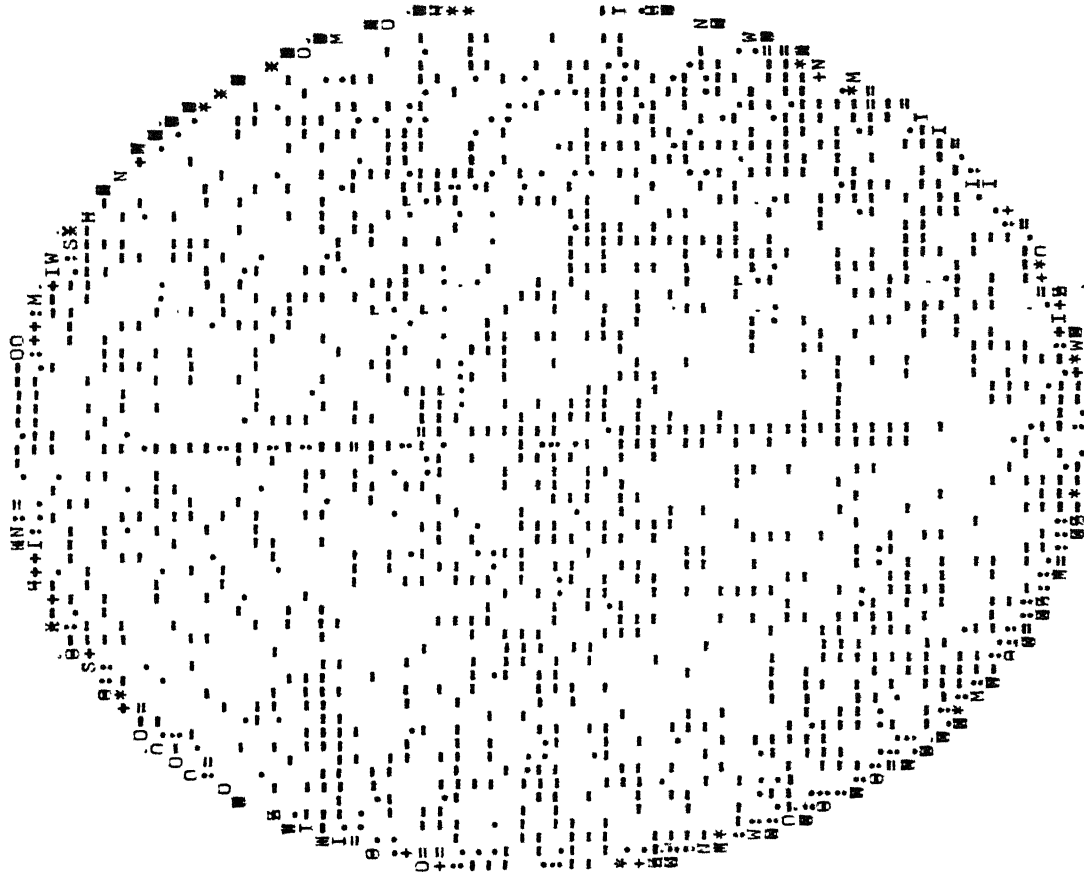
INITIAL=CAT

DATA=FACE OF A GIRL

ITERATION NUMBER= 5

NO. OF DETECTORS = 128

NRAY = 128



RKSFIL

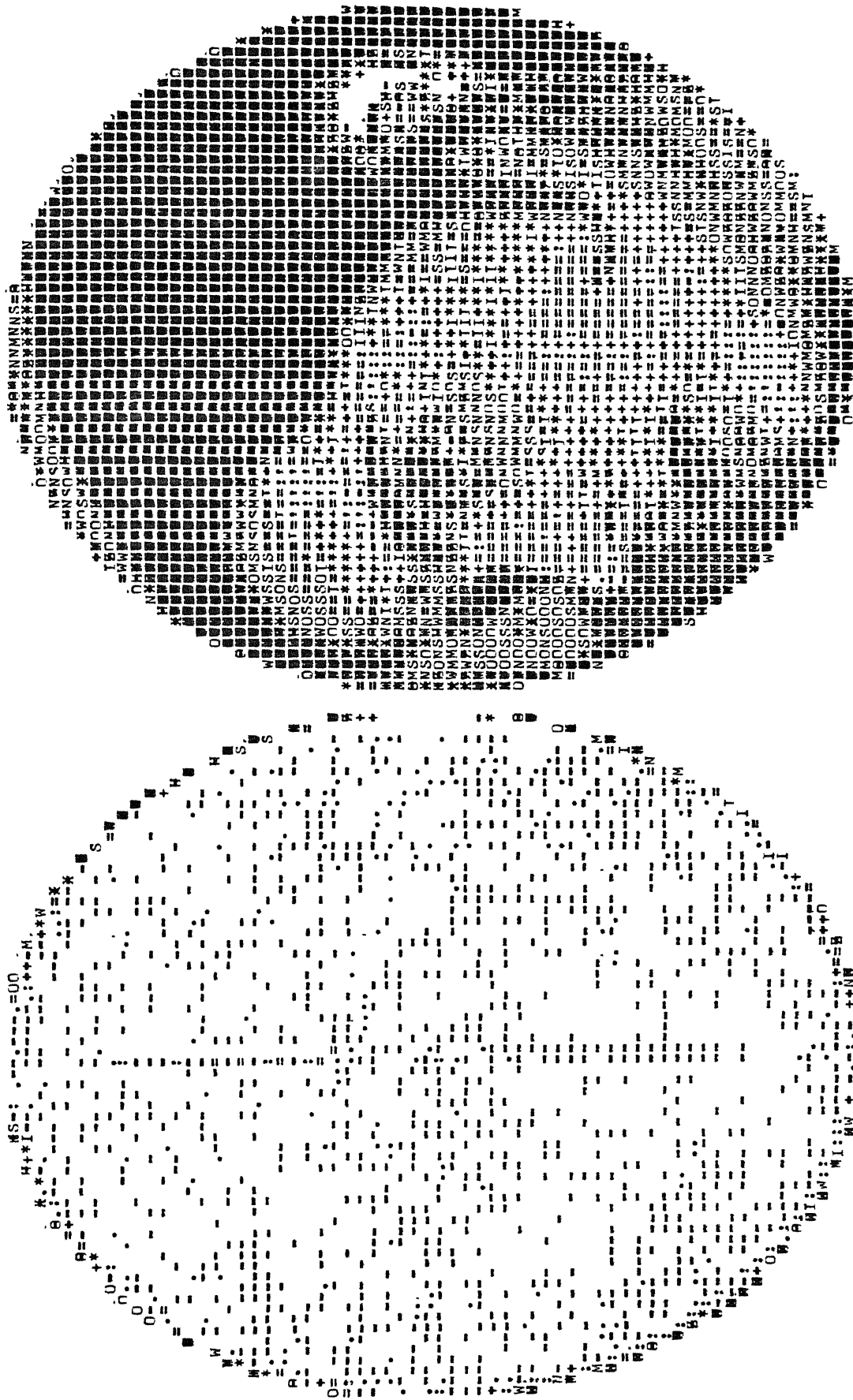
INITIAL=CAT

DATA=PAOF OF A GIRL

ITERATION NUMBER= 6

NO. OF DETECTORS = 128

NRAY = 128



PIXEL, CONSIDERED = 4096 ERMIN = -5 ERMAX = 5 ERSUM = 1165 ERSOSUM = 1700 FRL1 = 0.350587 ERL2 = 0.717143

RKSFIL

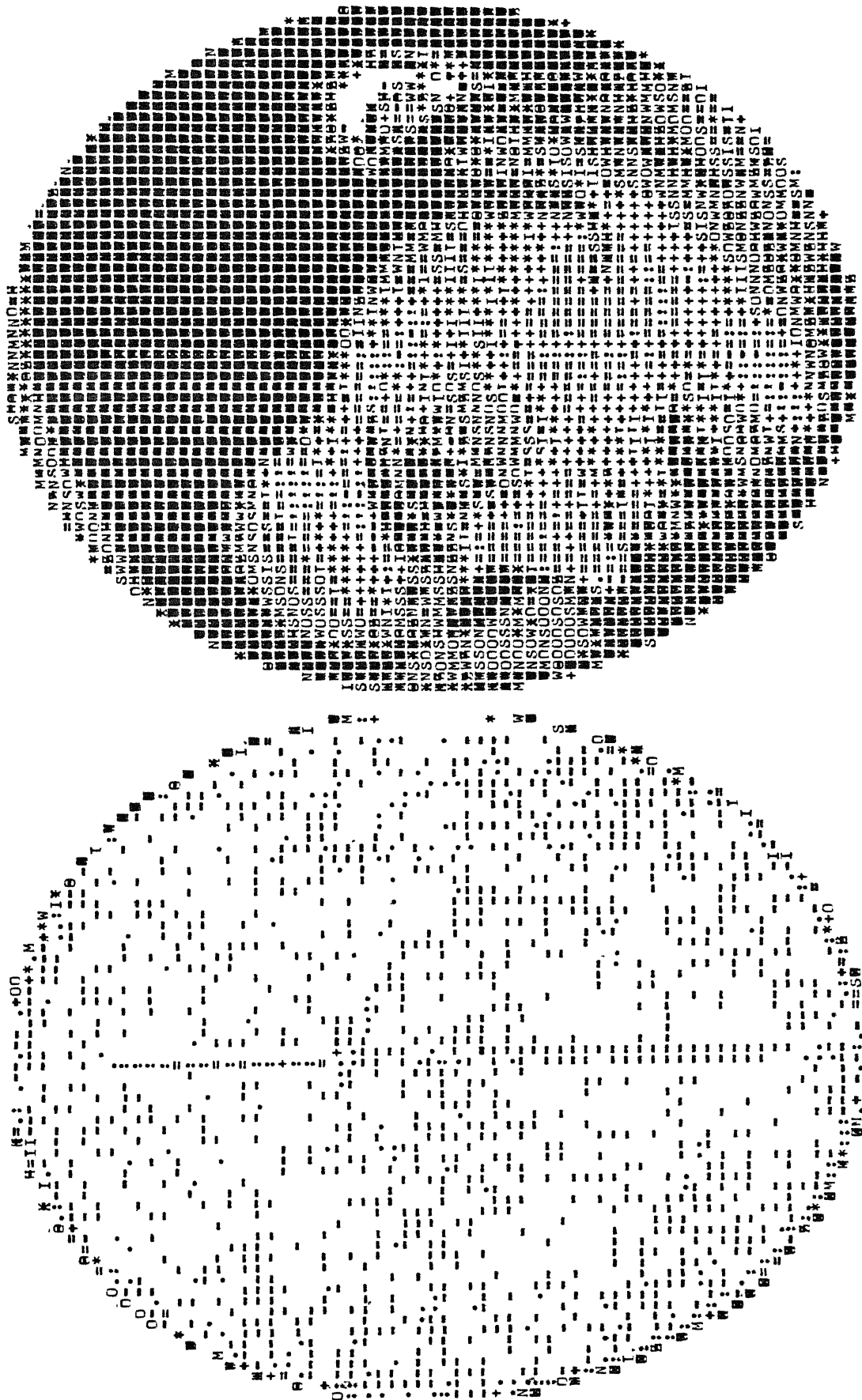
INITIAL=CAT

DATA=FACE OF A GIRL

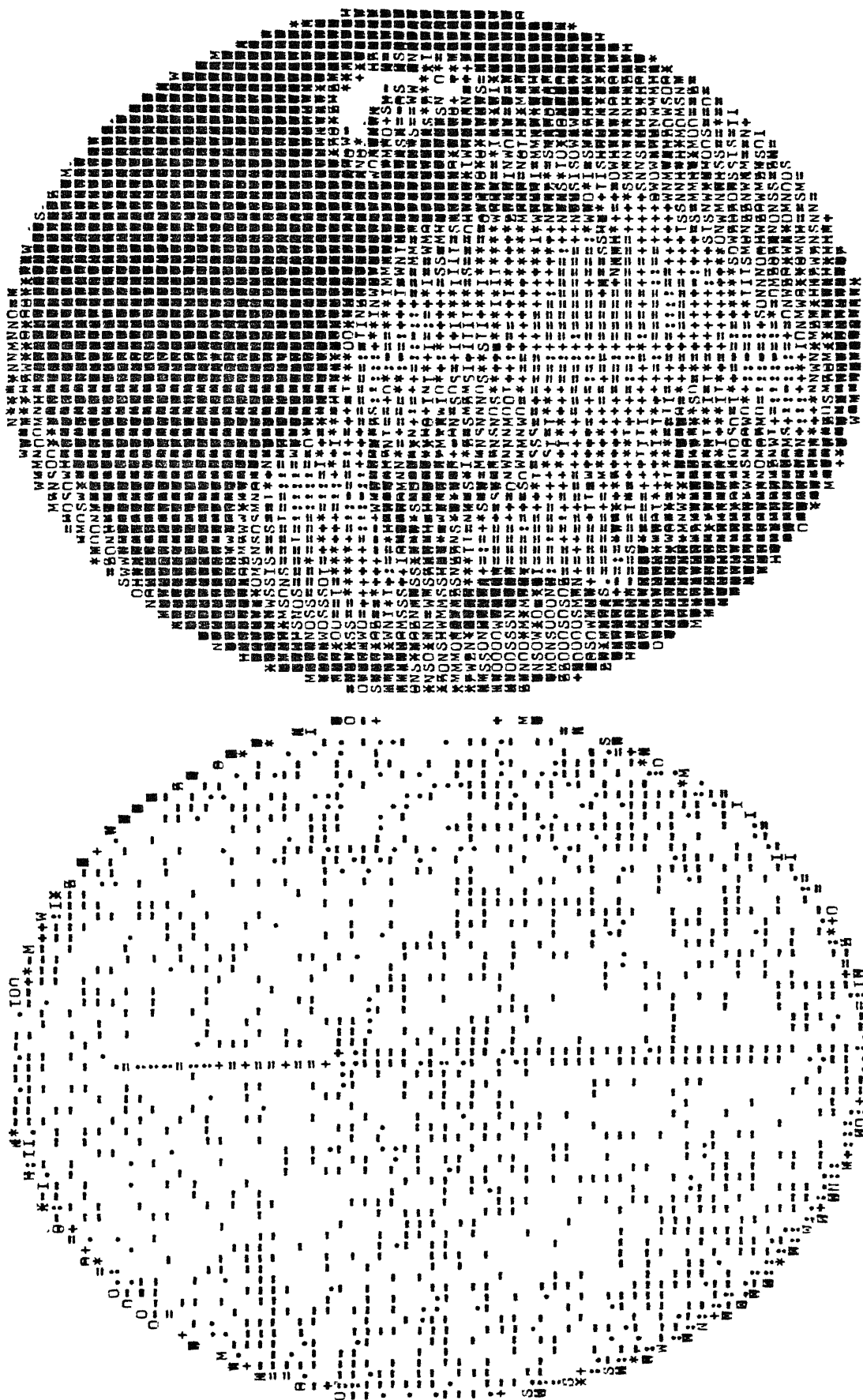
ITERATION NUMBER= 7

NO. OF DETECTORS = 128

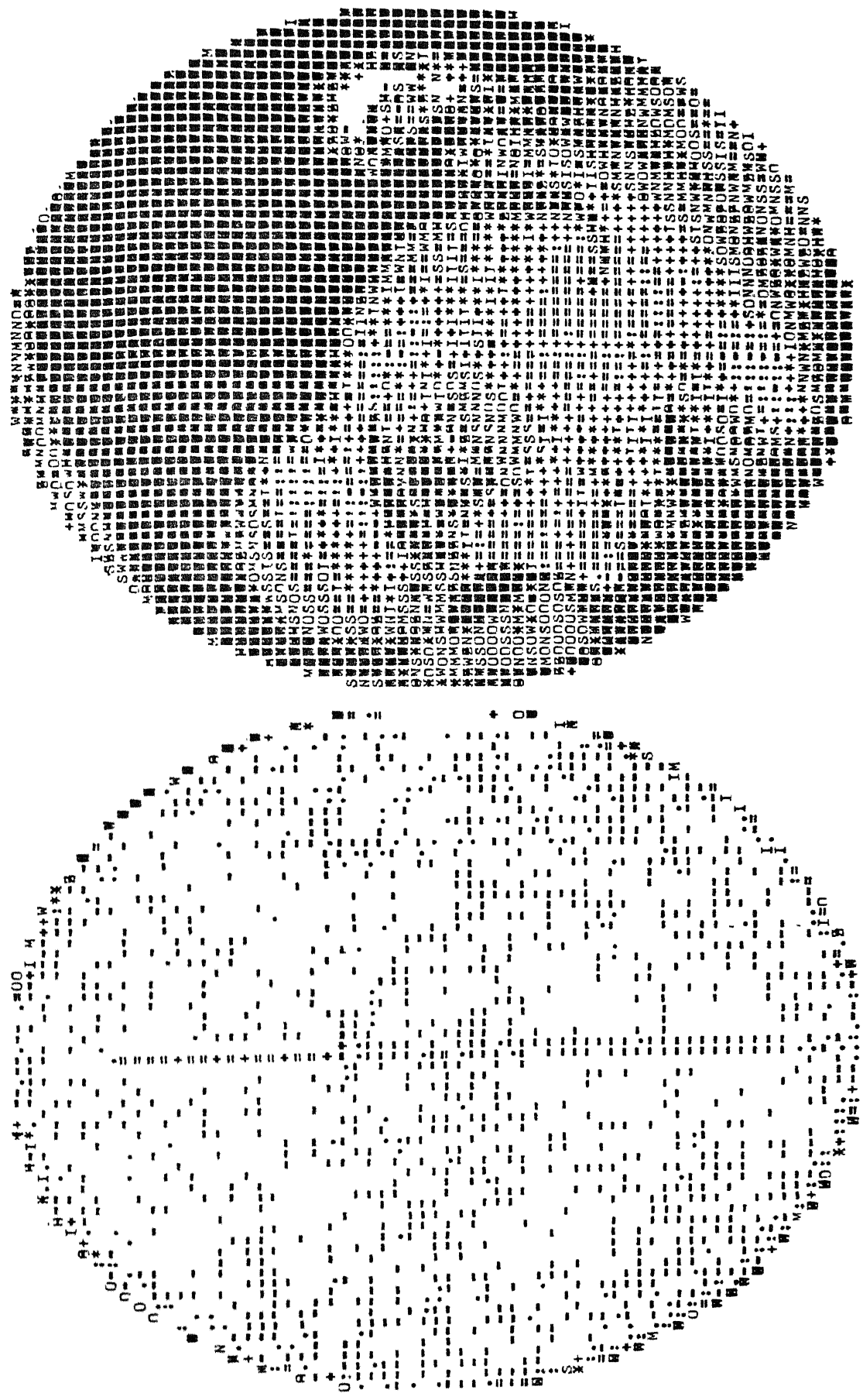
NRAY = 128



RKSFIL INITIAL=CAT DATA=FACE OF A GIRL ITERATION NUMBER= 8 NO. OF DETECTORS = 128 NRAY = 128



PIXEL CONSIDERED = 4096 ERMIN = -6 ERMAX = 7 ERSUM = 1145 ERSOSUM = 1811 FUL1 = 0.344568 ERL2 = 0.738234

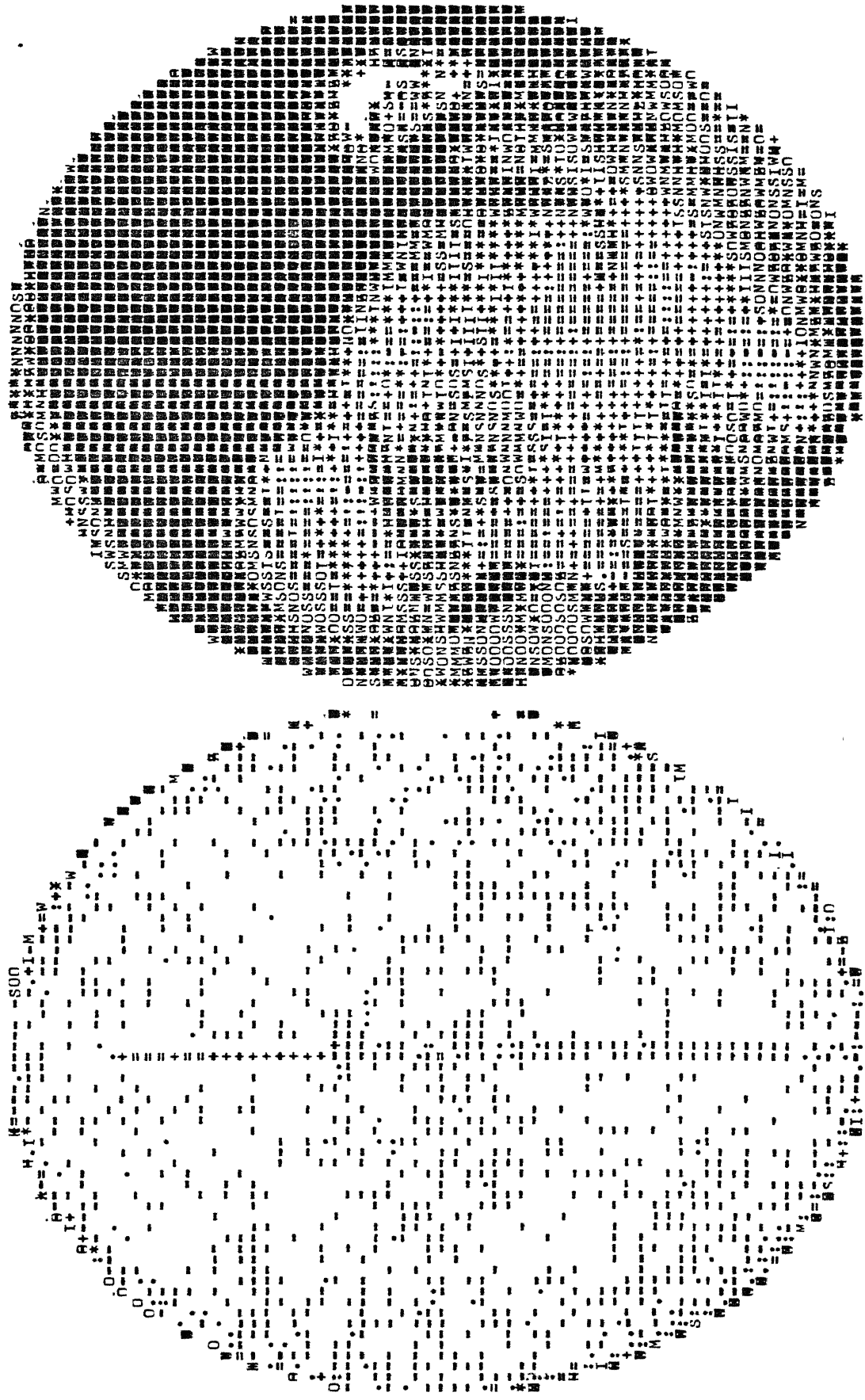


ITERATION NUMBER= 10 NO. OF DETECTORS = 128 NRAY = 128

DATA=FACE OF A GLOBE

INITIAL=CAT

RKSFTL

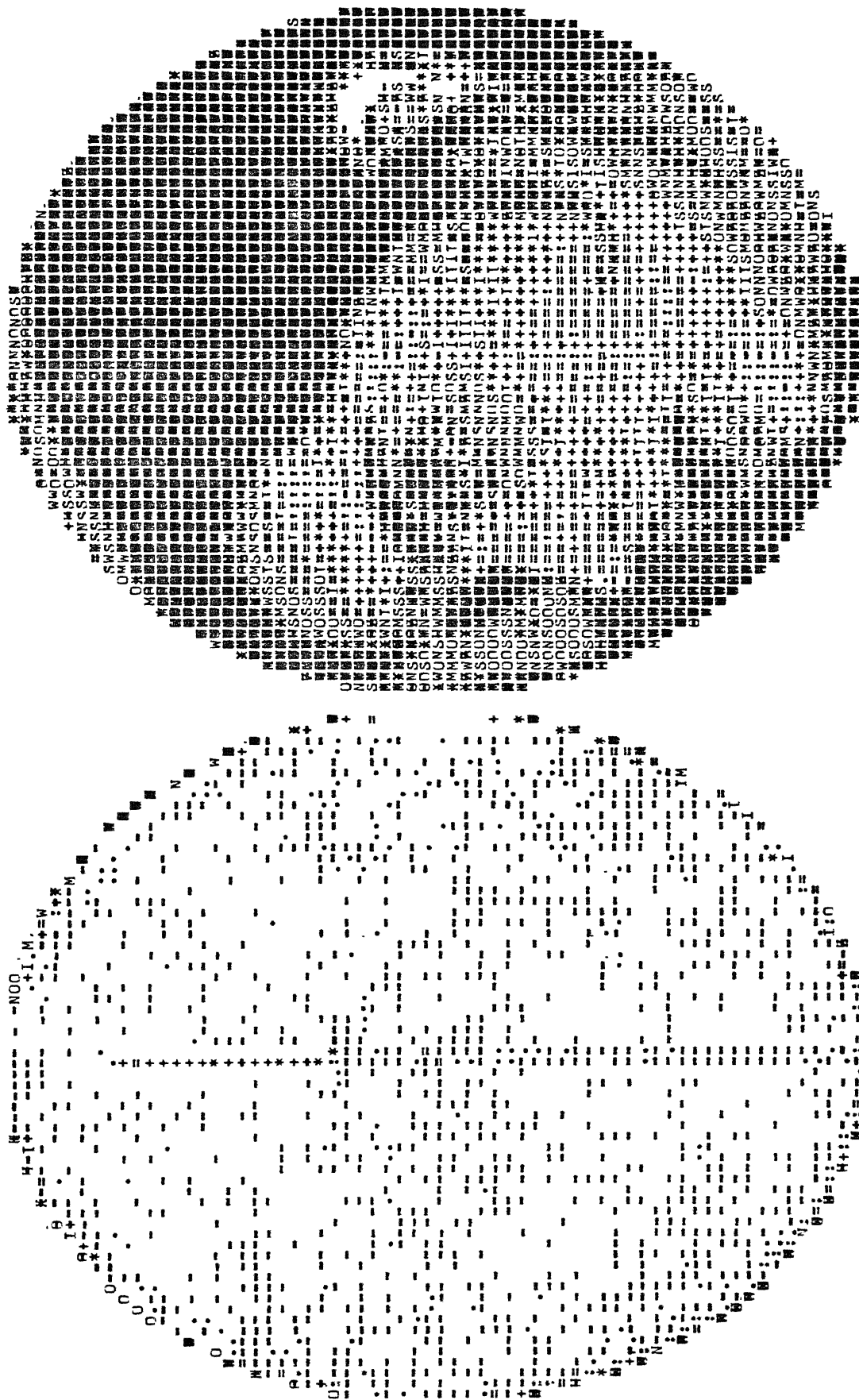


ITERATION NUMBER= 11 NO. OF DETECTORS = 128 NRAY = 128

DATA=FACE OF A GIRL

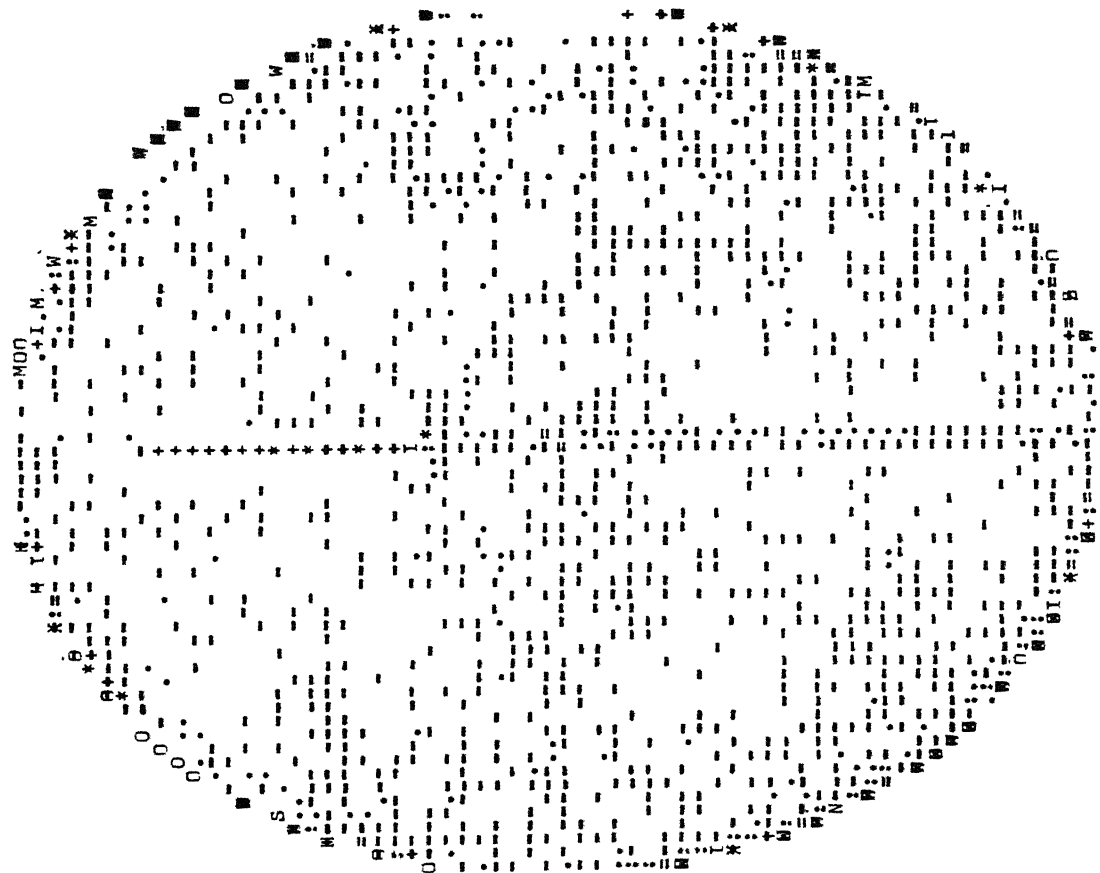
INITIAL=CAT

RKSPIL





PKSFIL INITIAL=CAT DATA=FACE OF A GIRL ITERATION NUMBER= 12 NO. OF DETECTORS = 128 NRAY = 128



PIXEL CONSIDERPO = 4096 ERMIN = -9 ERMAX = 8 EPSUM = 1136 ERSOSUM = 2180 FRL1 = 0.341860 ERL2 = 0.809959



RASFIL

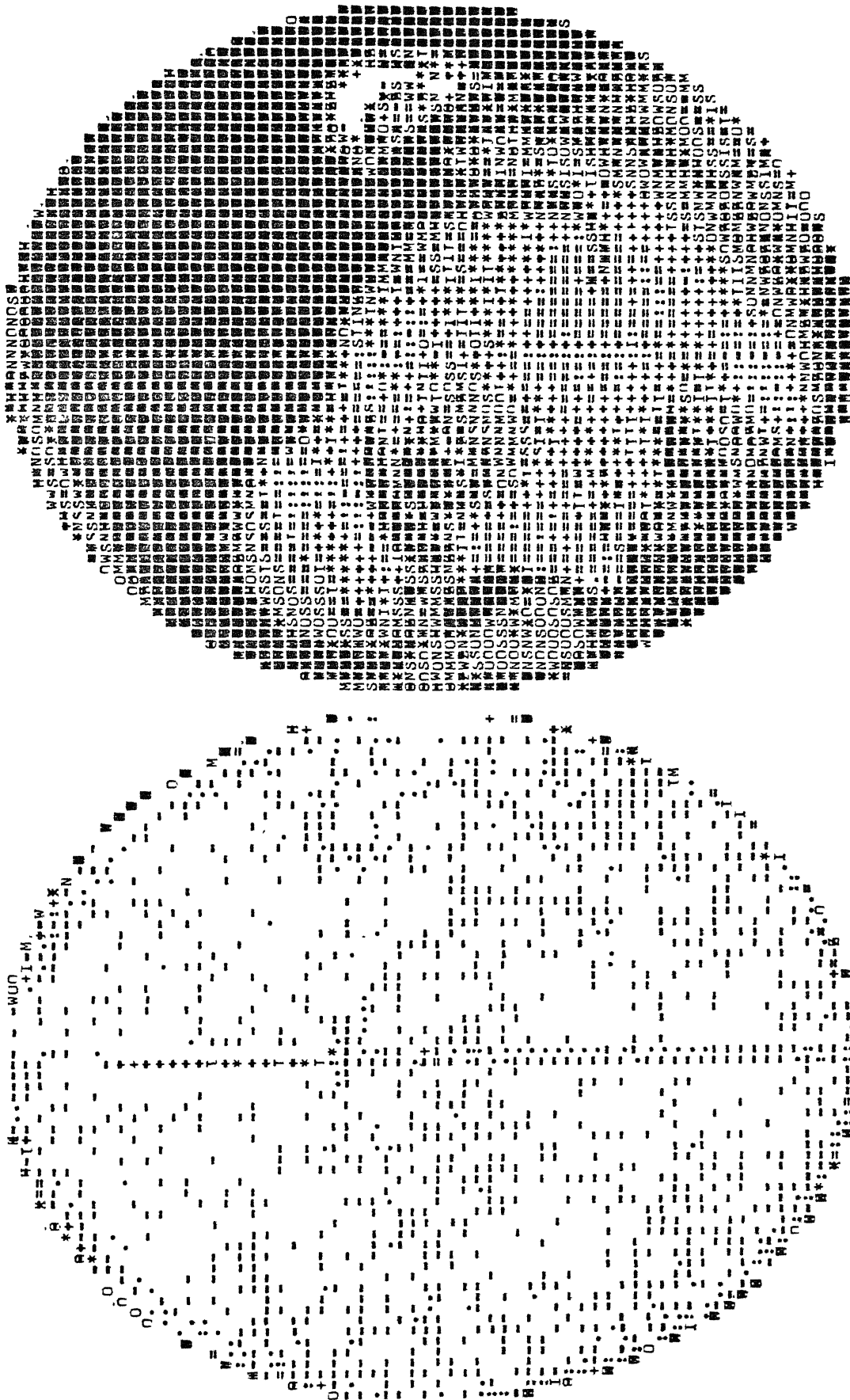
INITIAL=CAT

DATA=FACE OF A GIRL

ITERATION NUMBR= 13

NO. OF DETECTORS = 128

NRAY = 128



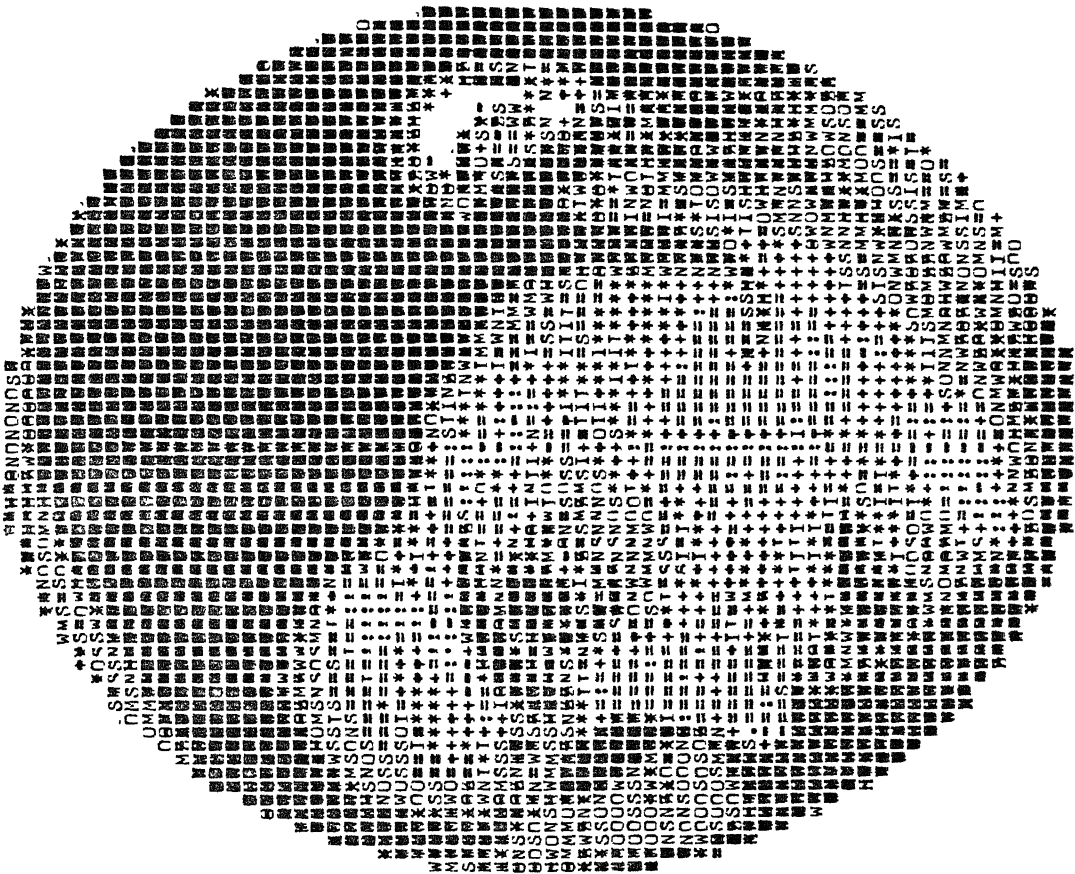
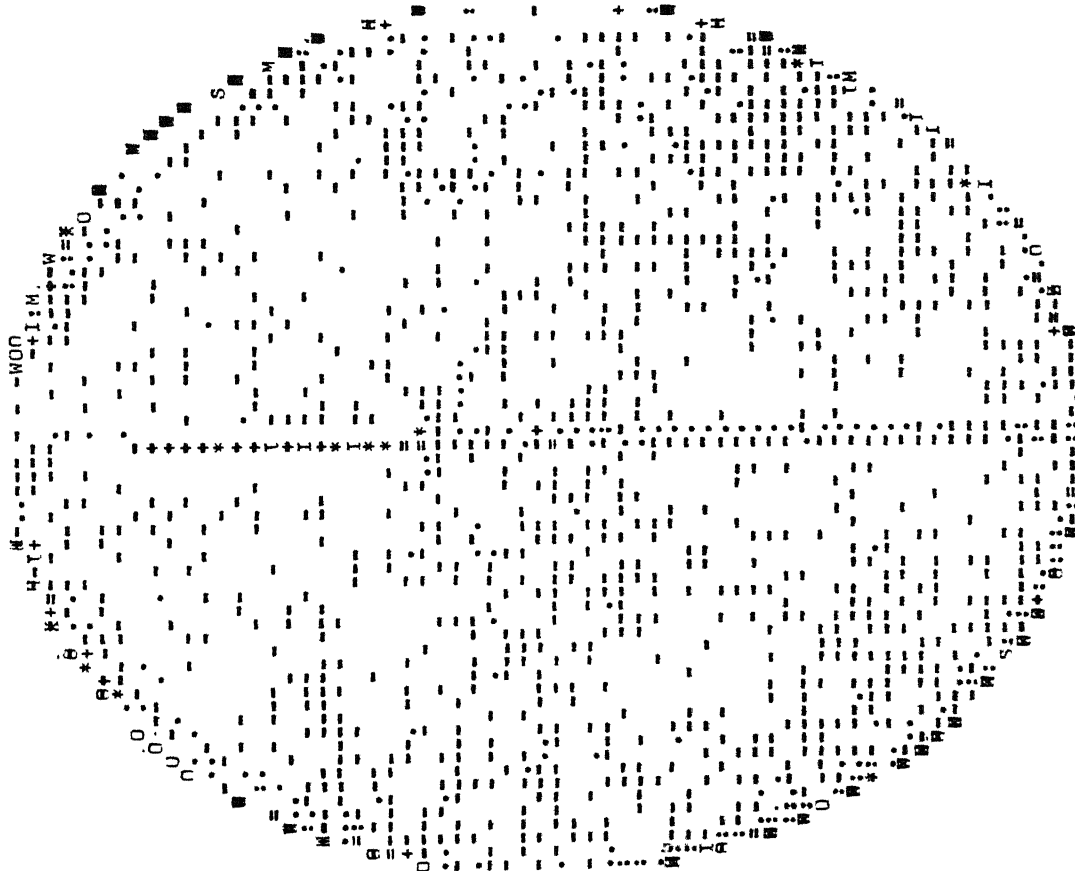
DATA=FACE OF A GIRL

INITIAL=CAT

ITERATION NUMBER= 14

NO. OF DETECTORS = 128

NRAY = 128



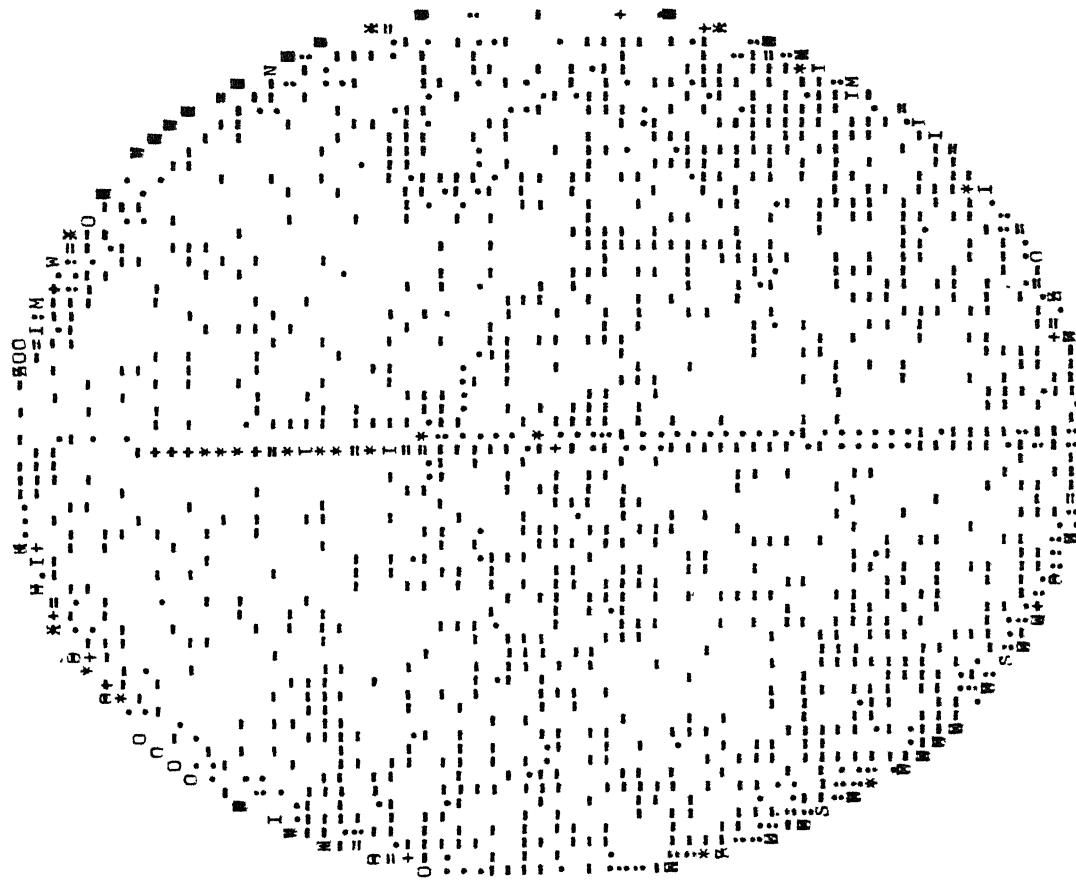
PIXEL CONSIDERED = 4096 ERMIN = -10 EPMAX = 8 ERSUM = 1143 ERSOSUM = 2423 ERL1 = 0.343966 ERL2 = 0.853909

RMSFIL

INITIAL=CAT

DATA=FACE OF A GIRL

ITERATION NUMBER=15 NO. OF DETECTORS = 128 NRAY = 128



APPENDIX C  
PROGRAM LISTING

```

*****
PROGRAM FOR ITERATIVE EM METHOD
*****
* SUM=N(N);PICOLD=OLD VALUE OF EMISSION DENSITY;PICNEW=NEW *
* VALUE OF LAMBDA;TOTCON=N(N).I.E.,TOTAL CONTRIBUTION OF THE *
* PIXEL E; *****
REAL IG
INTEGER P
DIMENSION C(260),S(260),TOTCON(64,64),PROJ(32)
DIMENSION NBT(128),PICOLD(64,64),PICNEW(64,64),II(201),JJ(201)
DIMENSION CODE(32),SUM(128,128),TITLE(40)
DO 576 L,KY=1,1
OPEN(UNIT=32,FILE='L',ACCESS='SEQIN')
READ(32,*) NPIC,NPIC,N,NRAY,H,TROUND
READ(32,2) (CODE(J),J=1,32)
CLOSE(UNIT=32,FILE='L')
OPEN(UNIT=31,DEVICE='DSKD',FILE='TOTCON',ACCESS='SEQIN')
READ(31,*) ((TOTCON(I,J),J=1,64),I=1,64)
CLOSE(UNIT=31,FILE='TOTCON')
OPEN(UNIT=32,DEVICE='DSKD',FILE='PSUM',ACCESS='SEQIN')
READ(32,*) ((SUM(I,J),J=1,N),I=1,N)
CLOSE(UNIT=32,FILE='PSUM')
OPEN(UNIT=30,DEVICE='DSKD',FILE='PICOLD',ACCESS='SEQIN')
READ(30,2) (TITLE(J),J=1,40)
DO 232 K=1,32
PROJ(K)=SORT(FLOAT(32-K))
DO 110 I=1,NPIC
READ(30,2) (PICOLD(I,J),J=1,NPIC)
DO 110 J=1,NPIC
DO 233 F=1,32
IF(PICOLD(I,J).NE.CODE(K)) GO TO 233
PICOLD(I,J)=PROJ(K)
GO TO 110
CONTINUE
CONTINUE
CLOSE(UNIT=30,FILE='PICOLD')
FORMAT(132A1)
*****
PI=3.141592654
PI2=PI/2.
PI42=2.0*PI
DT=2.*PI/FLOAT(N)
NITER=15
R=1.0
N=2.0/FLOAT(NPIC)
NN=2*N
NBT(1)=0
DO 100 J=1,NN
IF(J.EQ.1.OR.J.EQ.2) GO TO 145
TH=(PI-(J-2)*DT)/2.0
GO TO 21
TH=0.0
C(J)=COS(TH)
S(J)=SIN(TH)
CONTINUE
DO 50 K=2,N
IF(ABS(S(I+K)).LT.1.E-5) GO TO 11
T=FLOAT(K-1)*DT
DIST=SIN(T)*R/S(1+K)

```

```

11      GO TO 17
17      DIST=2.0
50      NBT(K)=DIST/H
50      CONTINUE
      DO 501 ITER=1,NITER
      WRITE(24,3)ITER
3      FORMAT(' ITERATION NUMBER=',I3)
      DO 105 I=1,MPIC
      DO 105 J=1,NPIC
105     PICNEW(I,J)=0.0
      DO 300 P=1,n
      DO 400 F=1,n
      DSUM=0.0
      J=P+K
      IF(J.LE.0) GO TO 44
      GO TO 300
44     XD=P*COS(PI-(P-1)*DT)
      YD=P*SIN(PI-(P-1)*DT)
      XJ=H*C(P+J)
      YJ=H*S(P+J)
      XJ=XD
      YJ=YD
      IF(K.EQ.0) GO TO 300
      N=K+1
      NBTT=NBTT(N)
      DO 600 IK=1,NBTT
      XI=XO+XI
      YI=YO+YI
      JI(IK)=IFIX((1.0-YI)/W+1.0)
      JJ(IK)=IFIX((1.0+XI)/W+1.0)
      IF(JI(IK).GT.NPIC) JI(IK)=JI(IK)-1
      IF(JJ(IK).GT.NPIC) JJ(IK)=JJ(IK)-1
      III=JI(IK)
      JJJ=JJ(IK)
      DSUM=PICOLD(III,JJJ)+DSUM
600     CONTINUE
      T=0
      IF(DSUM.EQ.0.0)GO TO 601
      T=SUM(P,J)/DSUM
601     CONTINUE
      DO 701 IC=1,NBTT
      III=JI(IC)
      JJJ=JJ(IC)
701     PICNEW(III,JJJ)=PICNEW(III,JJJ)+T
400     CONTINUE
300     CONTINUE
      DO 801 I=1,MPIC
      DO 801 J=1,NPIC
      IF(TOTCON(I,J).NE.0.)GOTO 802
      PICOLD(I,J)=0.
      GO TO 801
802     PICOLD(I,J)=PICNEW(I,J)*PICOLD(I,J)/TOTCON(I,J)
801     CONTINUE
      DO 901 I=1,MPIC
      DO 901 J=1,NPIC
      IF(PICNEW(I,J).NE.0.0) GO TO 9
      PICNEW(I,J)=CODE(32)
      GO TO 901
9      K=(32.5-PICOLD(I,J)*PICOLD(I,J))
      IF(K.LT.1)K=1

```

```

IF(M.GT.32)N=32
PICMEN(I,J)=CODE(K)
901 CONTINUE
DO 543 I=1,NPIC
WRITE(24,2) (PICMEN(I,J),J=1,NPIC)
543 CONTINUE
501 CONTINUE
576 CONTINUE
STOP
END

```